Electronic Supplementary Information

Chiral Proline-derived Zn(II) Complexes as Catalysts for Ring-Opening Polymerization and Ring-Opening Copolymerization Reactions

Ranay Kumar Ray[a], Manoj Kumari[a], Kartik Chandra Mondal*[a] and Debashis Chakraborty*[a]

dchakraborty@iitm.ac.in

[a] *Department of Chemistry, Indian Institute of Technology Madras, Chennai 600036, Tamil Nadu, India*

Contents

Experimental Section

1 Methods

All the NMR experiments were performed in Bruker Avance-500 instrument with the chemical shift (δ) referenced to residual solvent (δ^{H}, δ^{C} = 0 for $Si(CH_3)_4$. All spectra were processed using Topspin software. The HRMS data were recorded on an Agilent Micromass Q-TOF mass spectrometer. The GPC analysis of the polymers was carried out on a WATERS LC-20AD instrument equipped with a refractive index (RI) detector at 40 °C and with a flow rate of 0.8 mL/min. The samples were dissolved in HPLC-grade THF and were filtered through 0.2 μm PTFE filters prior to the analysis. The instrument was calibrated using narrow-M_n polystyrene standards. MALDI-TOF measurements were done on Bruker Daltonics MALDI-TOF spectrometer. Samples for MALDI-TOF MS analysis were prepared by mixing the copolymer (1.0 wt% in THF) with the matrix 1,8-dihydroxy-9(10H)-anthracenone (dithranol, 5.0 wt% in THF) and the cationizing agent potassium trifluoroacetate (1.0 wt%). The components were combined in a weight ratio of 1:40:1. Aliquots (1.0 μL) of the resulting mixture were deposited onto the wells of a gold-coated target plate and dried under ambient conditions before analysis. Single crystals suitable for X-ray diffraction analysis were grown inside the glove box from a toluene solution of the zinc complex **1** and **3**. Bruker D8 VENTURE Single Crystal X-ray diffractometer equipped with Mo(Kα) radiation source of λ = 0.71073 Å was used to collect the diffraction data for structure analysis. The selected crystal was picked using a fiber loop, mounted on the goniometer and centered. Data collection was performed at liquid nitrogen temperatures of 150 K for **1** and 100 K for **3**. An optimized strategy was adopted for the full data collection by keeping an average 4-fold redundancy for the reflections. The program APEX4-SAINT[S1] was used for integrating the frames, followed by a multi-scan absorption correction using the program SADABS[S2]. The structure was solved by direct methods using SHELXT-2018[S3] and refined by full-matrix least squares techniques using SHELXL-2019[S4] software package incorporated in WingX suite[S5]. Hydrogens on all carbon atoms were fixed at calculated positions and refined as a riding model with respect to its parent atom with Uiso (H) = 1.5 or 1.2 Ueq of C. The crystallographic data are summarized in **Table S1**. These data were deposited with CCDC with the numbers 2480534 and 2480535. HPLC analysis were performed on Waters e2695 spectrometer equipped with AD-H column by dissolving sample in hexane/isopropanol (90:10) with a flow rate of 1.0 ml/min.

2 Materials

All moisture and air-sensitive reactions were conducted under an inert argon atmosphere using a MBraun glovebox. The reagents *L*-proline, *D*-proline, thionyl chloride, triethylamine, di-tert-butyl dicarbonate, bromobenzene, 1-bromo-4-fluorobenzene, methylmagnesium bromide solution (3 M in diethyl ether), diethylzinc solution (1 M in hexane), Mg turnings, *rac*-lactide, *L*-lactide, cyclohexene oxide (CHO), propylene oxide (PO), *tert*-Butyl glycidyl ether (^{t}BGE), phthalic anhydride (PA), maleic anhydride (MA), succinic anhydride (SA), Bicyclo[2.2.1]hept-5-ene-2,3-dicarboxylic anhydride (NBA), tetraphenylphosphonium chloride (TPPCl), tetrabutylammonium bromide (TBAB), bis(triphenylphosphine)iminium chloride (PPNCl) were purchased from Sigma-Aldrich and used as received unless otherwise specified. Tetrahydrofuran (THF) and toluene were dried over sodium/benzophenone and freshly distilled prior to use. *L*-lactide and *rac*-lactide was sublimed under vacuum prior to use. CHO, PO and ^{t}BGE were dried over calcium hydride (CaH_2) and freshly distilled before use. Phthalic anhydride (PA) was crystallized twice from hot chloroform ($CHCl_3$) and sublimed under vacuum before use. Monomer MA, SA and NBA also sublimed in vacuum prior to use. NMR solvent $CDCl_3$ purchased from Cambridge Isotope Laboratories, Inc. and dried over CaH_2 and distilled prior to use. Tetra-n-butylammonium bromide (TBAB) was purified by crystallization from toluene and then dried under vacuum before use. Tetraphenylphosphonium chloride (TPPCl) and bis(triphenylphosphine)iminium chloride (PPNCl) were purified by crystallizing from chloroform and hexane, followed by drying under vacuum. Argon and nitrogen gas was purchased from Indogas, Bangalore, India.

3 Synthesis

3.1 Synthesis of Zn(II) compounds

3.1.1 Compound **1**

In an argon-filled glove box, $ZnEt_2$ (1 M in hexane, 0.28 mL, 0.28 mmol) was added dropwise to a stirred solution of $\mathbf{L_1H}$ (0.100g, 0.28 mmol) in 8 mL toluene at -24 ^{o}C. The solution was allowed to attain room temperature and stirred for an additional period of 12 h. The solvent was removed under vacuo giving a white solid product which was then recrystallised from concentrated dry toluene at –24 °C to give white crystals of **1** (Yield = 82 %). ^{1}H NMR ($CDCl_3$, 500 MHz, 298 K) : δ (ppm) : 7.14-7.43 (m, 10H, Ph**H**), 4.75-4.77 (dd, J = 7.6, 1.3 Hz, 1H, N**H)**, 3.22-3.28 (m, 1H,

NC**H**$_2$), 2.87-2.91 (m, 1H, NC**H**$_2$), 2.05-2.10 (m, 1H, NCHC**H**$_2$), 1.81-1.92 (m, 1H, NCH$_2$C**H**$_2$), 1.71 (s, 9H, C(C**H**$_3$)$_9$), 1.23-1.29 (m, 1H, (NCH$_2$C**H**$_2$), 0.48-0.52 (t, 3H, ZnCH$_2$C**H**$_3$, J = 10 Hz), 0.01-0.52 (m, 1H, NCHC**H**$_2$), -0.80 - -0.66 (m, 2H, Zn-C**H**$_2$CH$_3$). ^{13}C {^{1}H} NMR ($CDCl_3$, 500 MHz, 298 K) : δ (ppm) : 159.40, 150.23, 147.68, 128.66, 127.90, 127.46, 126.96, 126.48, 126.32, 82.22, 80.91, 68.30, 48.86, 29.54, 29.03, 22.05, 12.10, 0.11. HRMS m/z calculated for $[M+H]^+$ $C_{24}H_{31}NO_3Zn$: 446.1628 found 446.1630.

3.1.2 Compound **2**

In an argon-filled glove box, $ZnEt_2$ (1 M in hexane, 0.44 mL, 0.44 mmol) was added dropwise to a stirred solution of **L$_2$H** (0.100g, 0.44 mmol) in 8 mL toluene at -24 ^{o}C. The solution was allowed to attain room temperature and stirred for an additional period of 12 h. The solvent was removed under vacuo giving a white solid product which was then recrystallised from concentrated dry toluene at –24 °C to give white crystals of **2** (Yield = 76 %). ^{1}H NMR ($CDCl_3$, 500 MHz, 298 K) : δ (ppm) : 3.74-3.75 (dd, J = 8.9, 3.7 Hz, 1H, N**H)**, 3.50-3.55 (m, 1H, NC**H**$_2$), 3.10-3.15 (m, 1H, NC**H**$_2$), 1.84-1.96 (m, 2H, NCHC**H**$_2$), 1.61-1.84 (m, 1H, NCH$_2$C**H**$_2$), 1.48 (s, 9H, C(CH$_3$)$_9$, 1.18-1.21 (t, 3H, ZnCH$_2$C**H**$_3$, J = 10 Hz), 1.35 (s, 3H, -C-C**H**$_3$), 1.00 (s, 3H, -C-C**H**$_3$), 0.01-0.06 (q, 2H, ZnC**H**$_2$CH$_3$**,** J = 8 Hz). ^{13}C {^{1}H} NMR ($CDCl_3$, 500 MHz, 298 K) : δ (ppm) : 158.45, 80.74, 74.55, 69.91, 48.42, 30.93, 28.99, 28.34, 26.36, 24.38, 13.46, -0.16. HRMS m/z calculated for $[M+H]^+$ $C_{14}H_{27}NO_3Zn$: 322.1315 found 322.2021.

3.1.3 Compound **3**

In an argon-filled glove box, $ZnEt_2$ (1 M in hexane, 0.25 mL, 0.25 mmol) was added dropwise to a stirred solution of **L$_3$H** (0.100g, 0.25 mmol) in 8 mL toluene at -24 ^{o}C. The solution was allowed to attain room temperature and stirred for an additional period of 12 h. The solvent was removed under vacuo giving a white solid product which was then recrystallised from concentrated dry toluene at –24 °C to give white crystals of **3** (Yield = 88 %). ^{1}H NMR ($CDCl_3$, 500 MHz, 298 K) : δ (ppm) : 6.83-7.36 (m, 8H, Ph**H**), 4.67-4.69 (dd, J = 7.6, 1.3 Hz, 1H, N**H)**, 3.73-3.75 (m, 1H, NC**H**$_2$), 3.22-3.29 (m, 1H, NC**H**$_2$), 2.84-2.89 (m, 1H, NCHC**H**$_2$), 2.05-2.13 (m, 1H, NCH$_2$C**H**$_2$), 1.68 (s, 9H, C(C**H**$_3$)$_9$), 1.25-1.35 (m, 1H, (NCH$_2$C**H**$_2$), 0.50-0.54 (t, 3H, ZnCH$_2$C**H**$_3$, J = 10 Hz), -0.05-0.07 (m, 1H, NCHC**H**$_2$), -0.70- -0.63 (AB octet, 2H, Zn-C**H**$_2$CH$_3$). ^{13}C {^{1}H} NMR ($CDCl_3$, 500 MHz, 298 K) : δ (ppm) : 159.40, 150.23, 147.68, 128.66, 127.90, 127.46, 126.96, 126.48,

126.32, 82.22, 80.91, 68.30, 48.86, 29.54, 29.03, 22.05, 12.10, 0.11. HRMS m/z calculated for $[M+H]^+$ $C24H29NO_3F_2Zn$: 482.15 found 482.25.

3.1.4 Compound **4**

In an argon-filled glove box, $ZnEt_2$ (1 M in hexane, 0.28 mL, 0.28 mmol) was added dropwise to a stirred solution of $\mathbf{L_4H}$ (0.100g, 0.28 mmol) in 8 mL toluene at -24 °C. The solution was allowed to attain room temperature and stirred for an additional period of 12 h. The solvent was removed under vacuo giving a white solid product which was then recrystallised from concentrated dry toluene at –24 °C to give white crystals of **4** (Yield = 86 %). ^{1}H NMR ($CDCl_3$, 500 MHz, 298 K) : δ (ppm) : 7.06-7.34 (m, 10H, Ph**H**), 4.66-4.68 (dd, J = 7.6, 1.3 Hz, 1H, N**H)**, 3.13-3.19 (m, 1H, NC$\mathbf{H}_2$), 2.79-2.83 (m, 1H, NC$\mathbf{H}_2$), 1.95-2.03 (m, 1H, NCHC$\mathbf{H}_2$), 1.74-1.78 (m, 1H, $NCH_2C\mathbf{H}_2$), 1.63 (s, 9H, $C(C\mathbf{H_3})_9$), 1.15-1.20 (m, 1H, ($NCH_2C\mathbf{H}_2$), 0.39-0.43 (t, 3H, $ZnCH_2C\mathbf{H}_3$, J = 10 Hz), -0.17- -0.06 (m, 1H, NCHC$\mathbf{H}_2$), -0.89- -0.75 (m, 2H, Zn-C$\mathbf{H}_2CH_3$). ^{13}C {^{1}H} NMR ($CDCl_3$, 500 MHz, 298 K) : δ (ppm) : 159.27, 150.11, 147.55, 128.53, 127.78, 127.33, 126.83, 126.36, 126.18, 82.11, 80.79, 68.18, 48.73, 29.41, 28.90, 21.92, 11.97, -0.01. HRMS m/z calculated for $[M]^+$ $C_{24}H_{31}NO_3Zn$: 445.1595 found 427.1723.

3.2 General polymerization procedure for ROCOP of epoxide and anhydride

The reaction for the ROCOP of epoxide and anhydride was performed in a oven dried glass reaction tube equipped with a magnetic stirring bar. The constituents of the reaction were weighed inside the glove box and mixed such that CHO : PA : Cat : Cocat. = 400:100:1:1 followed by the addition of 1mL of dry toluene. The reaction tube was sealed properly by applying grease and taken out of the glove box. The tube was dipped in an oil bath maintained at 100 °C. The progress of the reaction was monitored by the analysis of the ^{1}H NMR spectra of the aliquots taken at different time interval. After the desired time interval, the solvent was evaporated under vacuum. Upon removal of the solvent, the crude product was dissolved in dichloromethane and precipitated by the addition of cold methanol. The polymer was filtered and dried under vacuum until the pure product gave constant weight.

3.2.1 Kinetics for the ROCOP of CHO with PA respect to PA

In order to determine the order of the reaction with respect to phthalic anhydride the reactions were performed with CHO : PA : Cat : Cocat. = 400:100:1:1. The aliquots were taken at different time interval and it was observed that PA decreases linearly over time indicating reaction is zero order with respect to PA.

3.2.2 Kinetics for the ROCOP of CHO with PA respect to CHO

In order to determine the order of the reaction with respect to CHO, the reactions were performed with CHO : PA : Cat : Cocat. = 400:100:1:1. The aliquots were taken at different time interval and amount of CHO reacted was determined at each time interval. The amount of CHO reacted was calculated by taking the integral for polyester linkage (δ = 4.80-5.26 ppm) and polyether linkage (δ = 3.22-3.64 ppm) relative to unreacted CHO (3.08 ppm). It was observed that the plot of $\ln([CHO]_0/[CHO]_t)$ versus time was linear indicating that the reaction is first order in concentration of monomer CHO.

3.2.3 Kinetics for the ROCOP of CHO with PA respect to catalyst

To determine the order of the reaction with respect to catalyst the reactions were performed such that CHO:PA:cocatalyst was kept constant to 400:100:1 and set of experiments were performed by varying the equivalents of catalyst from 0.5 to 2. In each case the percentage conversion of phthalic anhydride was determined by integrating the signals for unreacted PA (δ = 7.97 ppm) and phenylene signal in the polymer chain (7.30-7.83 ppm) at different time interval and initial rate (k_{obs}) was determined for each set of experiments, from the plot of $[PA]_t$ versus time. The plot of k_{obs} versus [cat] was linear.

3.2.4 Kinetics for the ROCOP of CHO with PA respect to cocatalyst

To determine the order of the reaction with respect to catalyst and the reactions were performed such that CHO:PA:catalyst was kept constant to 400:100:1 and set of experiments were performed by varying the equivalents of cocatalyst from 0.5 to 2. In each case the percentage conversion of phthalic anhydride was determined by integrating the signals for unreacted PA (δ = 7.97 ppm) and phenylene signal in the polymer chain (7.30-7.83 ppm) at different time interval and initial rate (k_{obs}) was determined for each set of experiments, from the plot of $[PA]_t$ versus time. The plot of k_{obs} versus [cat] was linear.

3.3. General procedure for ROP of *rac*-lactide

The reaction for the ROP of *rac*-LA was performed in a glass reaction tube equipped with a magnetic stirring bar. The monomer *rac*-LA and the catalyst were mixed in a 200:1 molar ratio in the tube followed by the addition of 1 mL of dry toluene. The reaction tube was sealed properly by applying grease and taken out of the glove box. The tube was dipped in an oil bath maintained at 100 ˚C. The progress of the reaction was monitored by the analysis of the ^{1}H NMR spectra of the aliquots taken at different time interval. After the desired time interval, the solvent was evaporated under vacuum. Upon removal of the solvent, the crude product was dissolved in dichloromethane and precipitated by the addition of cold methanol. The polymer was filtered and dried under vacuum until the pure product gave constant weight.

3.3.1. Kinetics for the ROP of *rac*-LA

subjected to ^{1}H NMR analysis and the percentage conversion was determined. The percentage conversion of *rac*-LA was determined by comparing the signal intensity of PLA (δ = 5.15-5.25 ppm) relative to unreacted *rac*-LA (δ = 4.98-5.05 ppm). The linear relationship between ln([*rac*-LA]$_0$/[*rac*-LA]$_t$) versus time well manifested that the polymerization reaction is first-order with respect to the monomer.

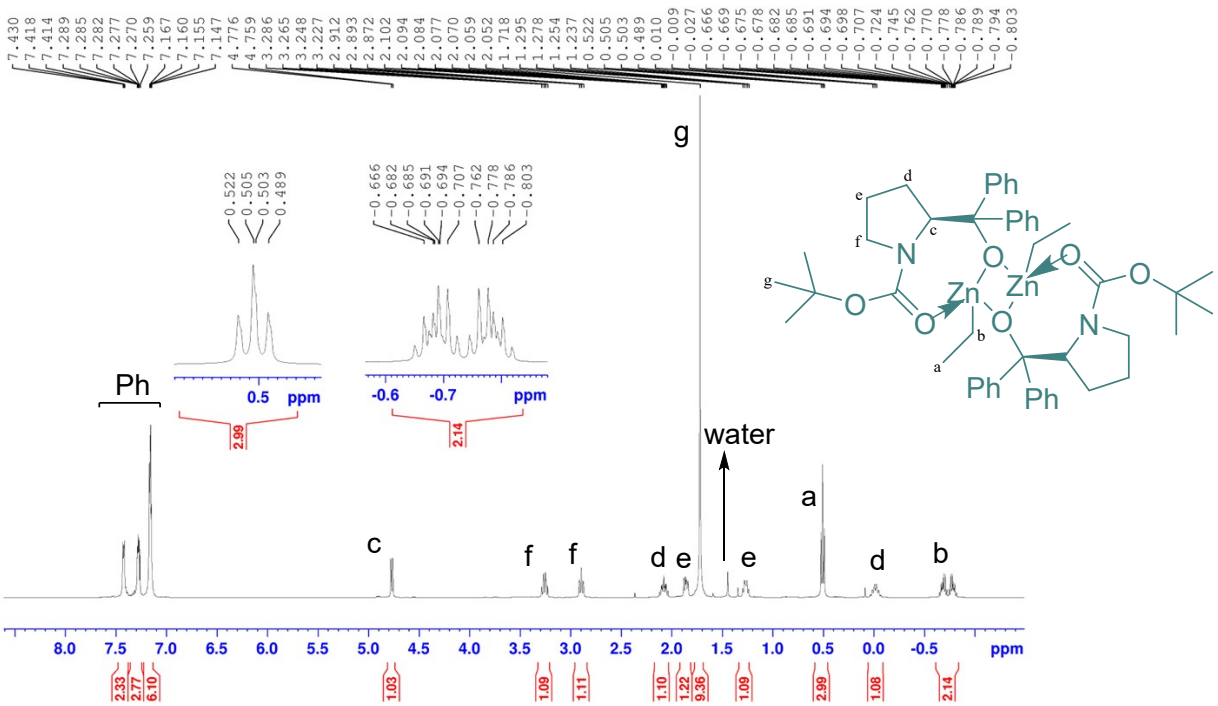

Fig. S1. ^{1}H NMR spectrum of **1** in $CDCl_3$ (300 K).

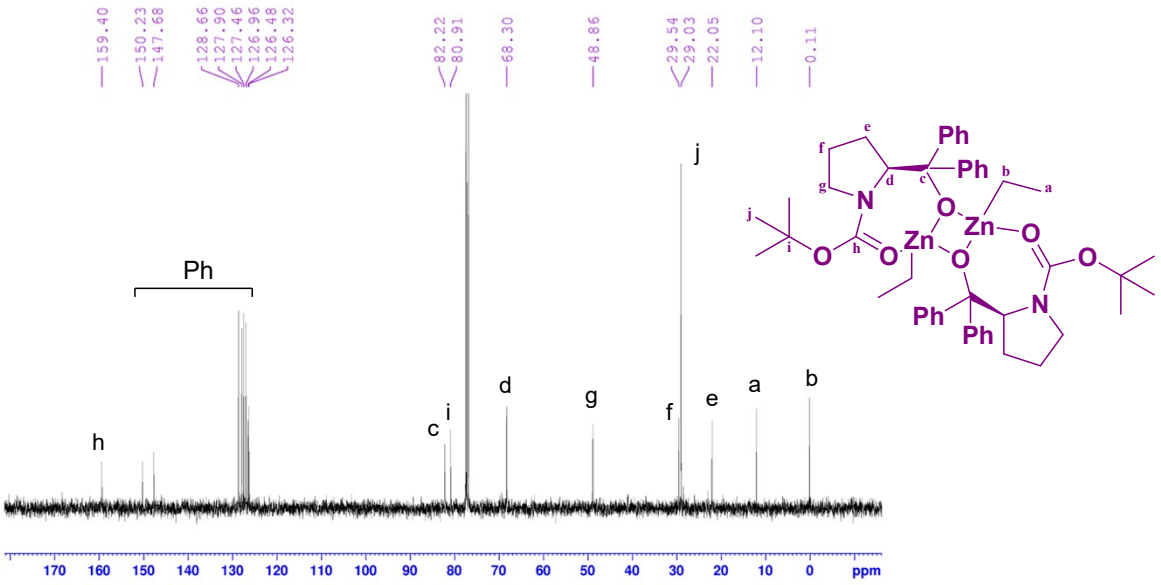

Fig. S2. ^{13}C NMR spectrum of **1** in $CDCl_3$ (300 K).

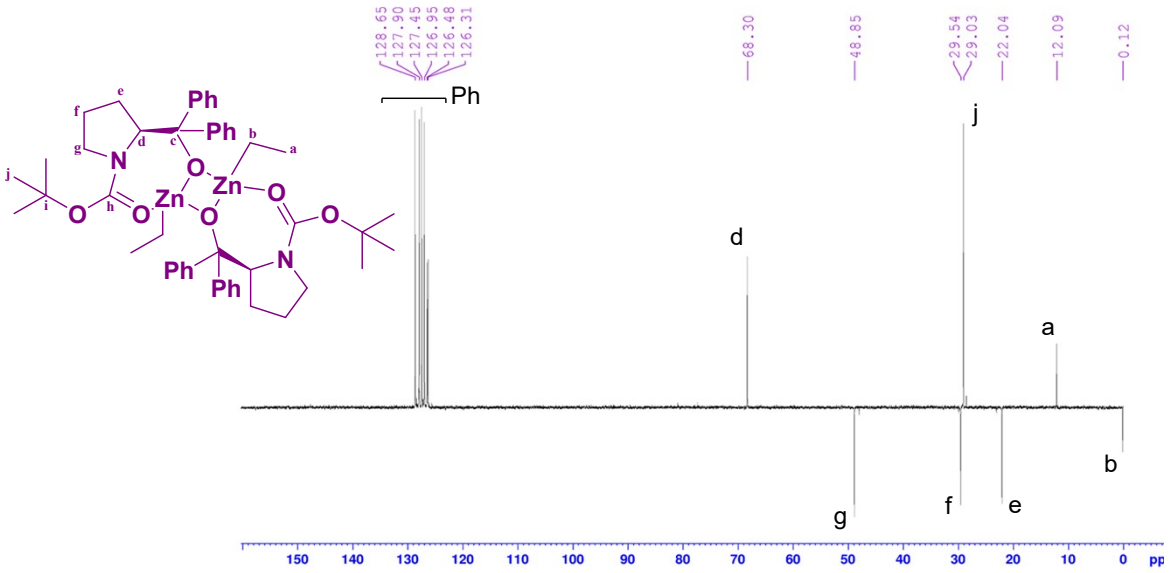

Fig. S3. ^{13}C DEPT NMR spectrum of **1** in $CDCl_3$ (300 K).

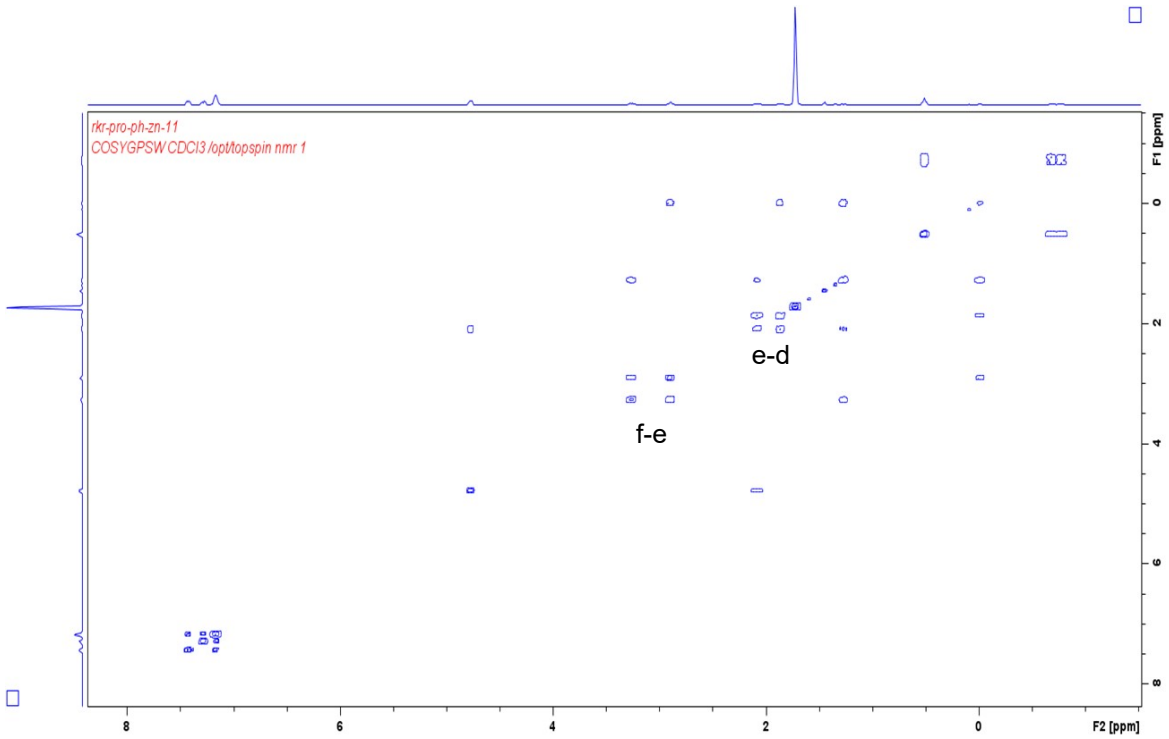

Fig. S4. ^{1}H-^{1}H COSY NMR spectrum of **1** in $CDCl_3$ (300 K).

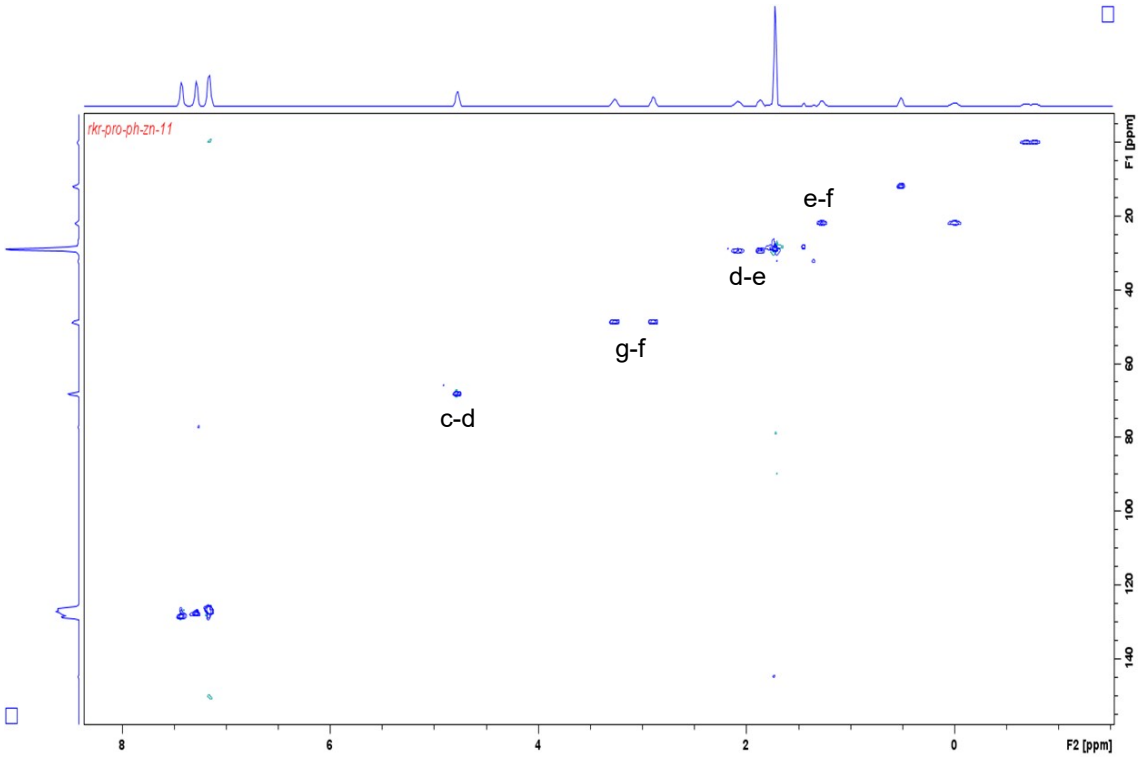

Fig. S5. ^{1}H-^{13}C HSQC NMR spectrum of **1** in $CDCl_3$ (300 K).

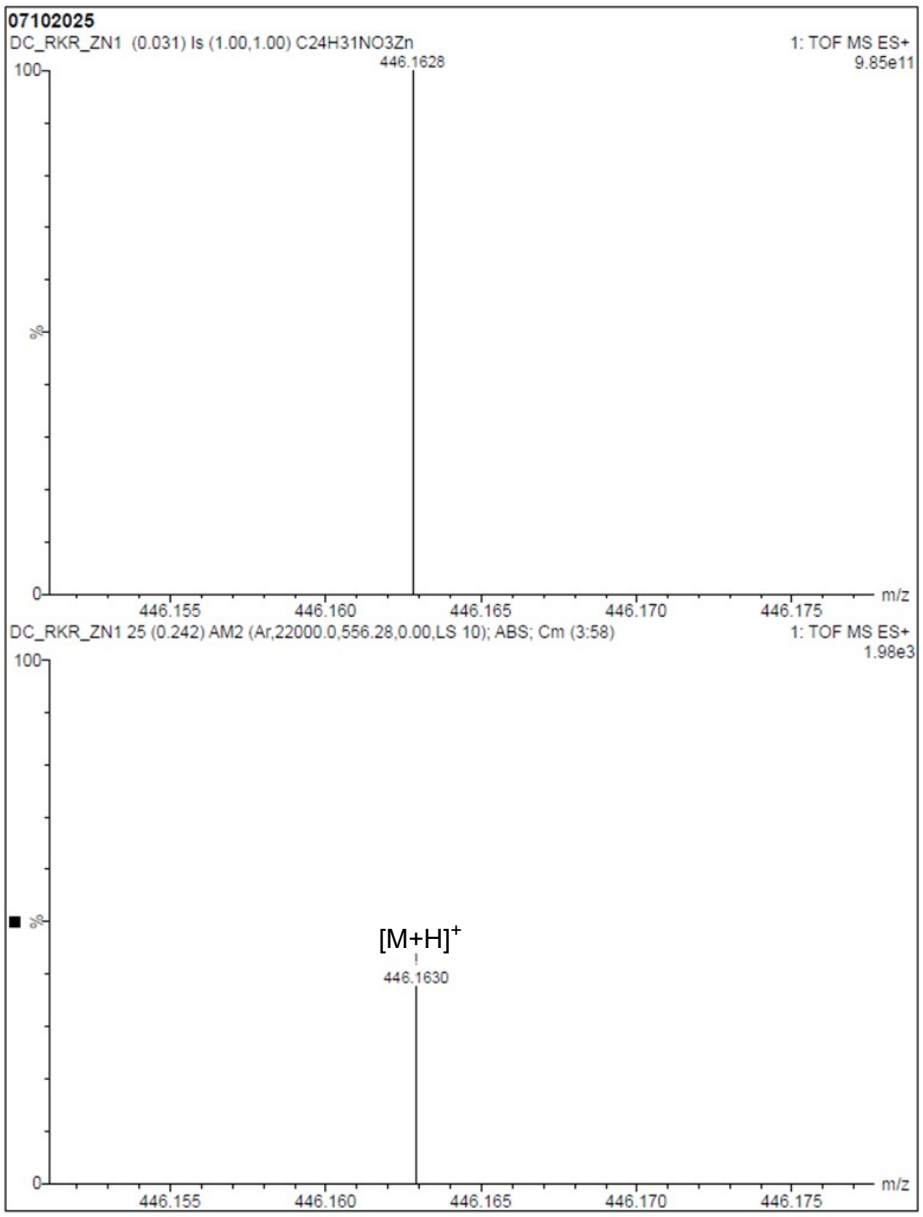

Fig. S6. Simulated (above) and experimental (below) ESI-MS spectrum of **1**

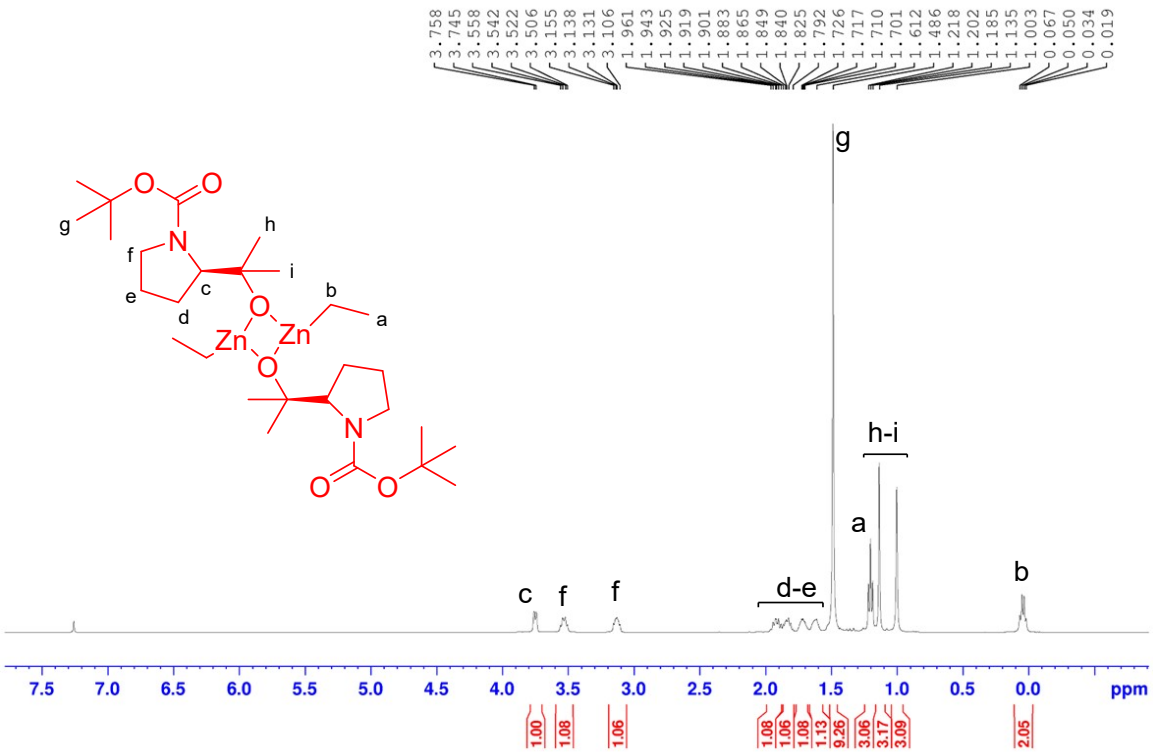

Fig. S7. ^{1}H NMR spectrum of **2** in $CDCl_3$ (300 K).

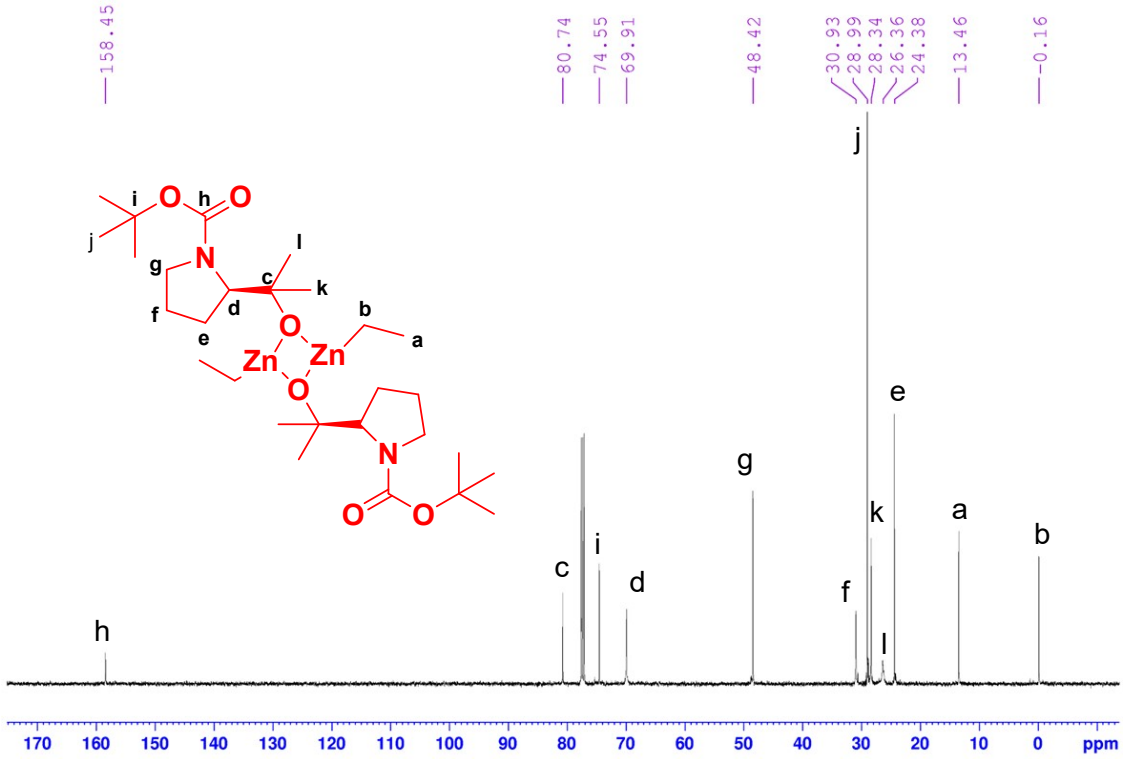

Fig. S8. ^{13}C NMR spectrum of **2** in $CDCl_3$ (300 K).

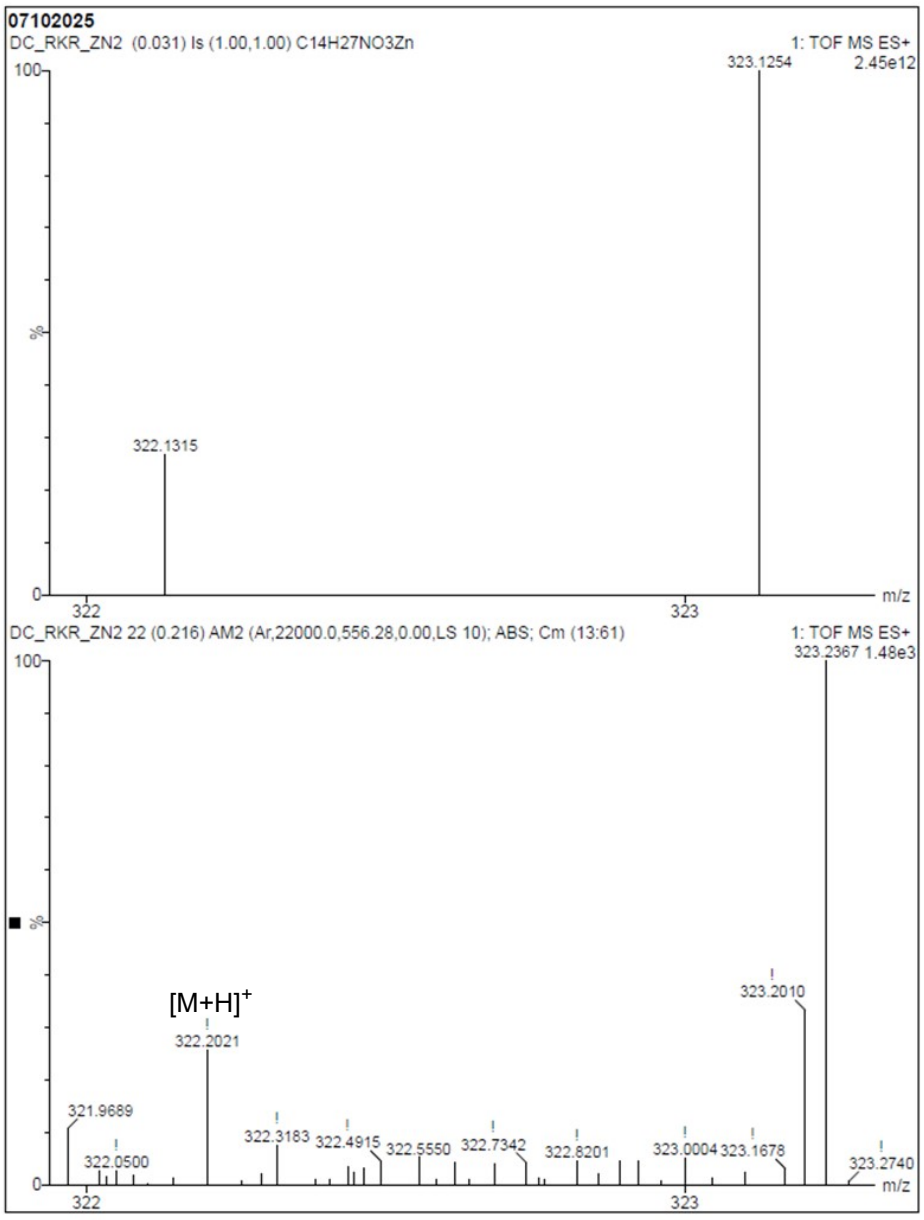

Fig. S9. Simulated (above) and experimental (below) ESI-MS spectrum of **2**

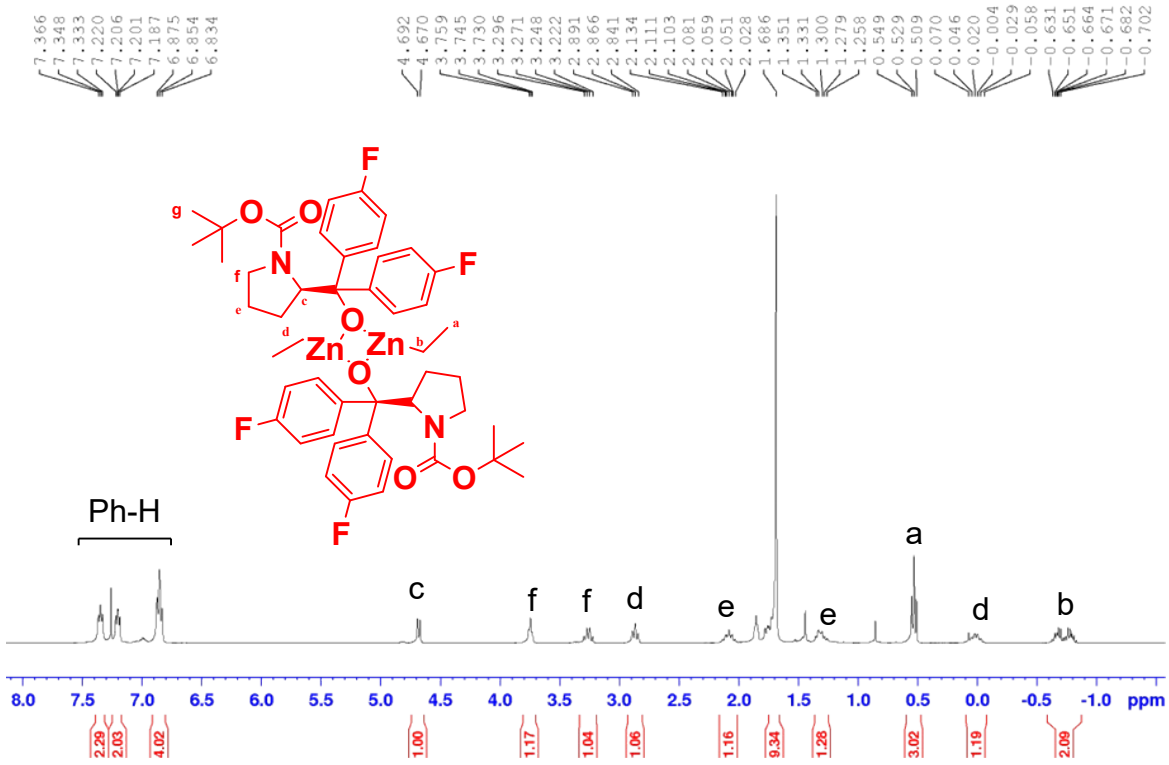

Fig. S10. ^{1}H NMR spectrum of **3** in $CDCl_3$ (300 K).

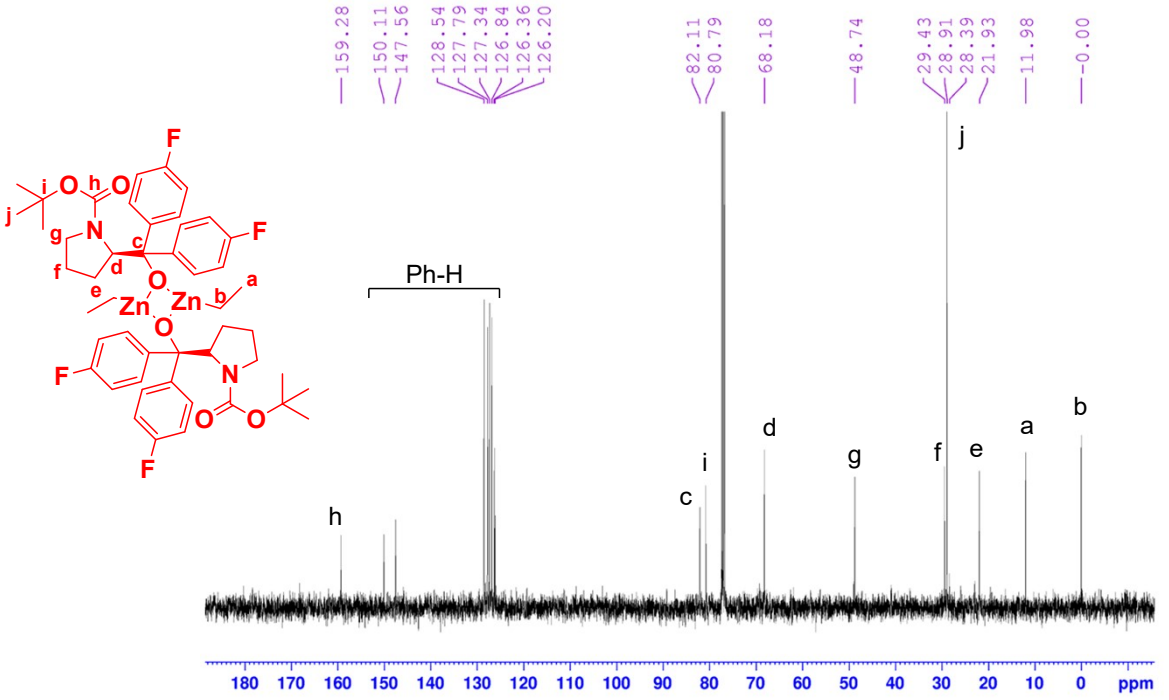

Fig. S11. ^{13}C NMR spectrum of **3** in $CDCl_3$ (300 K).

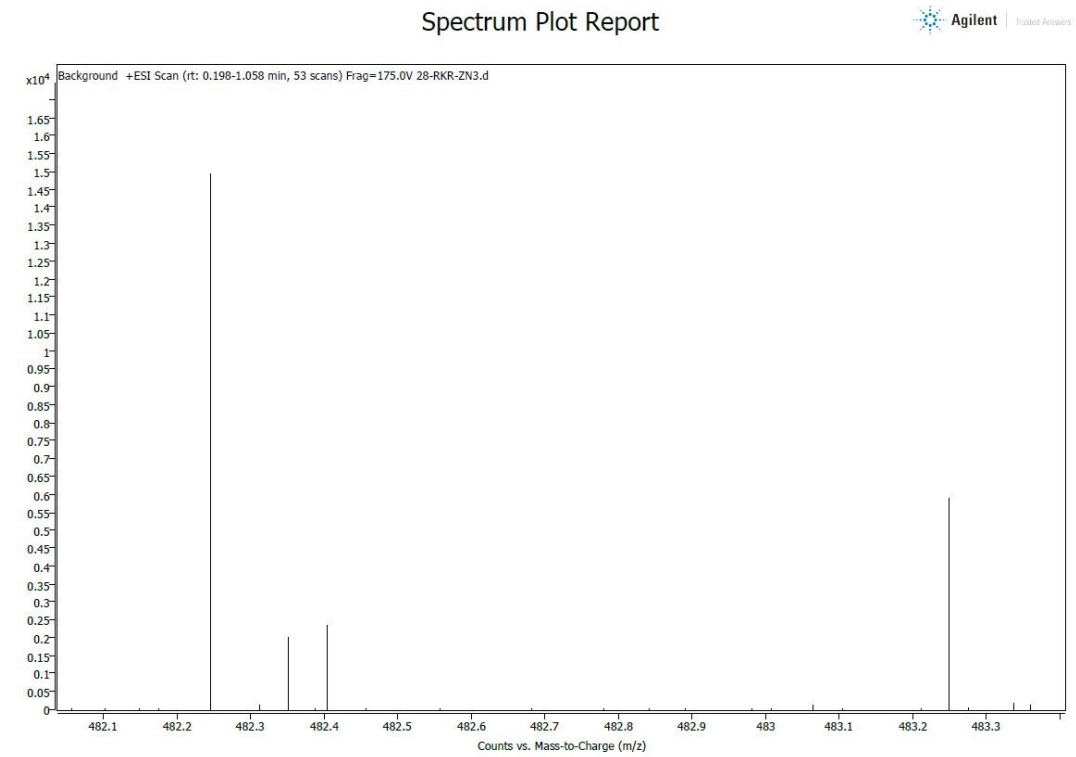

Fig. S12. ESI-MS spectrum of **3.**

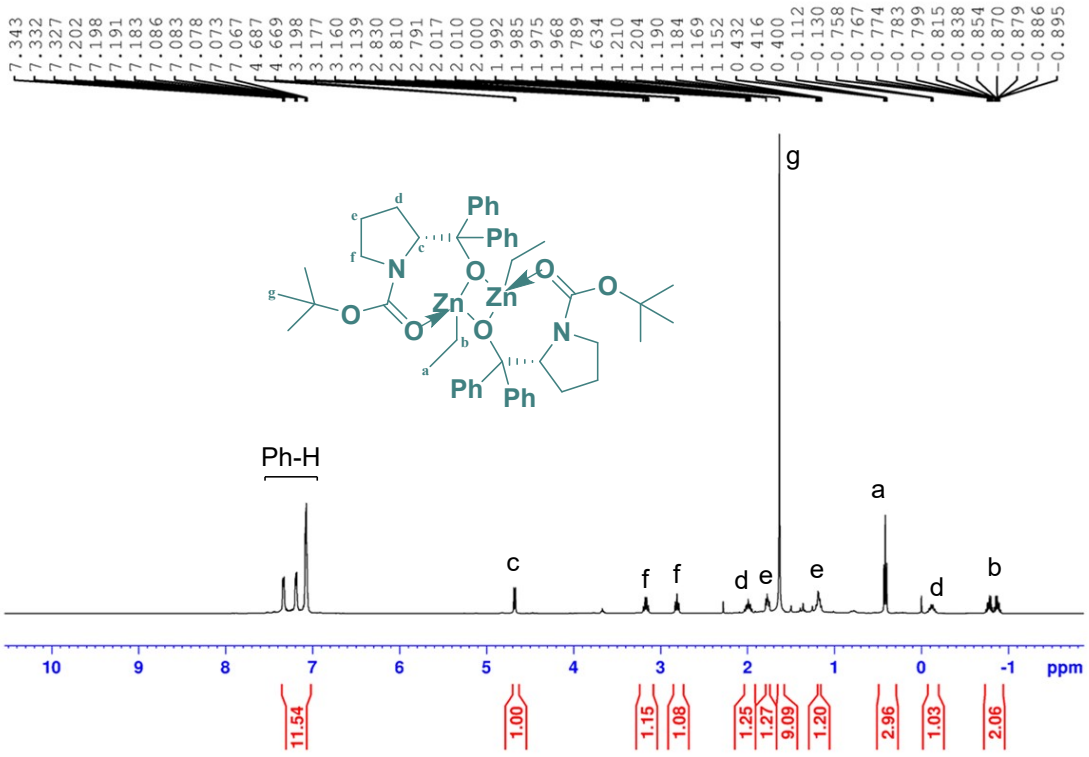

Fig. S13. ^{1}H NMR spectrum of **4** in $CDCl_3$ (300 K).

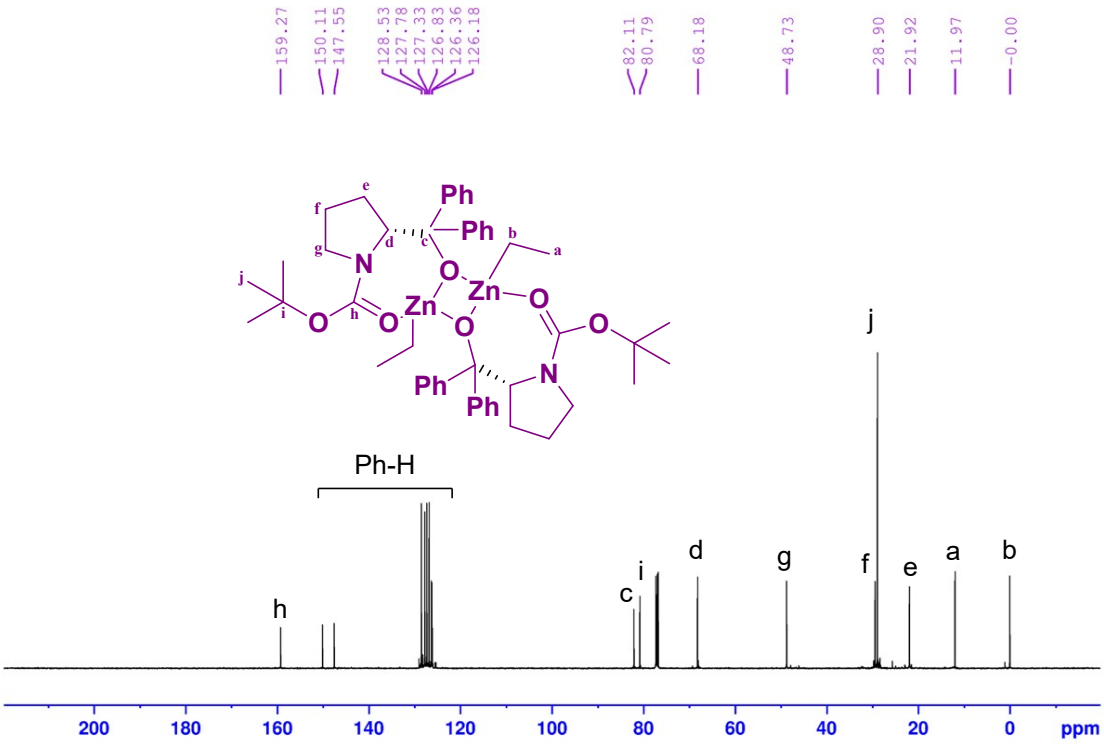

Fig. S14. ^{13}C NMR spectrum of **4** in $CDCl_3$ (300 K).

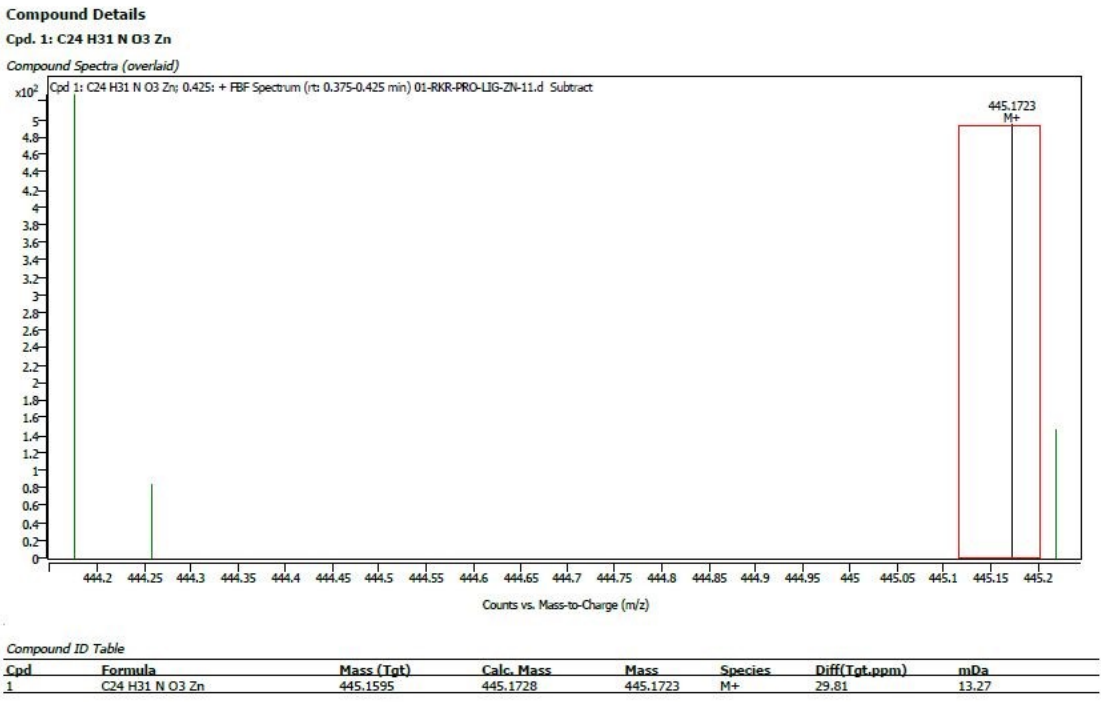

Fig. S15. HRMS of **4**.

DOSY

Diffusion-Ordered Spectroscopy (DOSY) experiments were conducted using a Bruker AVANCE III 500 MHz NMR spectrometer, operating at a proton resonance frequency of 499.9 MHz. The instrument was equipped with a z-gradient BBFO 5 mm tunable "SmartProbe™" and a GRASP II gradient accessory capable of delivering a maximum gradient strength of 53.5 G/cm (5.35 G/cmA).Data acquisition was performed using the Bruker pulse sequence ledbpgp2s. The spectral width was set to 5500 Hz, centered at 4.5 ppm, with 32,768 data points collected per scan. A relaxation delay of 12 s was applied to ensure complete longitudinal relaxation. The diffusion delay (Δ) was set to 100 ms, and the longitudinal eddy current delay (LED) was 5 ms.Bipolar gradient pulses (δ/2) of 2.2 ms duration were employed, along with homospoil gradient pulses of 0.6 ms. The gradient strengths for the homospoil pulses were set to −17.13% and −13.17%, respectively. A total of 32 gradient increments were recorded, starting from 5% gradient strength in the first increment and linearly increasing to 95% in the final increment. All gradient pulses were shaped using the smooth-square SMSQ10.100 profile, with a recovery delay of 200 μs following each gradient application.Each increment was acquired with 24 scans, utilizing a single stimulated echo sequence with two spoiling gradients. Data processing and generation of DOSY plots were performed using the DOSY module in Bruker TopSpin software. Diffusion coefficients were extracted by fitting the signal intensities to the Stejskal–Tanner equation.[S6] Molecular weights were estimated using the Stokes–Einstein Gierer–Wirtz Estimation (SEGWE) method.[S7]

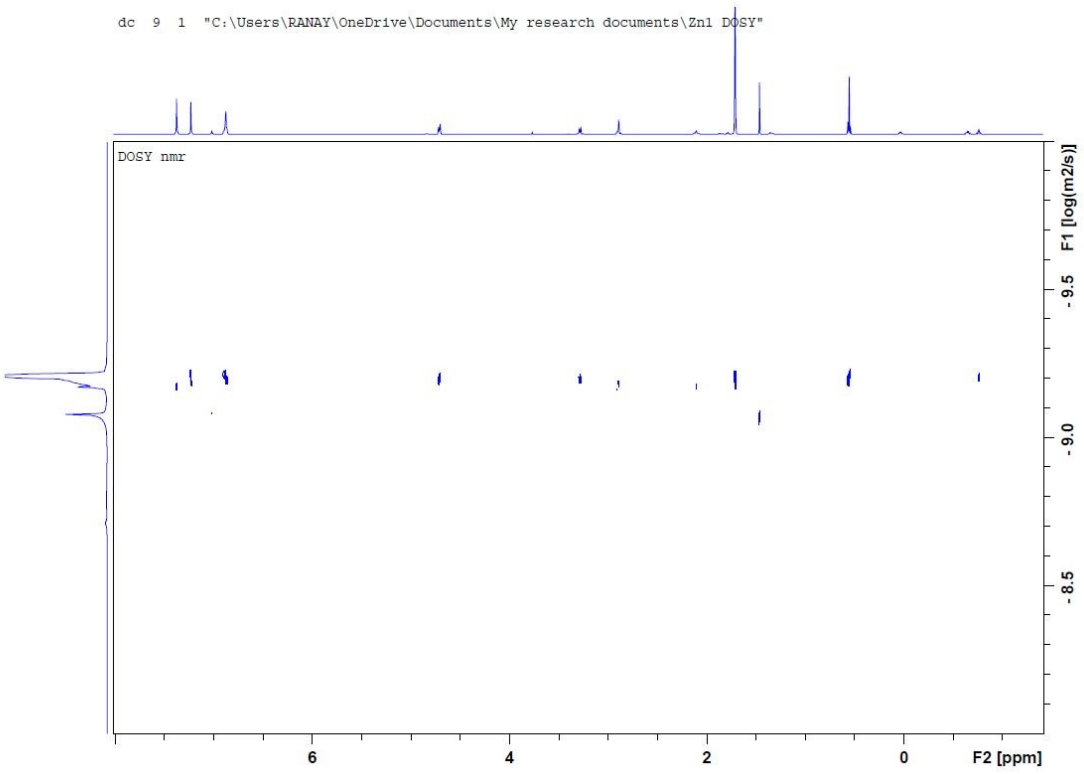

Fig. S16. DOSY NMR spectrum of **1** in $CDCl_3$ at r.t.

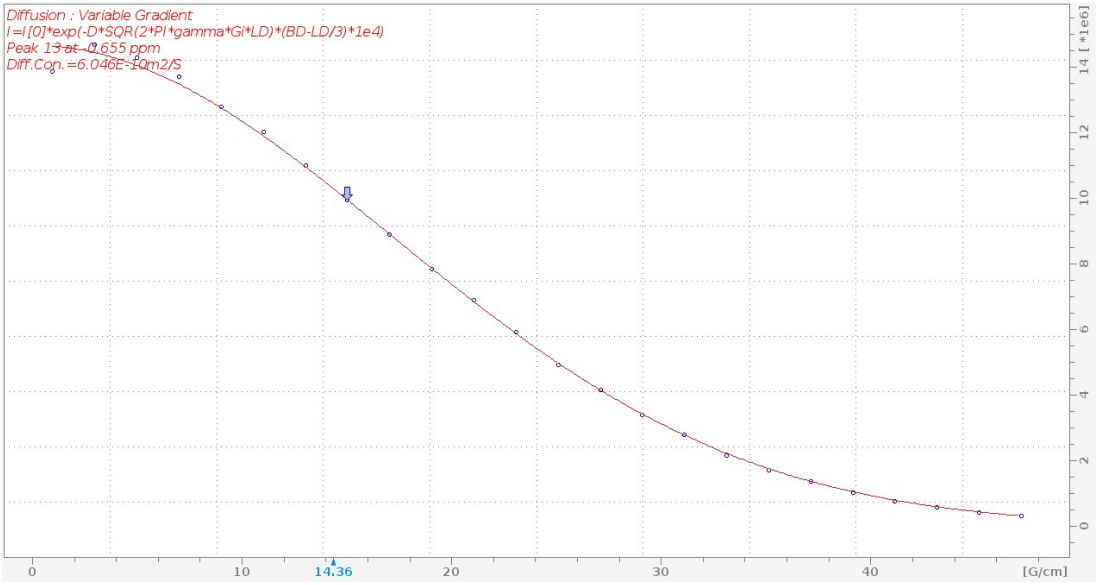

Fig. S17. DOSY fitting curve of **1** at r.t.

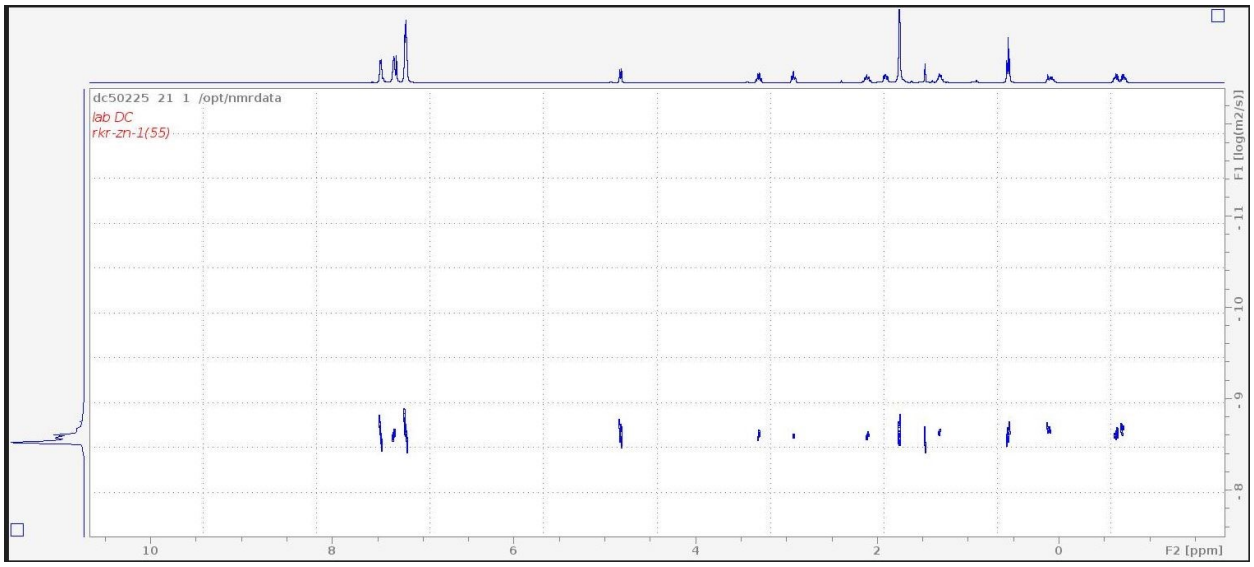

Fig. S18. DOSY NMR spectrum of **1** in $CDCl_3$ at 57 °C.

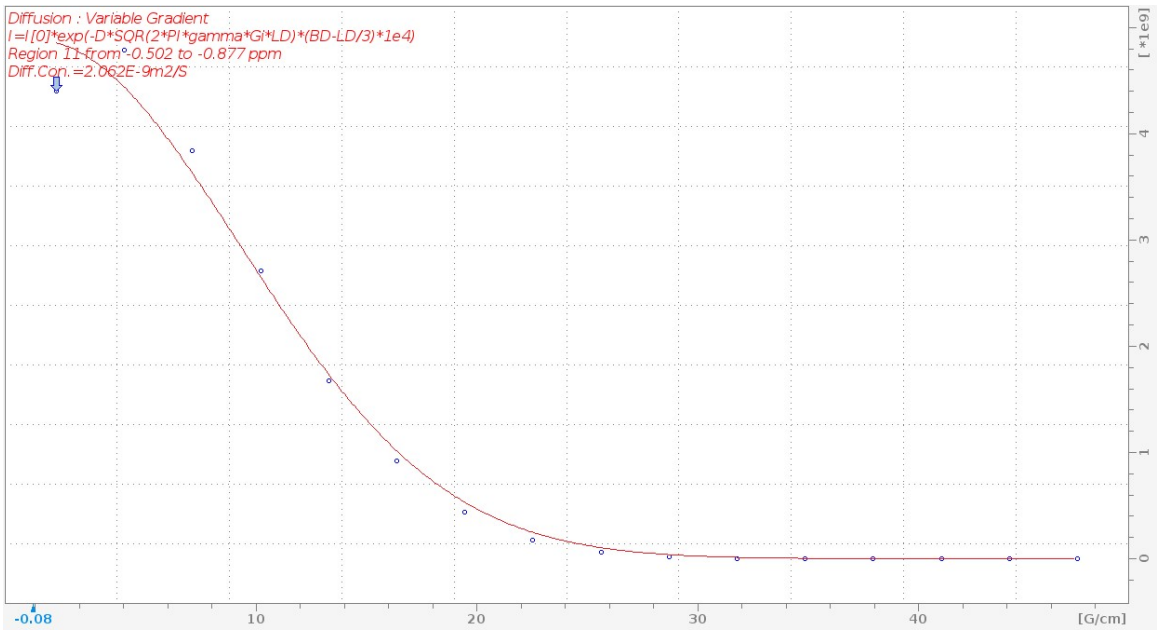

Fig. S19. DOSY fitting curve of **1** at 57 ºC.

Table S1. Crystallographic data and details of refinement for complexes **1** and **3.**

Compounds	**1**	**3**
Molecular formula	$C_{55}H_{70}N_2O_6Zn_2$	$C_{48}H_{58}F_4N_2O_6Zn_2$
Formula weight	985.87 g/mol	965.70 g/mol
T/K	150(2)	100(2)
Wavelength (Å)	0.71073	0.71073
Crystal system,	Trigonal	Orthorhombic
Space group	$P3_2$	$P2_12_12_1$
a/ Å	11.6080(4)	11.1571(4)
b/ Å	11.6080(4)	20.5403(9)
c/ Å	33.2403(16)	20.6397(7)
α (°)	90.00	90
β (°)	90.00	90
γ (°)	120.00	90
V/ Å^3	3878.9(3)	4730.0(3)
Z, Calculated density (Mg/m^3)	3, 1.266	4, 1.356
Absorption coefficient(mm^{-1})	0.977	1.078
θ range/°	2.026 to 28.287	3.342 to 28.304
Reflections collected	89516	78349
Unique Independent reflections	12794 [R(int) = 0.0449]	11741 [R(int) = 0.0557]
Data/restraints/parameters	12794 / 610 / 662	11741 / 0 / 560
Goodness-of-fit on F2	1.226	1.021
Final R indices [$I>2\sigma(I)$]	$R1$ = 0.0534, $wR2$ = 0.1162	$R1$ = 0.0280, $wR2$ = 0.0627
R indices (all data)	$R1$ = 0.0560, $wR2$ = 0.1172	$R1$ = 0.0339, $wR2$ = 0.0650
Max. and min. transmission	0.7457 and 0.6941	0.7457 and 0.5393

$R_1 = \sum||F_o| - |F_c||/\sum|F_o|$, $wR_2 = [\sum (F_o^2 - F_c^2)^2/\sum w(F_o^2)^2]^{1/2}$

Complex **3** crystallized in orthorhombic crystal system with space group $P2_12_12_1$. One full molecule of the complex **3** is present in the asymmetric unit of the crystal lattice. Whereas, the complex **1** crystallized in trigonal crystal system with space group $P3_2$. The asymmetric unit of the crystal lattice of complex **1** consists of one complex molecule and one molecule of toluene solvent. The solvent molecule is disordered in the lattice in the ratio of 57: 43 by 180-degree rotation. DFIX restraint was used to attain target bond distances of 1.53 Å for C-C bonds and 1.39 Å for aromatic C-C bonds in toluene. Anisotropic displacement parameters (Uij) of atoms in the disordered groups were restrained to be equal using SIMU restraint with an effective standard deviation of 0.02 Å^2.

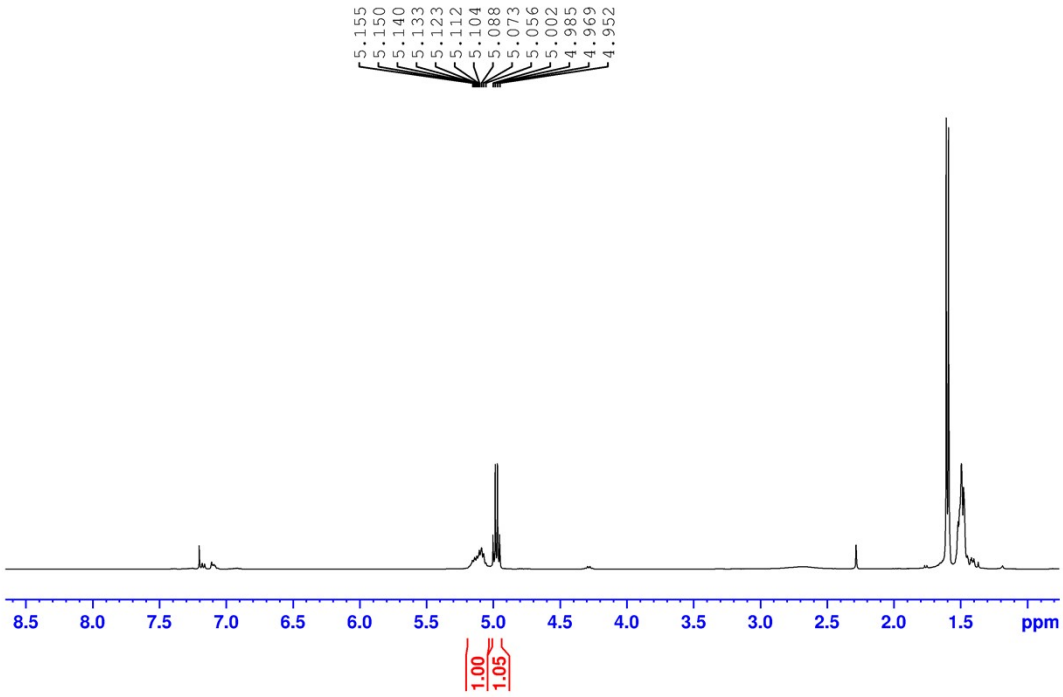

Fig. S20. ^{1}H NMR spectrum of crude PLA catalyzed by **1** ($CDCl_3$, 500 MHz).

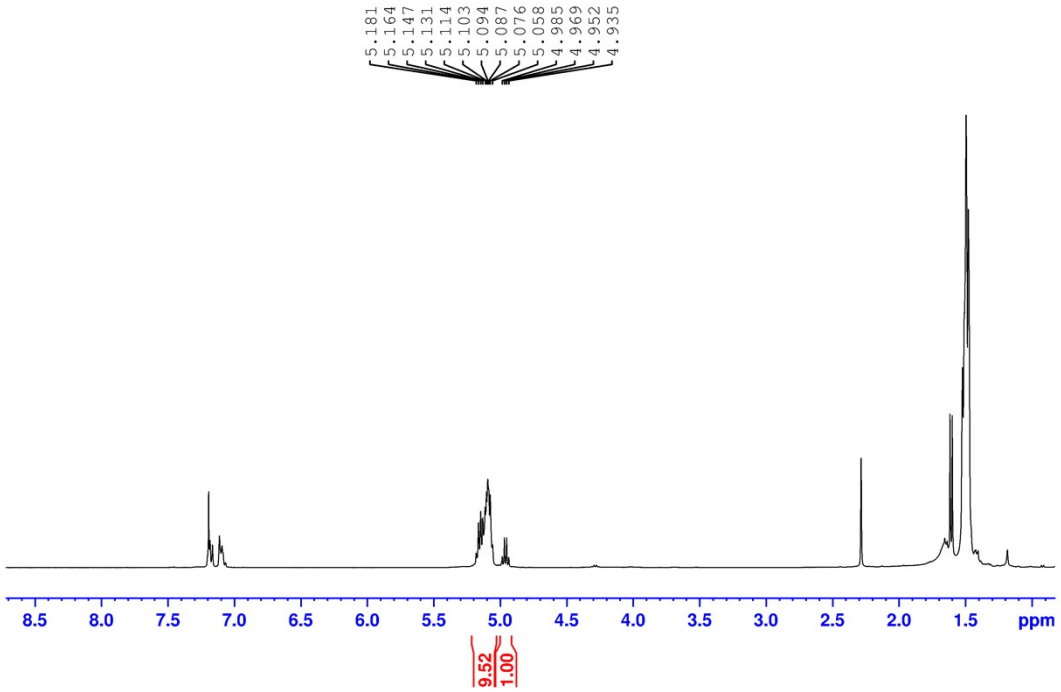

Fig. S21. ^{1}H NMR spectrum of crude PLA catalyzed by **2** ($CDCl_3$, 500 MHz).

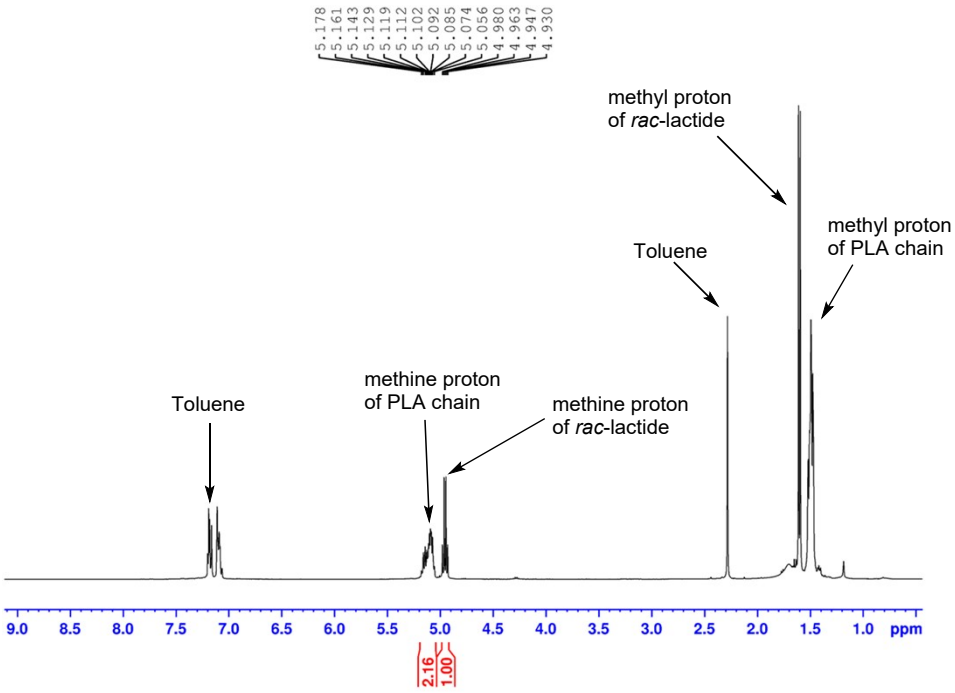

Fig. S22. ^{1}H NMR spectrum of crude PLA catalyzed by **3** ($CDCl_3$, 500 MHz).

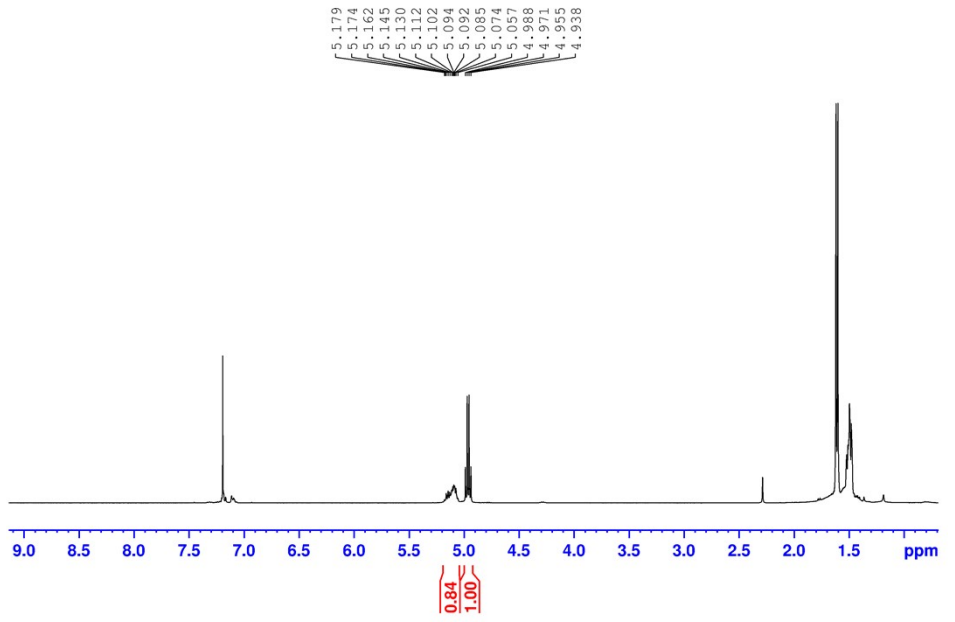

Fig. S23. ^{1}H NMR spectrum of crude PLA catalyzed by **4** ($CDCl_3$, 500 MHz).

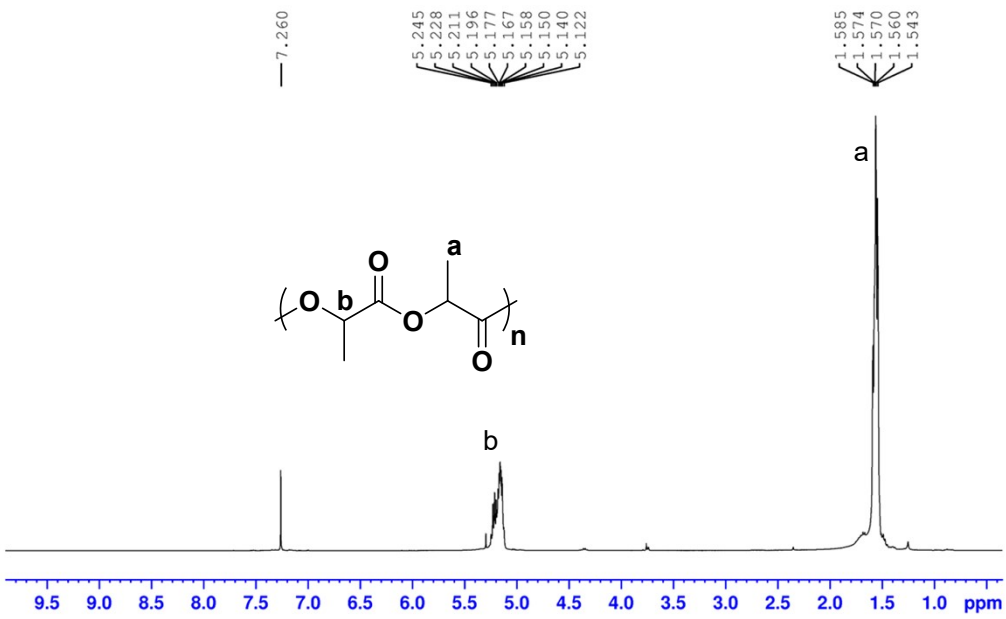

Fig. S24. ^{1}H NMR spectrum of pure PLA catalyzed by **2** ($CDCl_3$, 500 MHz).

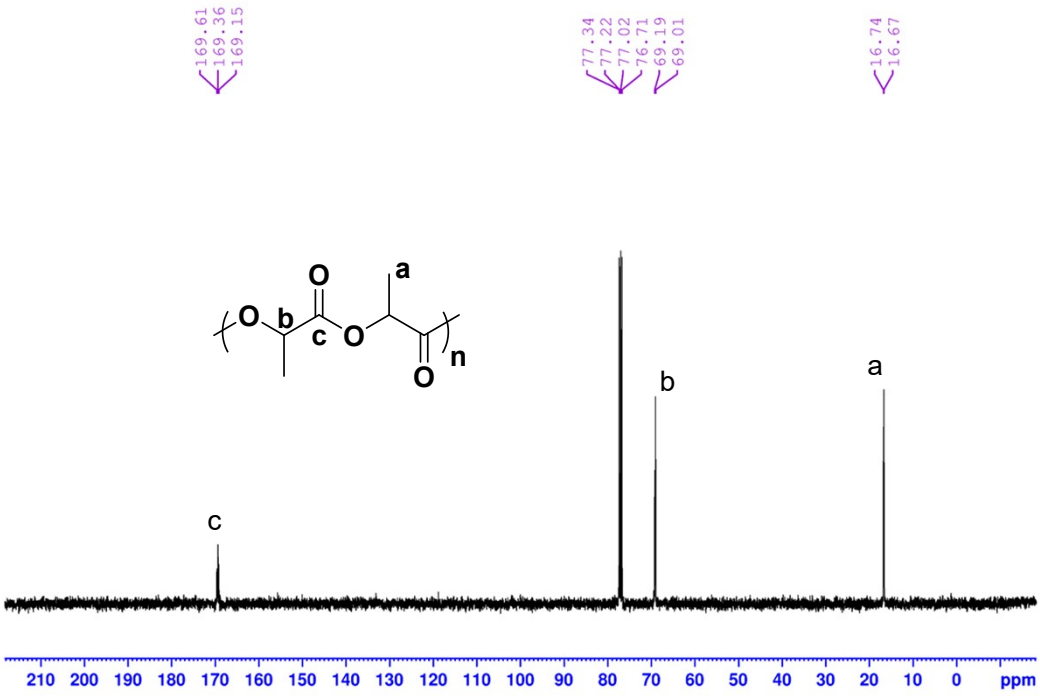

Fig. S25. ^{13}C NMR spectrum of pure PLA catalyzed by **2** ($CDCl_3$, 500 MHz).

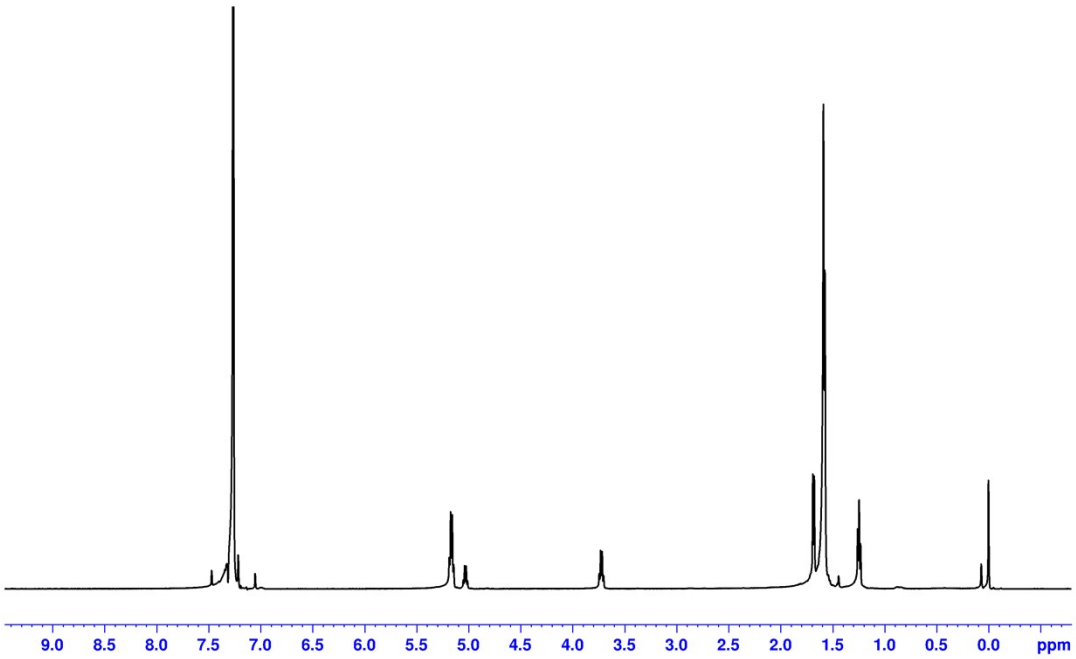

Fig. S26. ^{1}H NMR spectrum of crude PLLA catalyzed by **2** ($CDCl_3$, 500 MHz).

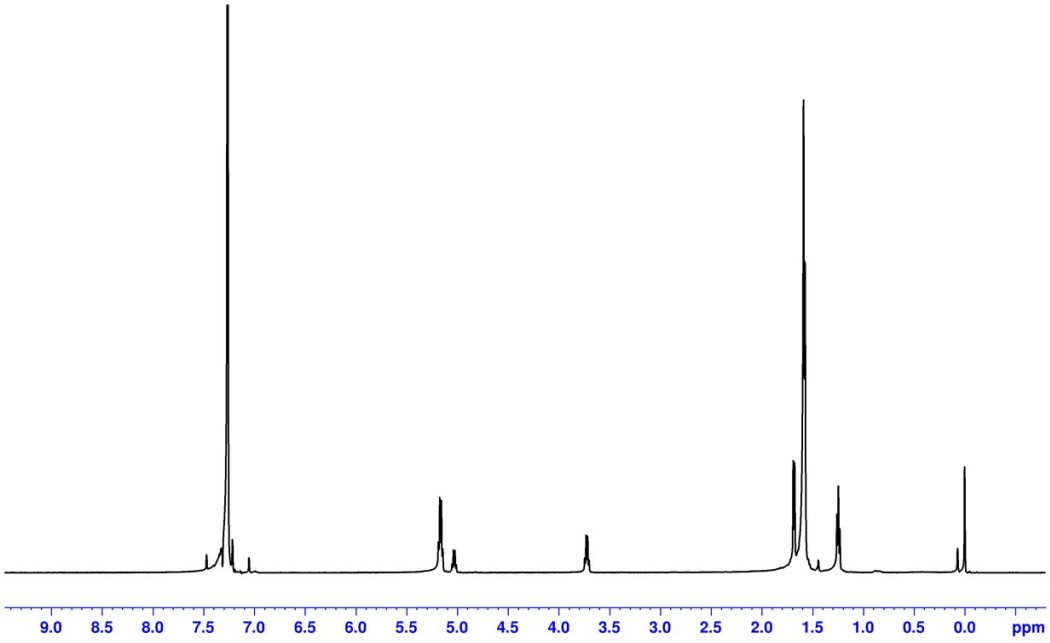

Fig. S27. ^{1}H NMR spectrum of crude PLLA catalyzed by **3** ($CDCl_3$, 500 MHz).

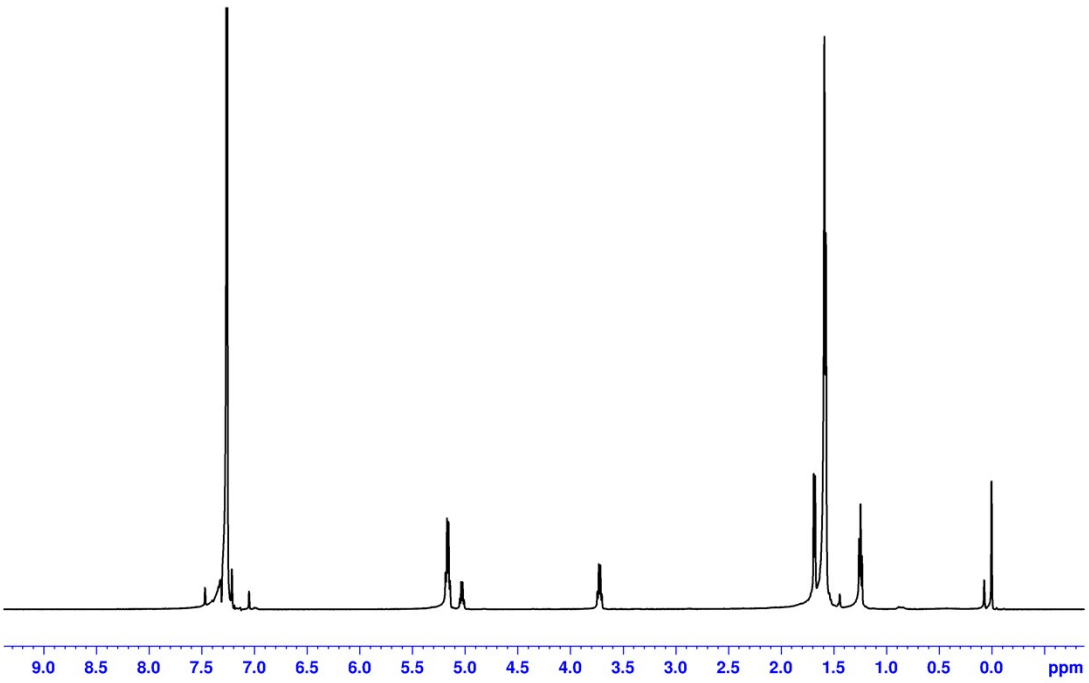

Fig. S28. ^{1}H NMR spectrum of crude PLLA catalyzed by **4** ($CDCl_3$, 500 MHz).

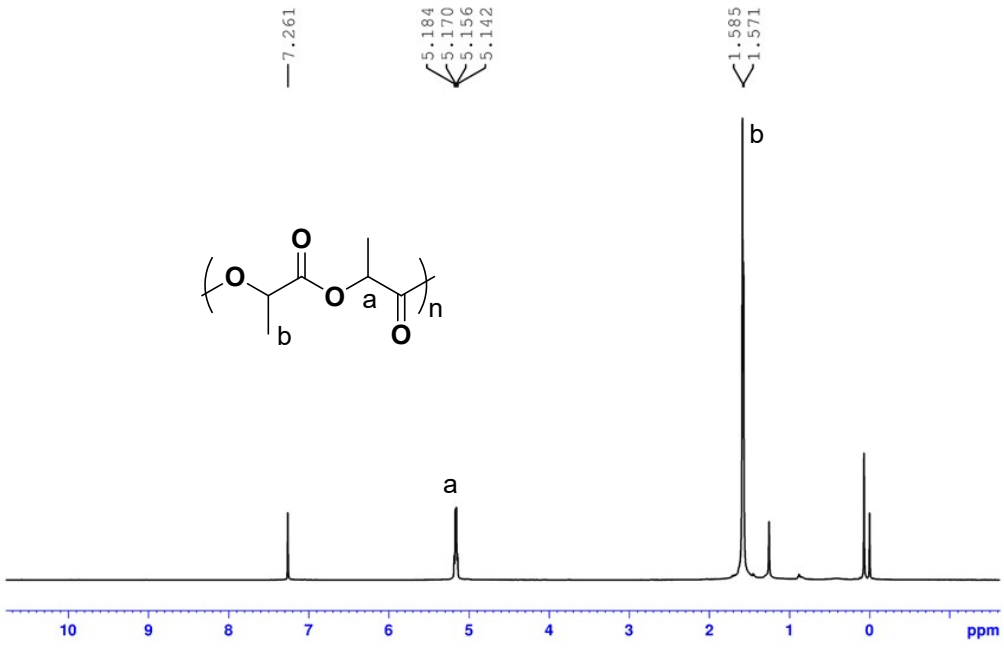

Fig. S29. ^{1}H NMR spectrum of pure PLLA catalyzed by **2** ($CDCl_3$, 500 MHz).

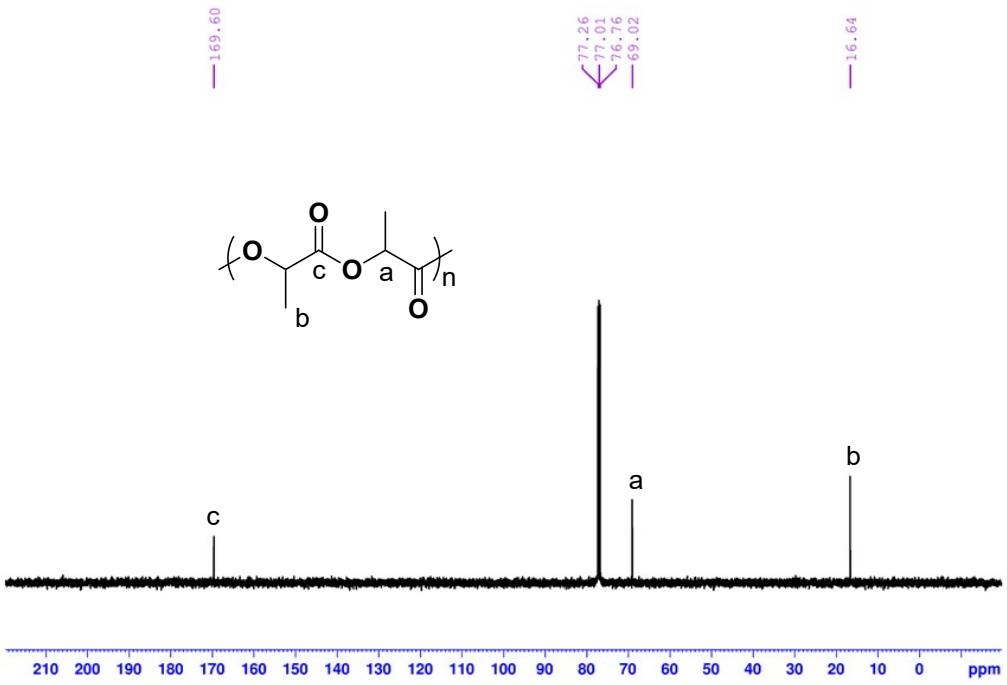

Fig. S30. ^{13}C NMR spectrum of pure PLLA catalyzed by **2** ($CDCl_3$, 500 MHz).

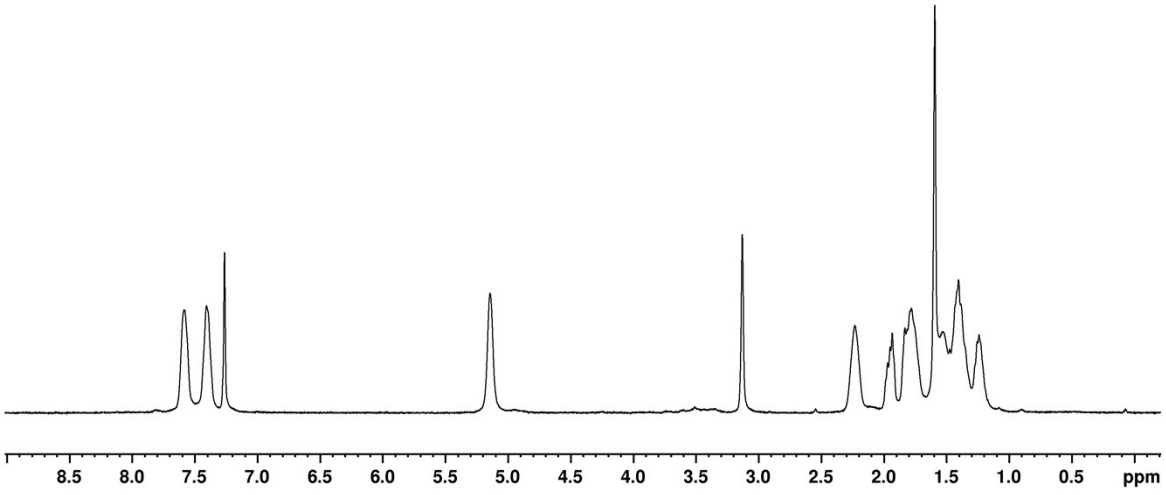

Fig. S31. ^{1}H NMR ($CDCl_3$) spectrum of the crude polyester of CHO/PA with **2**/PPNCl in neat condition (Table 3, Entry 6).

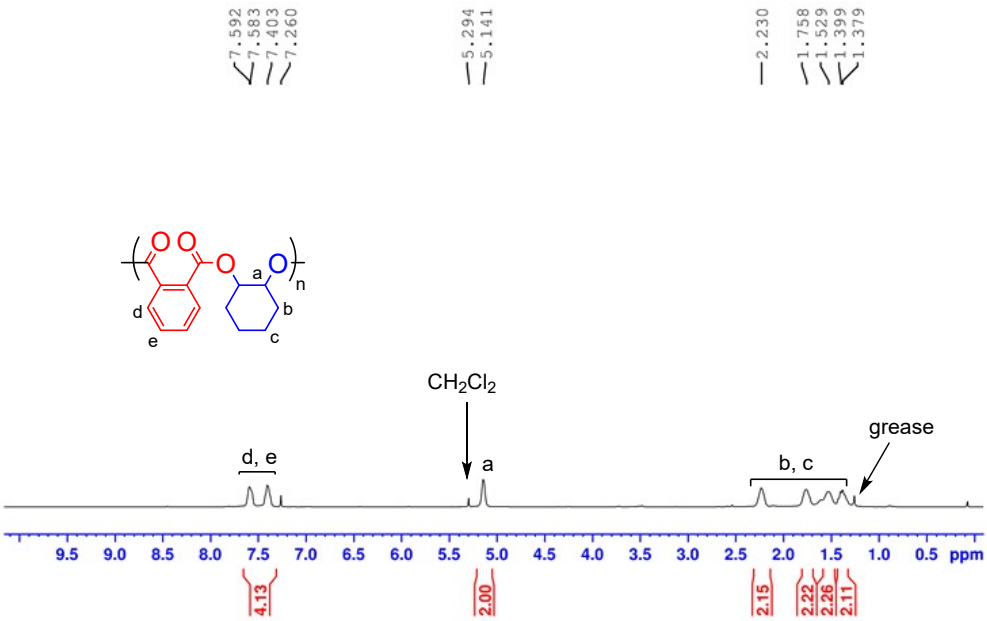

Fig. S32. ^{1}H NMR ($CDCl_3$) spectrum of poly(PA-*alt*-CHO) synthesized from CHO/PA/**2**/PPNCl (Table 3, Entry 6).

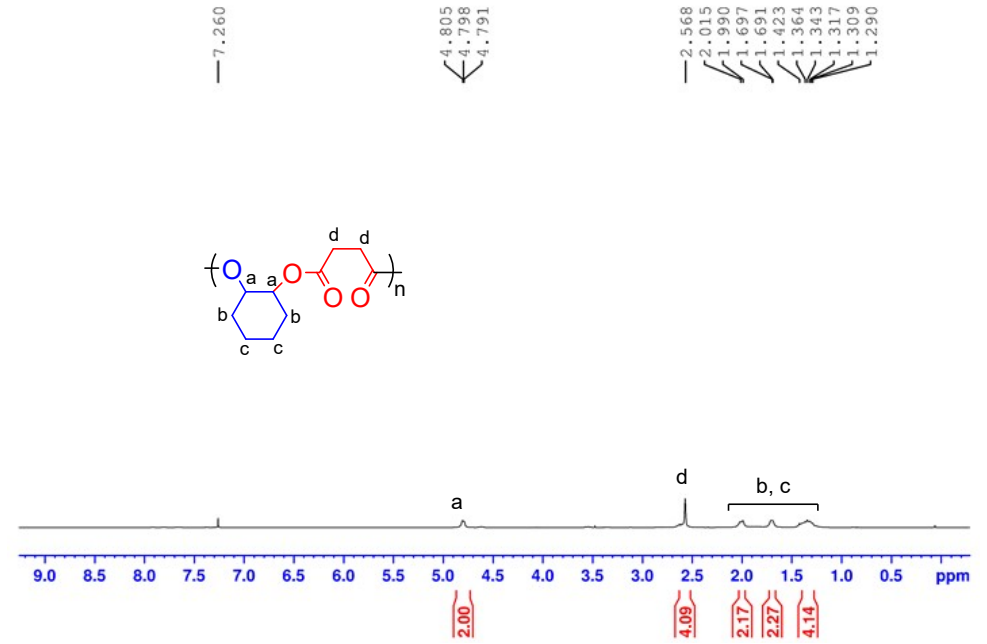

Fig. S33. ^{1}H NMR ($CDCl_3$) spectrum of poly(SA-*alt*-CHO) synthesized from CHO/SA/**2**/PPNCl (Table 4, Entry 1).

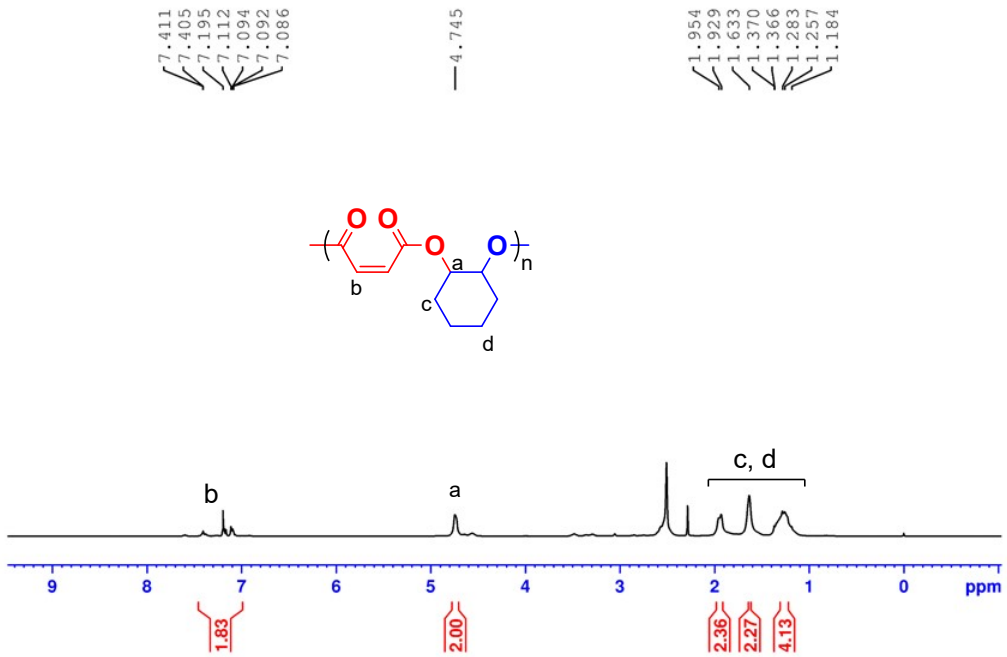

Fig. S34. ^{1}H NMR ($CDCl_3$) spectrum of poly(MA-*alt*-CHO) synthesized from CHO/MA/**2**/PPNCl (Table 4, Entry 2).

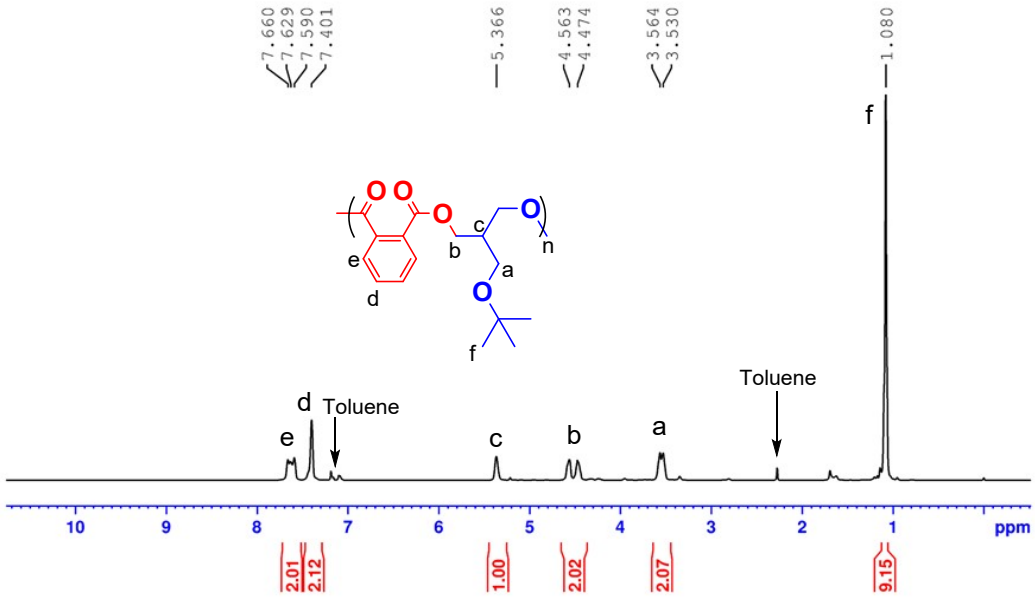

Fig. S35. ^{1}H NMR ($CDCl_3$) spectrum of poly(PA-*alt*-^{t}BGE) synthesized from ^{t}BGE/PA/**2**/PPNCl (Table 4, Entry 4).

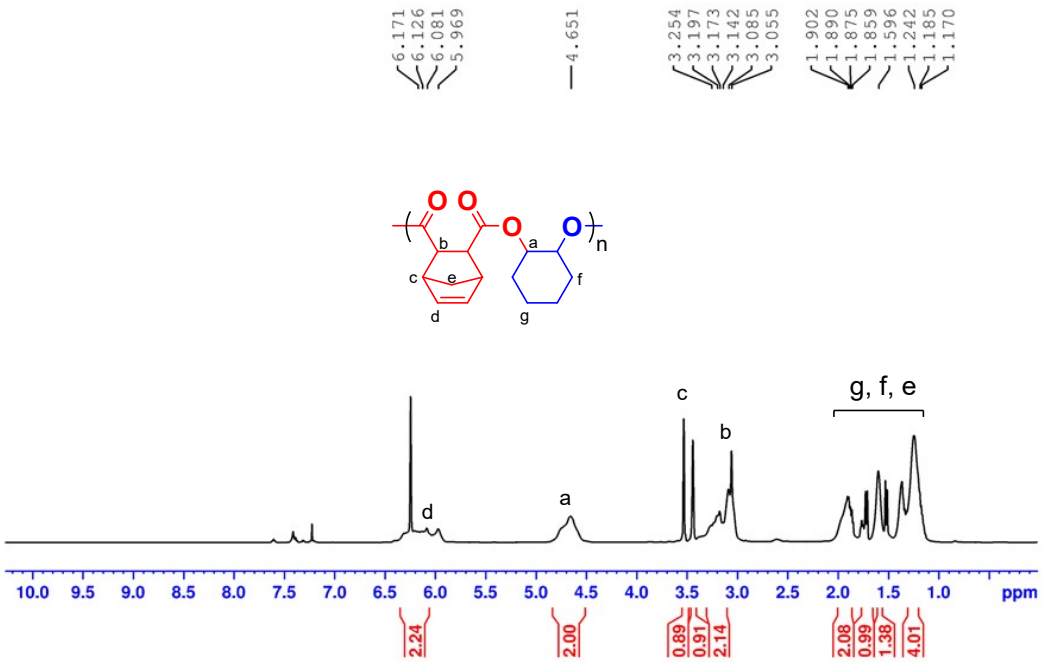

Fig. S36. ^{1}H NMR ($CDCl_3$) spectrum of poly(NDA-*alt*-CHO) synthesized from CHO/NDA/**2**/PPNCl (Table 4, Entry 3).

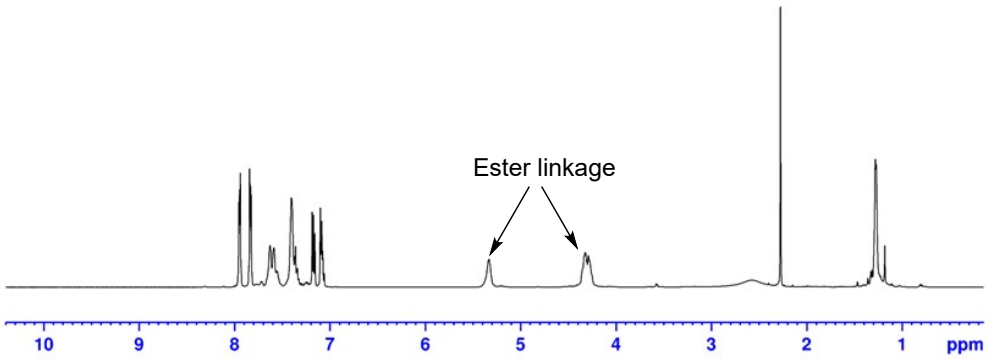

Fig. S37. ^{1}H NMR ($CDCl_3$) spectrum of the crude polyester of PO/PA with **2**/PPNCl in neat condition (Table 4, Entry 5).

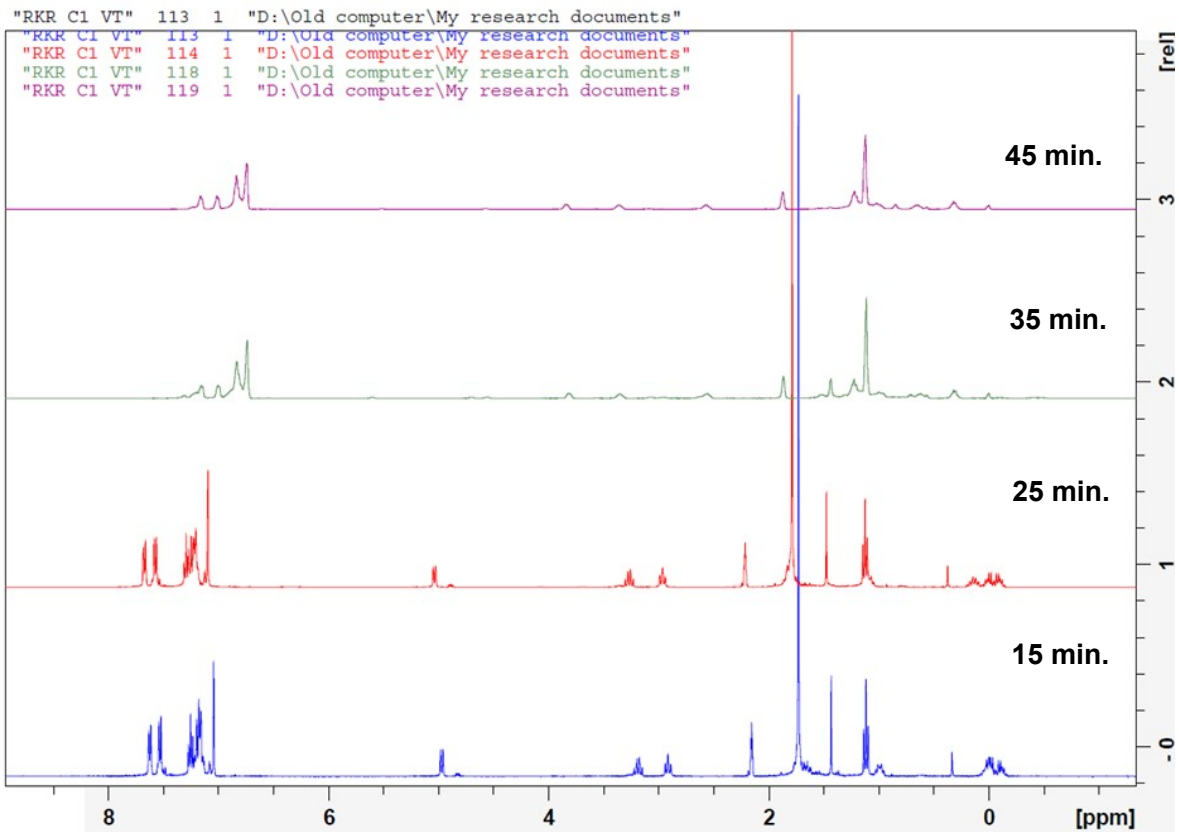

Fig. S38. Stacked ^{1}H NMR spectrum of complex **1** in toluene at 100 ^{o}C in different time intervals

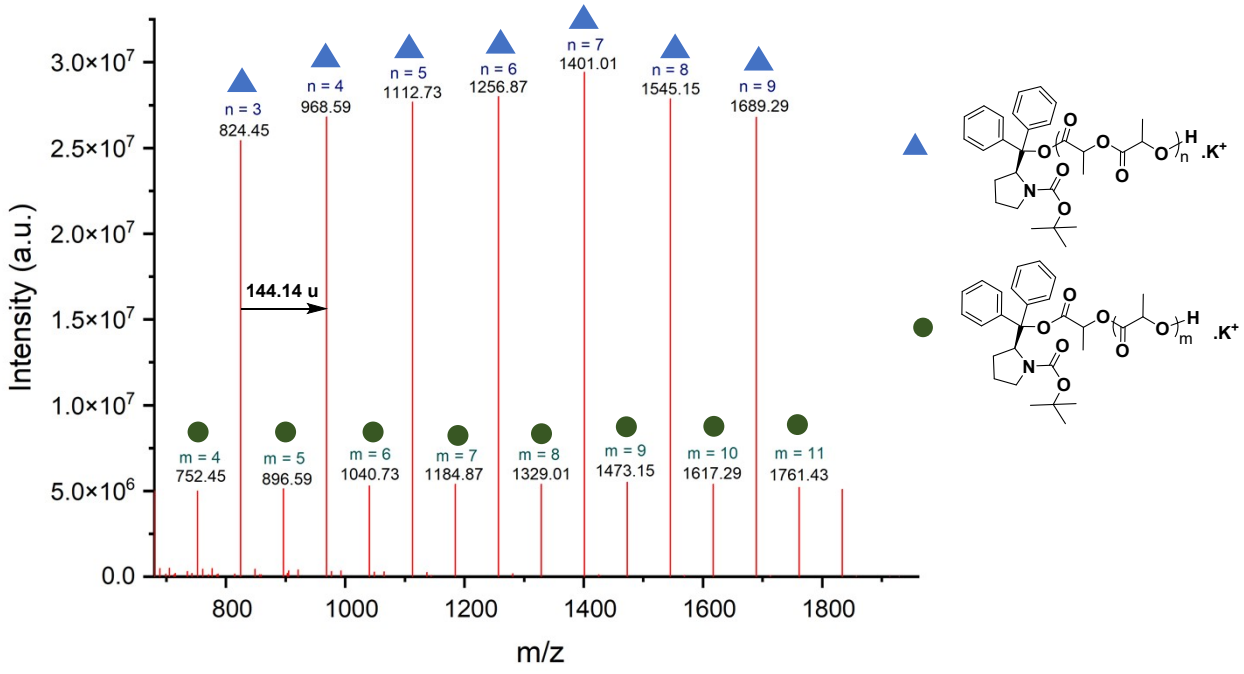

Fig. S39. MALDI-TOF spectrum of oligomer prepared from *rac*-LA using **1**.

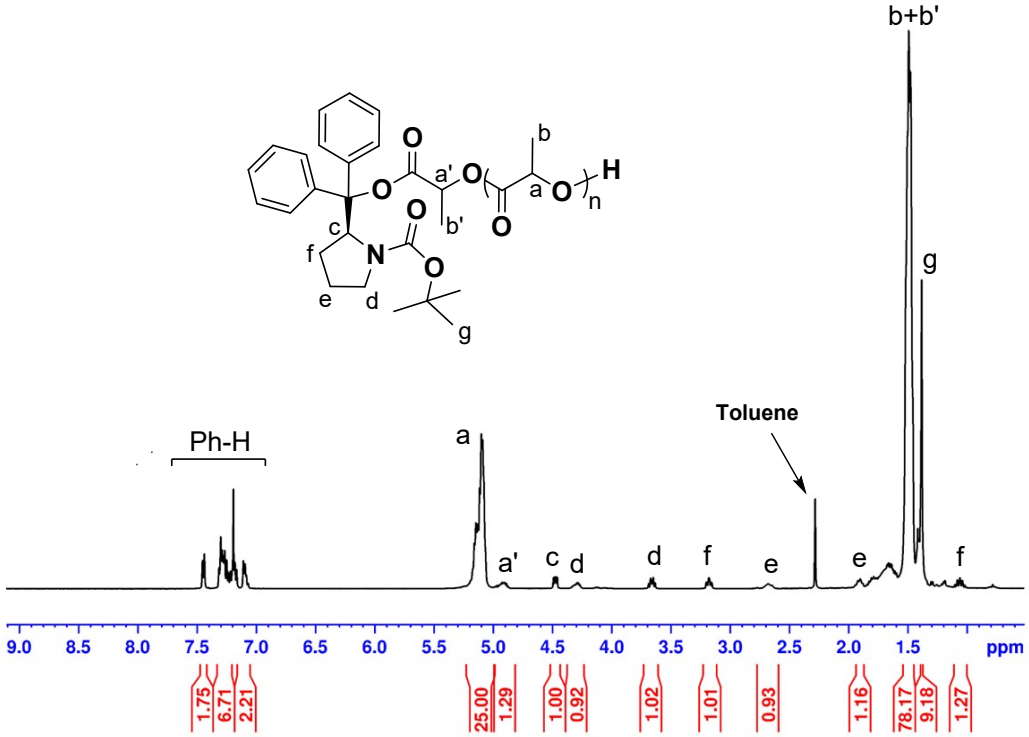

Fig. S40. ^{1}H NMR spectrum ($CDCl_3$, 500 MHz) of oligomer prepared from *rac*-LA using **1**.

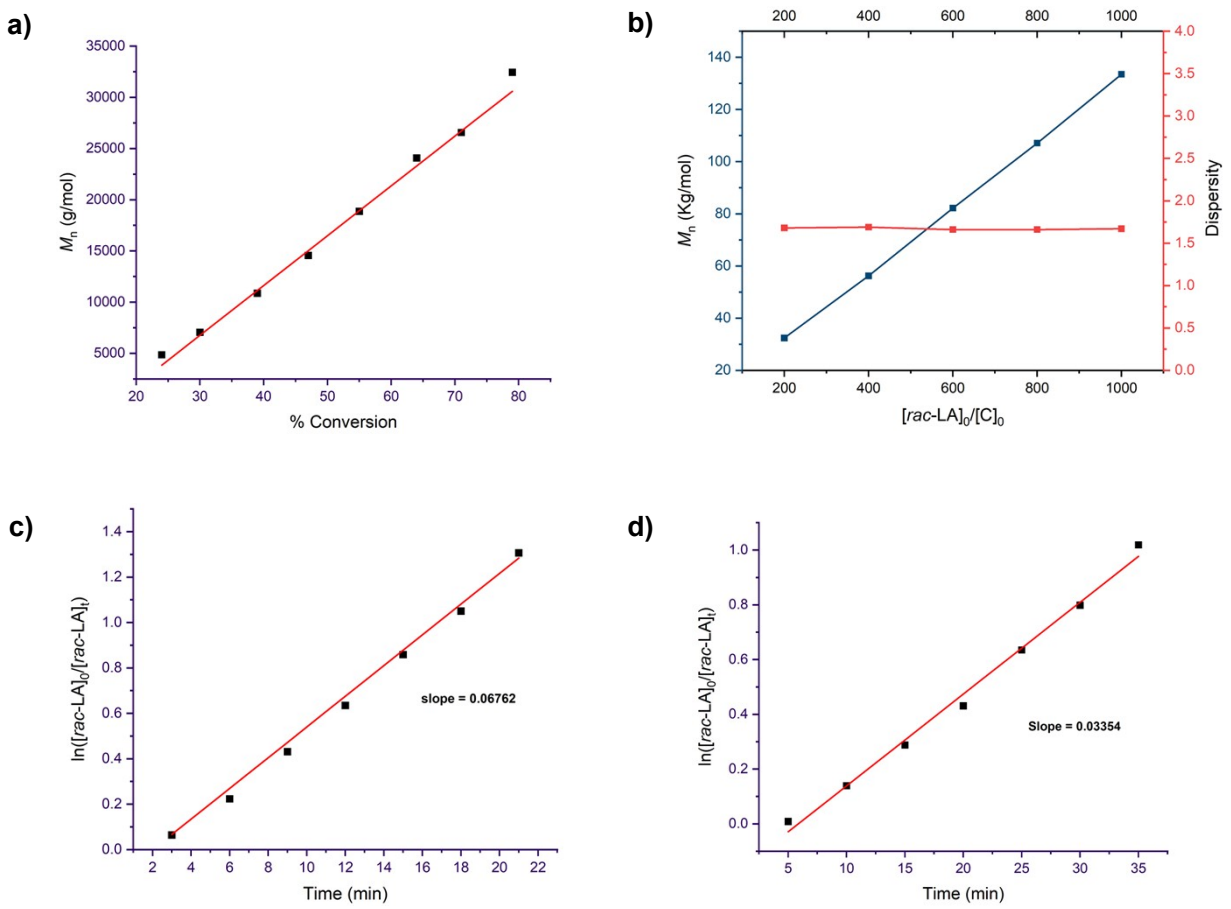

Fig. S41. a) Plot of M_n vs. % conversion for *rac*-LA polymerization with **1**. b) Plot of M_n and PDI vs. [Monomer]/[Zn catalyst] for *rac*-LA polymerization with **1**. c) Semi-logarithmic plot of *rac*-LA conversion with time initiated by **1**: $[\text{rac-LA}]_o/[C]_o = 200$. d) Semi-logarithmic plot of *rac*-LA conversion with time initiated by **4**: $[\text{rac-LA}]_o/[C]_o = 200$.

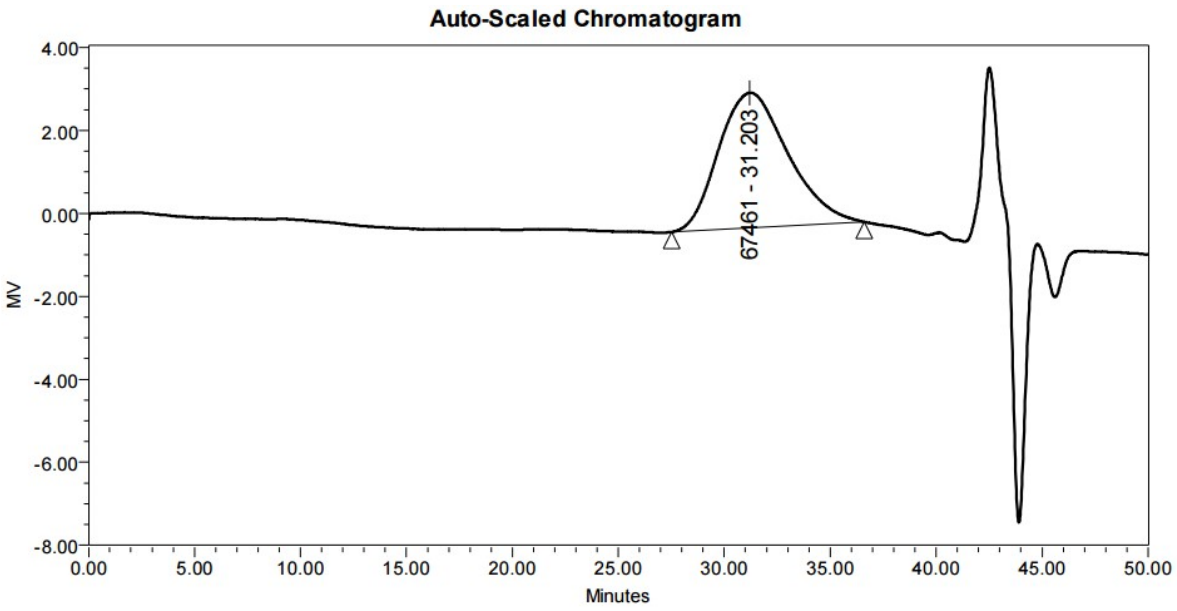

GPC Results

	Dist Name	Mn	Mw	MP	Mz	Mz+1	Mv	Polydispersity	MW Marker 1	MW Marker 2
1		44887	71864	67461	102482	132907		1.600996		

Fig. S42a. GPC trace of PLA synthesized using **1** (Table 1, Entry 1).

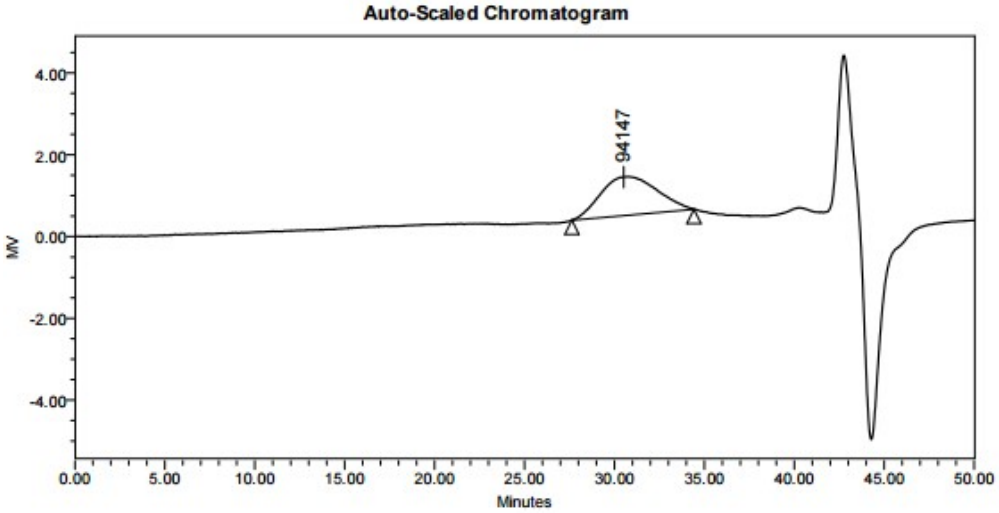

GPC Results

	Dist Name	Mn	Mw	MP	Mz	Mz+1	Mv	Polydispersity	MW Marker 1	MW Marker 2
1		66528	95183	94147	128325	160142		1.430720		

Fig. S42b. GPC trace of PLA synthesized using **2** (Table 1, Entry 2).

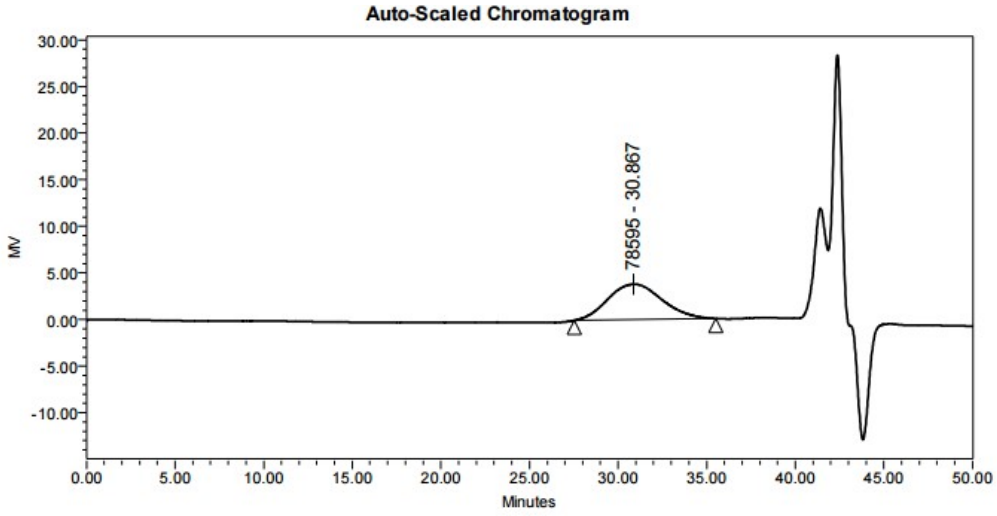

GPC Results

	Dist Name	Mn	Mw	MP	Mz	Mz+1	Mv	Polydispersity	MW Marker 1	MW Marker 2
1		59363	86912	78595	119051	151601		1.464080		

Fig. S42c. GPC trace of PLA synthesized using **3** (Table 1, Entry 3).

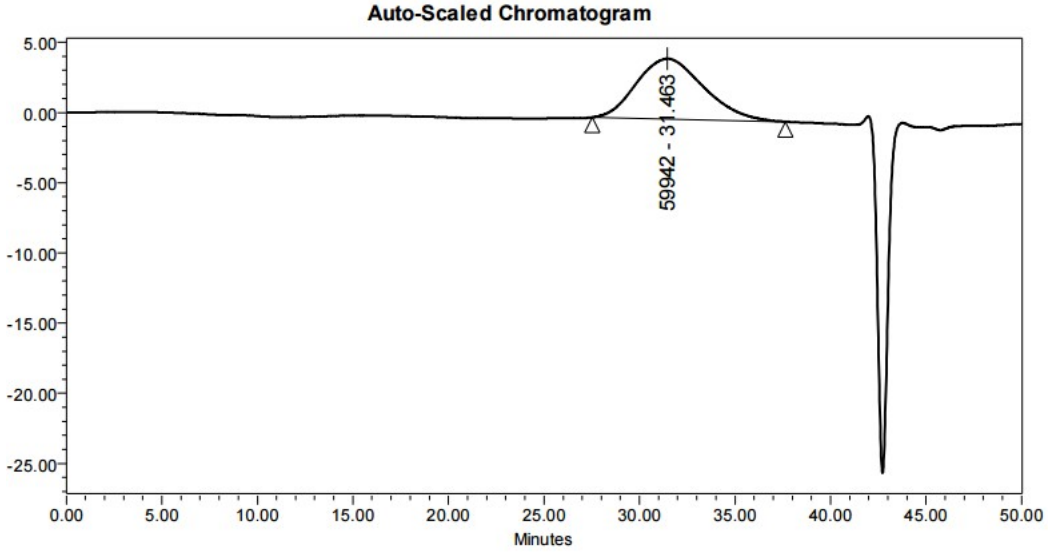

GPC Results

	Dist Name	Mn	Mw	MP	Mz	Mz+1	Mv	Polydispersity	MW Marker 1	MW Marker 2
1		38985	67061	59942	101007	135879		1.720198		

Fig. S42d. GPC trace of PLA synthesized using **4** (Table 1, Entry 4).

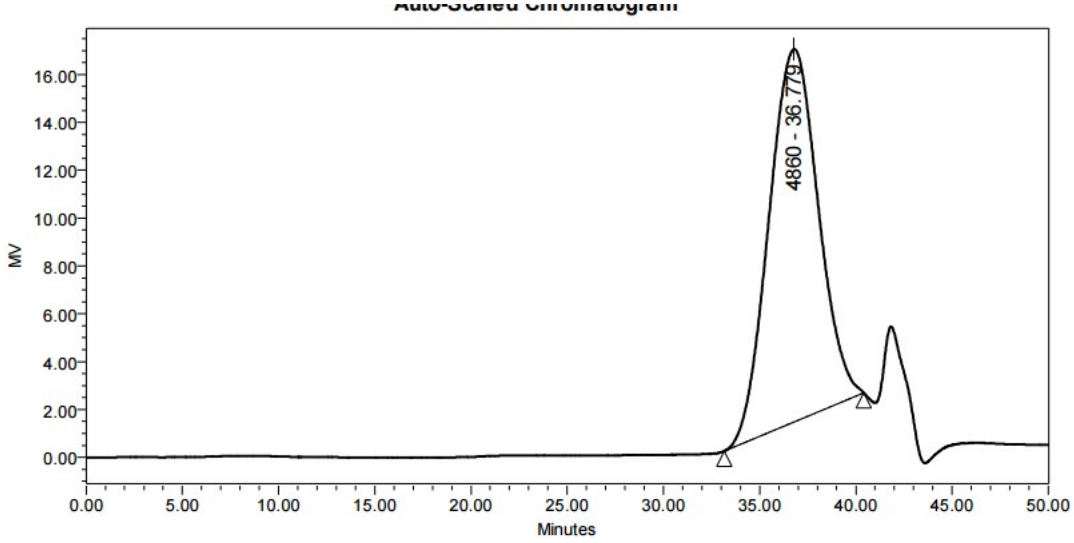

GPC Results

	Dist Name	Mn	Mw	MP	Mz	Mz+1	Mv	Polydispersity	MW Marker 1	MW Marker 2
1		4030	5564	4860	7362	9278		1.380669		

Fig. S42e. GPC trace of polyester synthesized from CHO/PA using **1** and TPPCl in neat condition (Table 3, Entry 3).

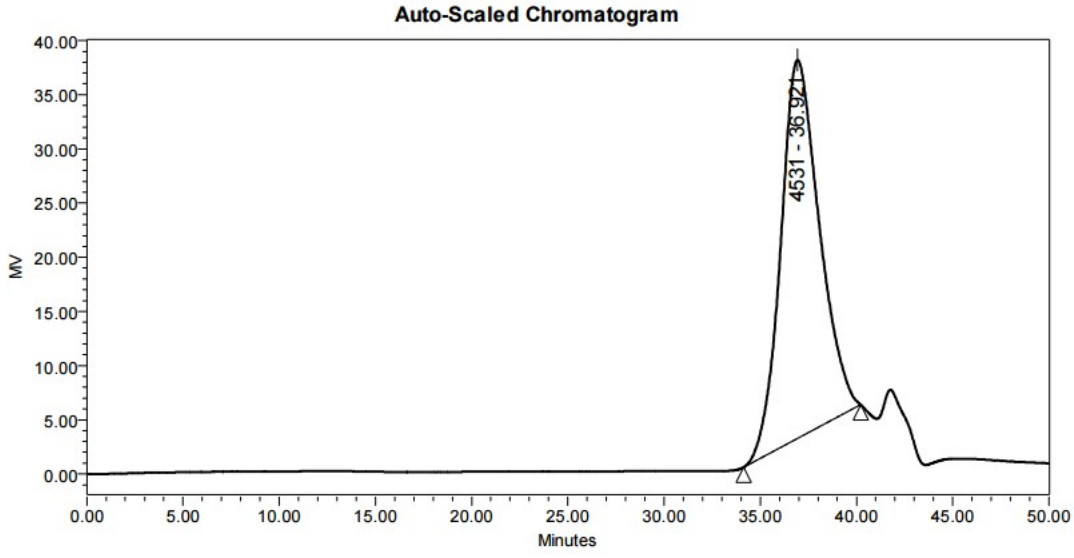

GPC Results

	Dist Name	Mn	Mw	MP	Mz	Mz+1	Mv	Polydispersity	MW Marker 1	MW Marker 2
1		3553	4464	4531	5430	6427		1.256505		

Fig. S42f. GPC trace of polyester synthesized from CHO/PA using **1** and TBAB in neat condition (Table 3, Entry 2).

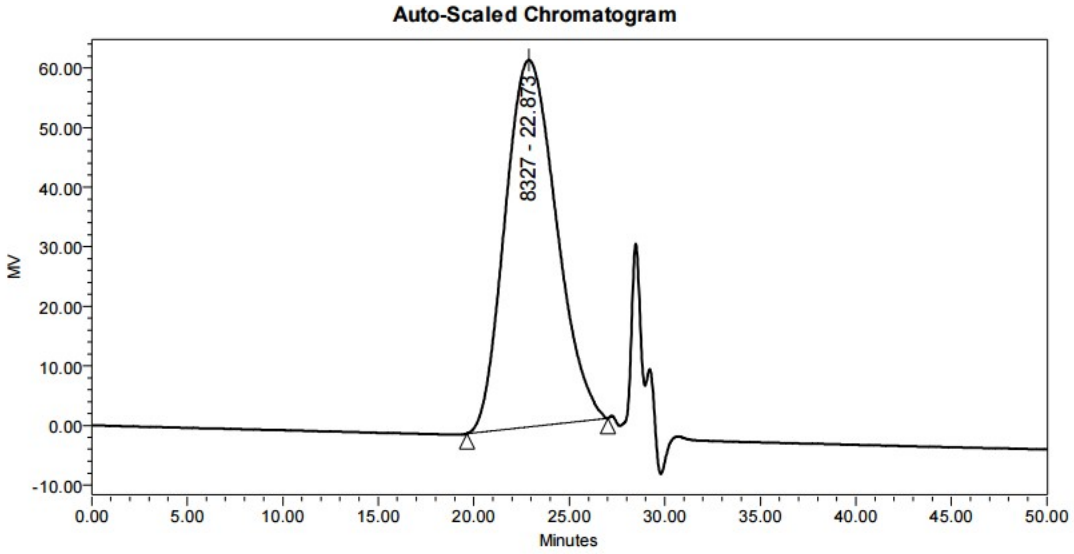

GPC Results

	Dist Name	Mn	Mw	MP	Mz	Mz+1	Mv	Polydispersity	MW Marker 1	MW Marker 2
1		5487	9155	8327	13427	17938		1.668347		

Fig. S42g. GPC trace of polyester synthesized from CHO/PA using **1** and PPNCl in neat condition (Table 3, Entry 4).

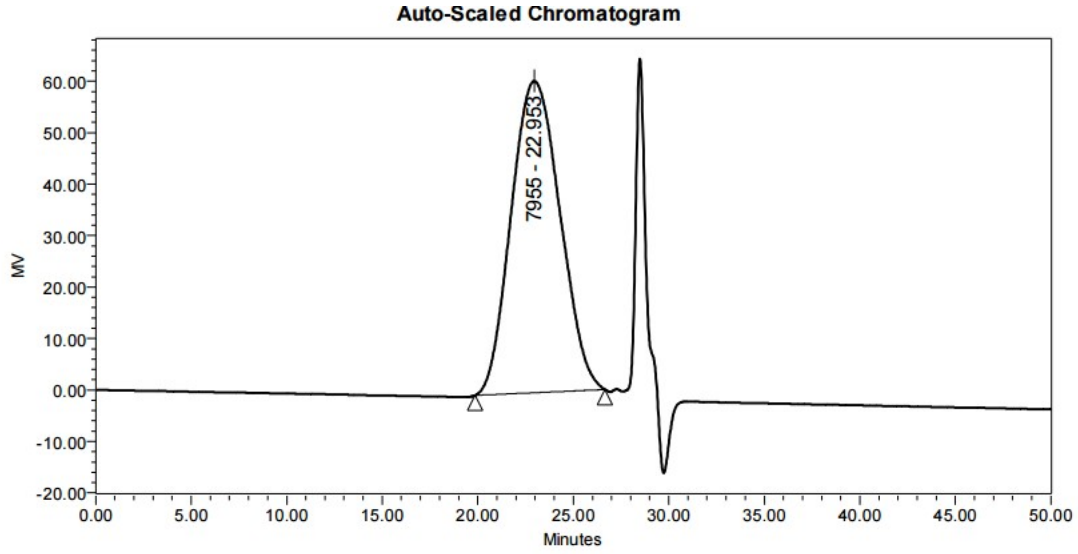

GPC Results

	Dist Name	Mn	Mw	MP	Mz	Mz+1	Mv	Polydispersity	MW Marker 1	MW Marker 2
1		5734	8867	7955	12618	16612		1.546515		

Fig. S42h. GPC trace of polyester synthesized from CHO/PA using **1** and PPNCl in toluene (Table 3, Entry 5).

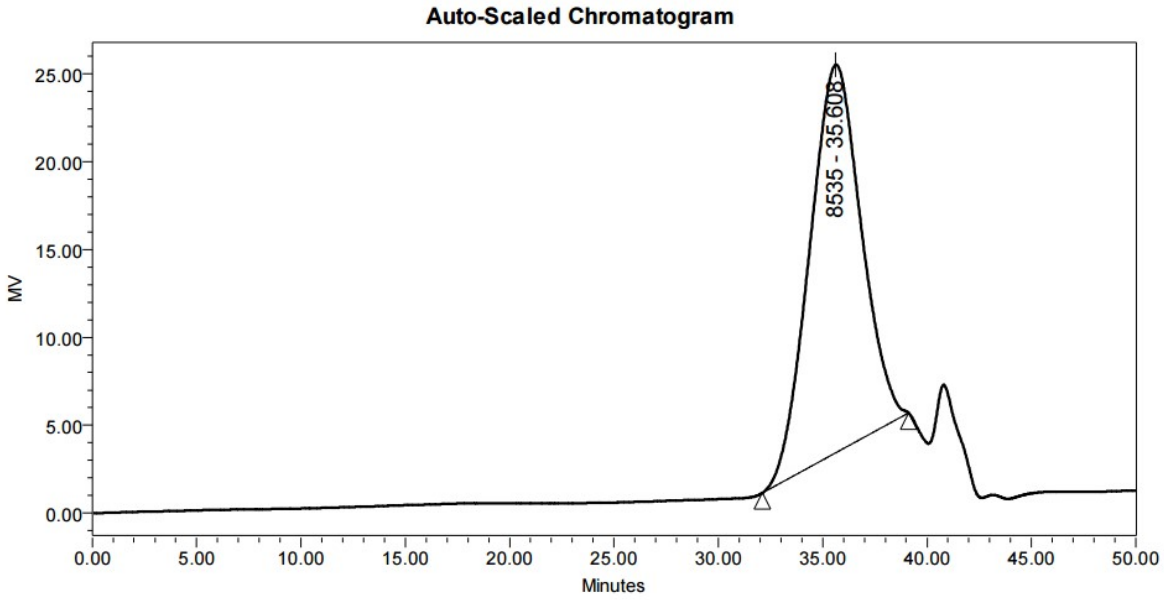

GPC Results

	Dist Name	Mn	Mw	MP	Mz	Mz+1	Mv	Polydispersity	MW Marker 1	MW Marker 2
1		7211	9642	8535	12515	15611		1.337126		

Fig. S42i. GPC trace of polyester synthesized from CHO/PA using **2** and PPNCl in toluene (Table 3, Entry 6).

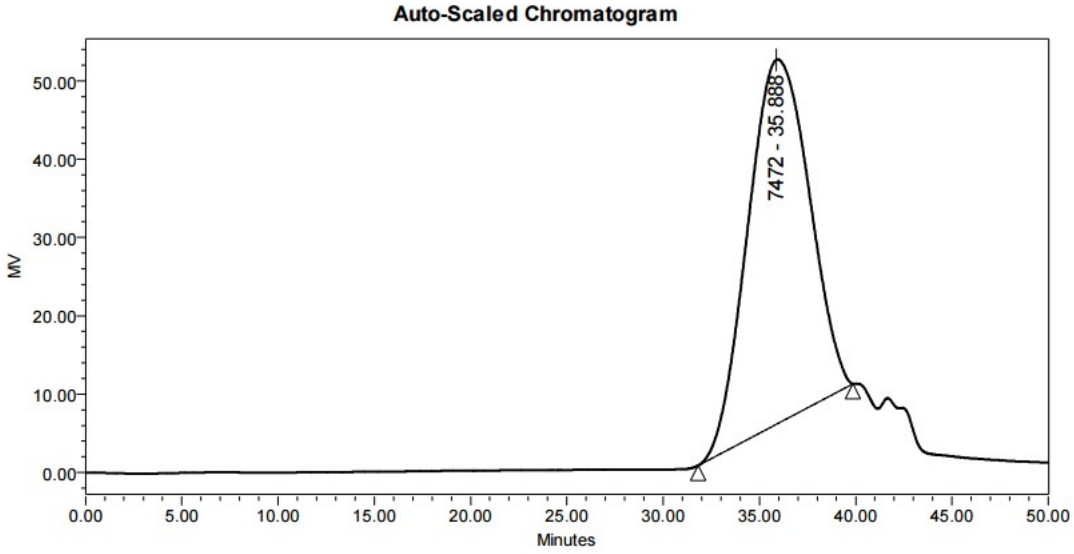

GPC Results

	Dist Name	Mn	Mw	MP	Mz	Mz+1	Mv	Polydispersity	MW Marker 1	MW Marker 2
1		5570	8561	7472	12415	16542		1.537055		

Fig. S42j. GPC trace of polyester synthesized from CHO/PA using **3** and PPNCl in toluene (Table 3, Entry 7).

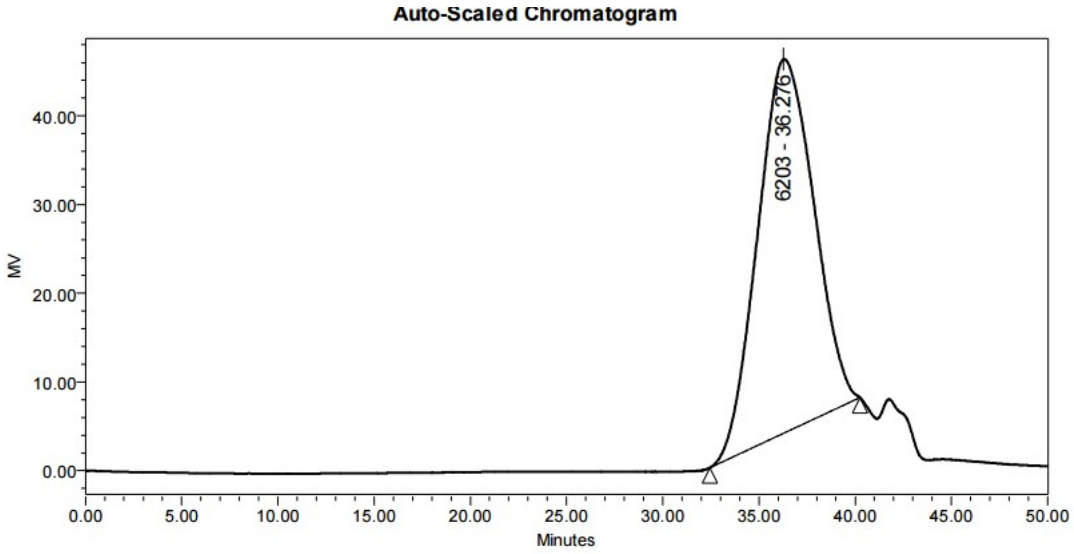

GPC Results

	Dist Name	Mn	Mw	MP	Mz	Mz+1	Mv	Polydispersity	MW Marker 1	MW Marker 2
1		4640	6874	6203	9651	12631		1.481320		

Fig. S42k. GPC trace of polyester synthesized from CHO/PA using **4** and PPNCl in toluene (Table 3, Entry 8).

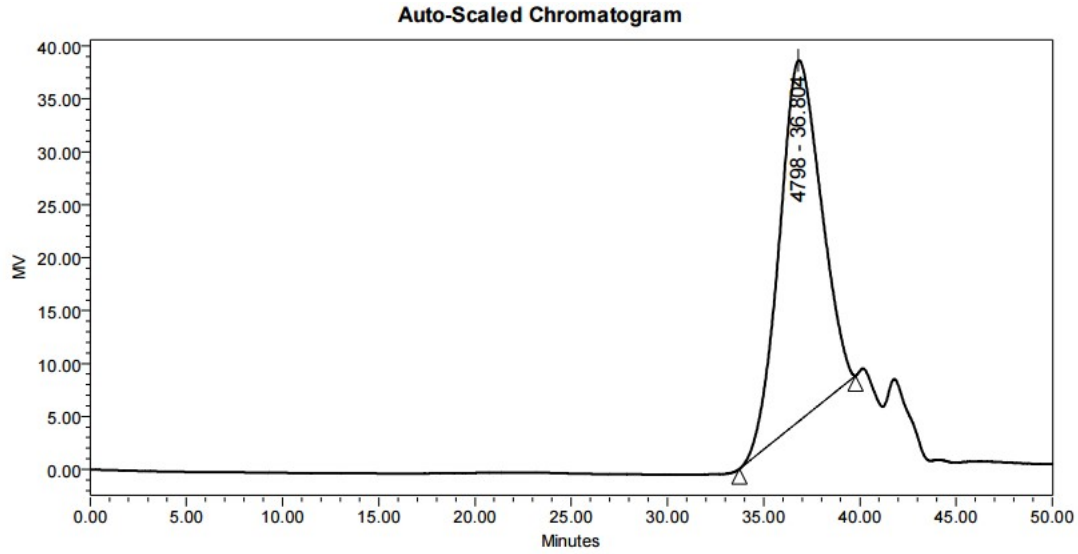

GPC Results

	Dist Name	Mn	Mw	MP	Mz	Mz+1	Mv	Polydispersity	MW Marker 1	MW Marker 2
1		3958	5007	4798	6215	7510		1.265102		

Fig. S42l. GPC trace of polyester synthesized from CHO/PA in 110:100 ratio using **1** and PPNCl in toluene (Table 3, Entry 9).

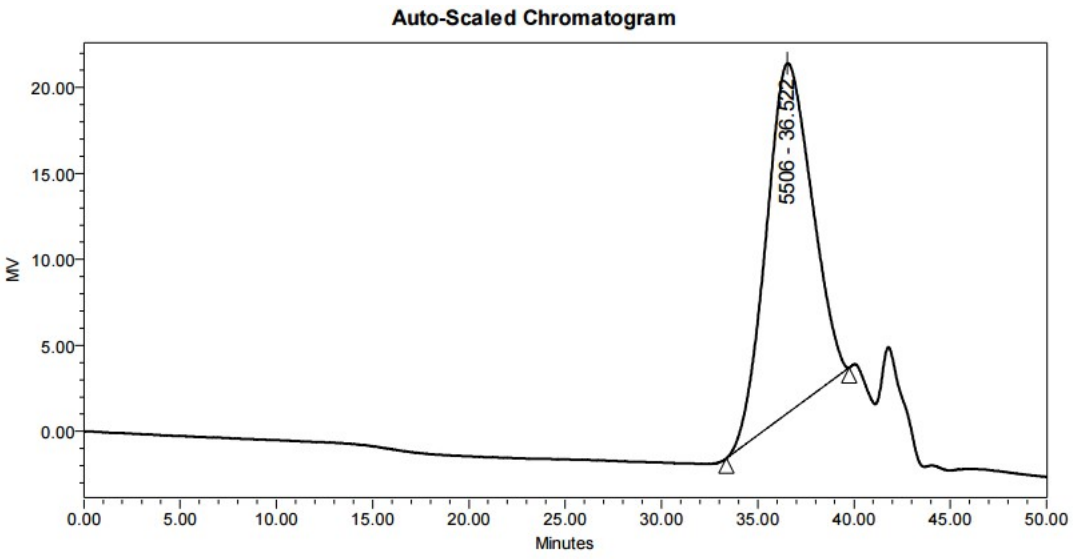

GPC Results

	Dist Name	Mn	Mw	MP	Mz	Mz+1	Mv	Polydispersity	MW Marker 1	MW Marker 2
1		4437	5817	5506	7421	9119		1.311083		

Fig. S42m. GPC trace of polyester synthesized from CHO/PA in 110:100 ratio using **2** and PPNCl in toluene (Table 3, Entry 10).

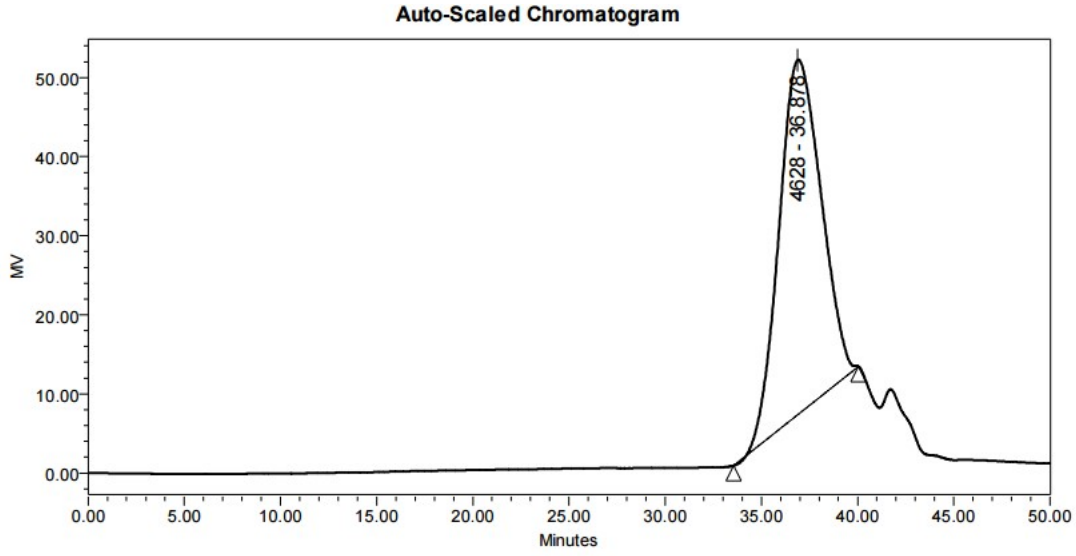

GPC Results

	Dist Name	Mn	Mw	MP	Mz	Mz+1	Mv	Polydispersity	MW Marker 1	MW Marker 2
1		3733	4712	4628	5797	6912		1.262149		

Fig. S42n. GPC trace of polyester synthesized from CHO/PA in 110:100 ratio using **3** and PPNCl in toluene (Table 3, Entry 11).

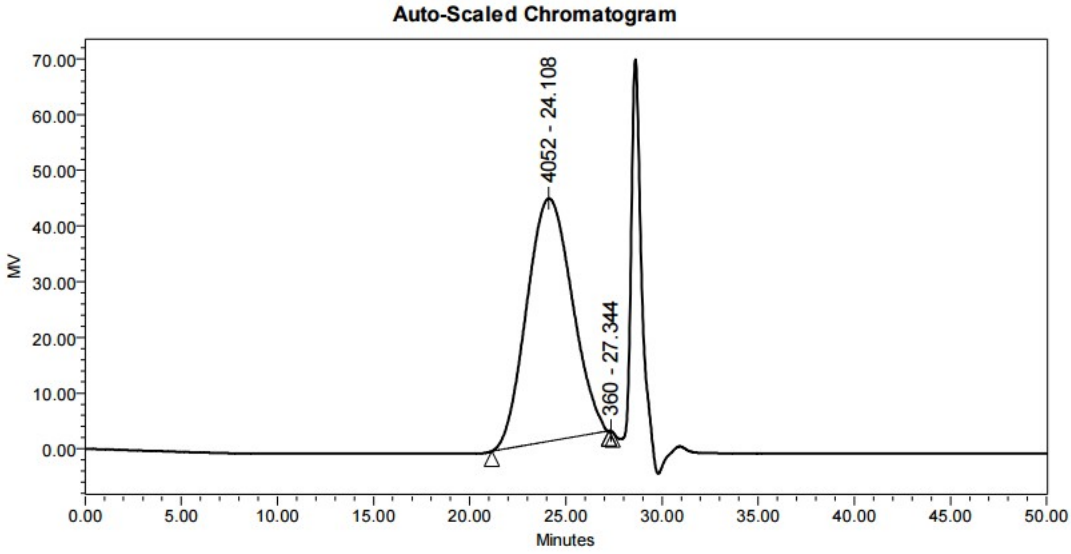

GPC Results

	Dist Name	Mn	Mw	MP	Mz	Mz+1	Mv	Polydispersity	MW Marker 1	MW Marker 2
1		2968	4556	4052	6370	8202		1.535058		
2				360						

Fig. S42o. GPC trace of polyester synthesized from CHO/PA in 110:100 ratio using **4** and PPNCl in toluene (Table 3, Entry 12).

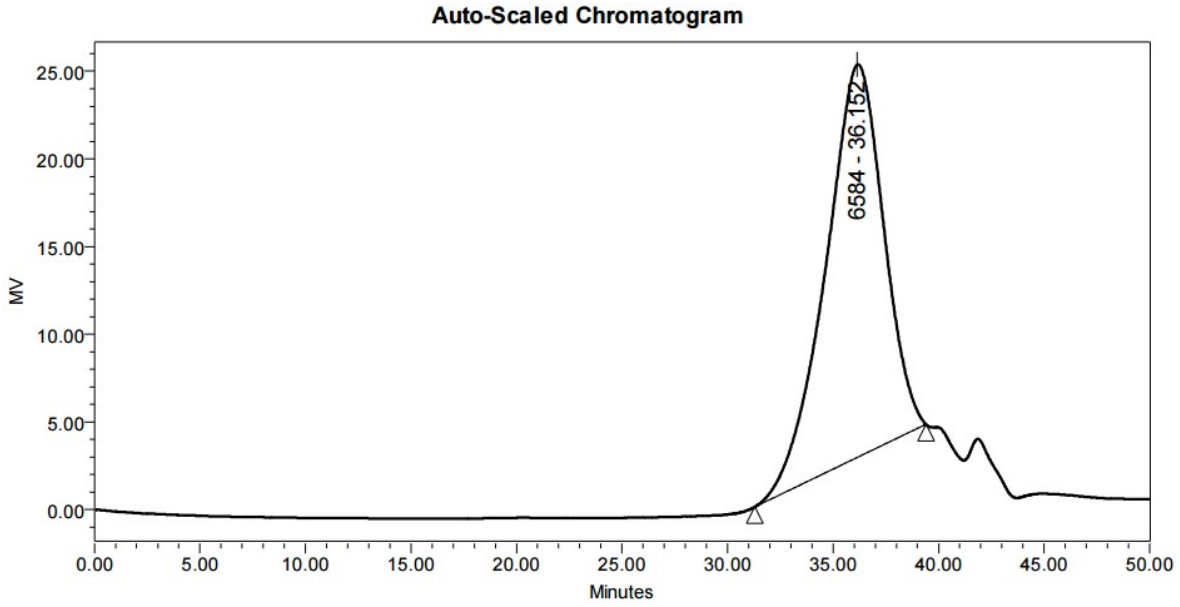

GPC Results

	Dist Name	Mn	Mw	MP	Mz	Mz+1	Mv	Polydispersity	MW Marker 1	MW Marker 2
1		6003	8828	6584	13225	19025		1.470484		

Fig. S42p. GPC trace of polyester synthesized from CHO/SA using **2** and PPNCl in toluene (Table 4, Entry 1).

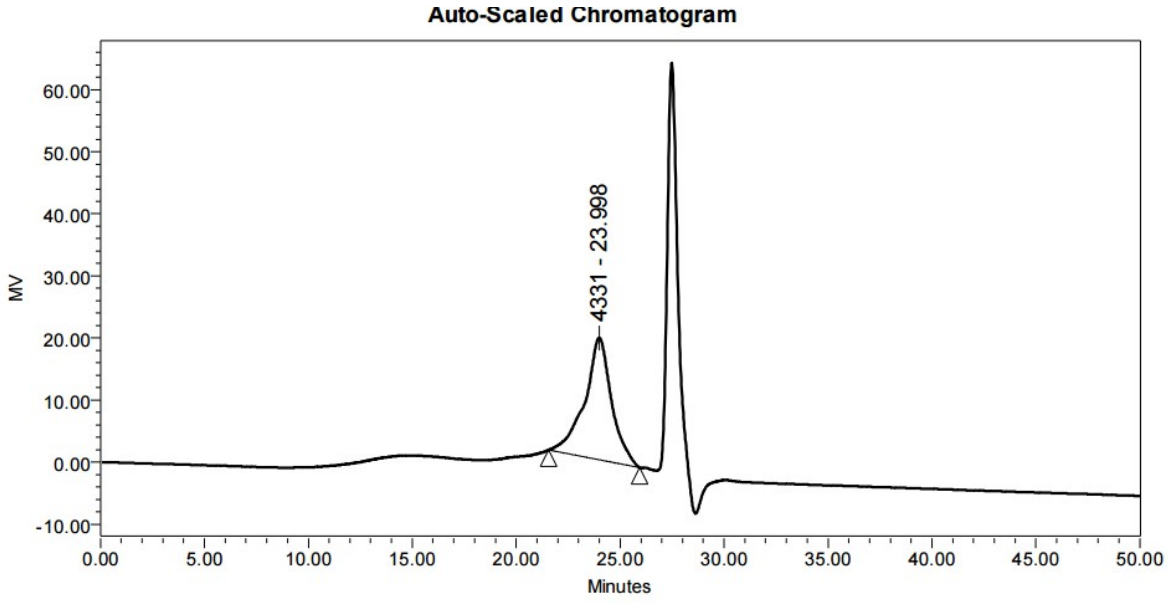

GPC Results

	Dist Name	Mn	Mw	MP	Mz	Mz+1	Mv	Polydispersity	MW Marker 1	MW Marker 2
1		4158	5007	4331	6072	7351		1.204161		

Fig. S42q. GPC trace of polyester synthesized from CHO/MA using **2** and PPNCl in toluene (Table 4, Entry 2).

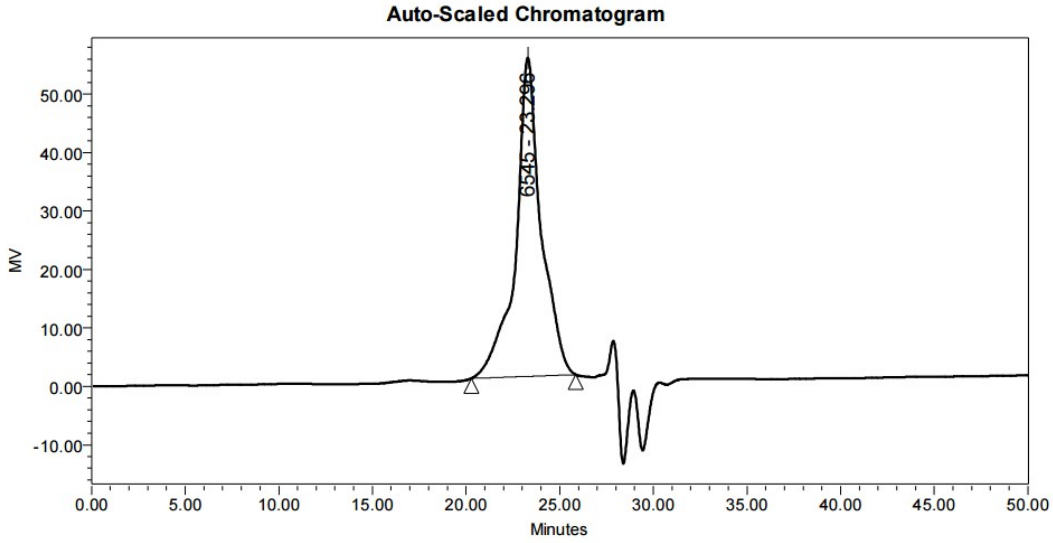

GPC Results

	Dist Name	Mn	Mw	MP	Mz	Mz+1	Mv	Polydispersity	MW Marker 1	MW Marker 2
1		5663	7221	6545	9454	12590		1.275100		

Fig. S42r. GPC trace of polyester synthesized from CHO/NBA using **2** and PPNCl in toluene (Table 4, Entry 3).

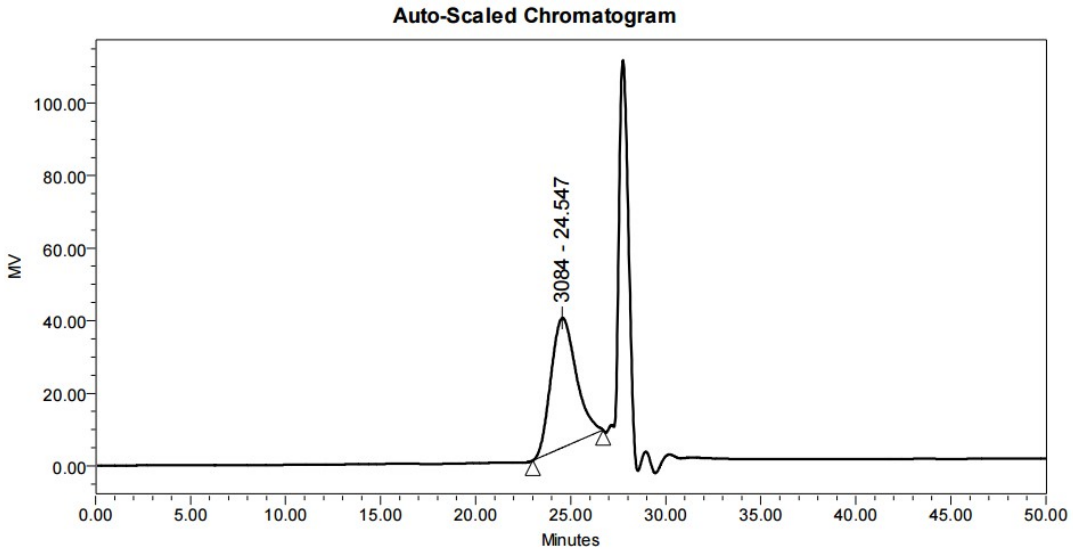

GPC Results

	Dist Name	Mn	Mw	MP	Mz	Mz+1	Mv	Polydispersity	MW Marker 1	MW Marker 2
1		2542	3007	3084	3436	3822		1.183032		

Fig. S42s. GPC trace of polyester synthesized from PO/PA using **2** and PPNCl in toluene (Table 4, Entry 5).

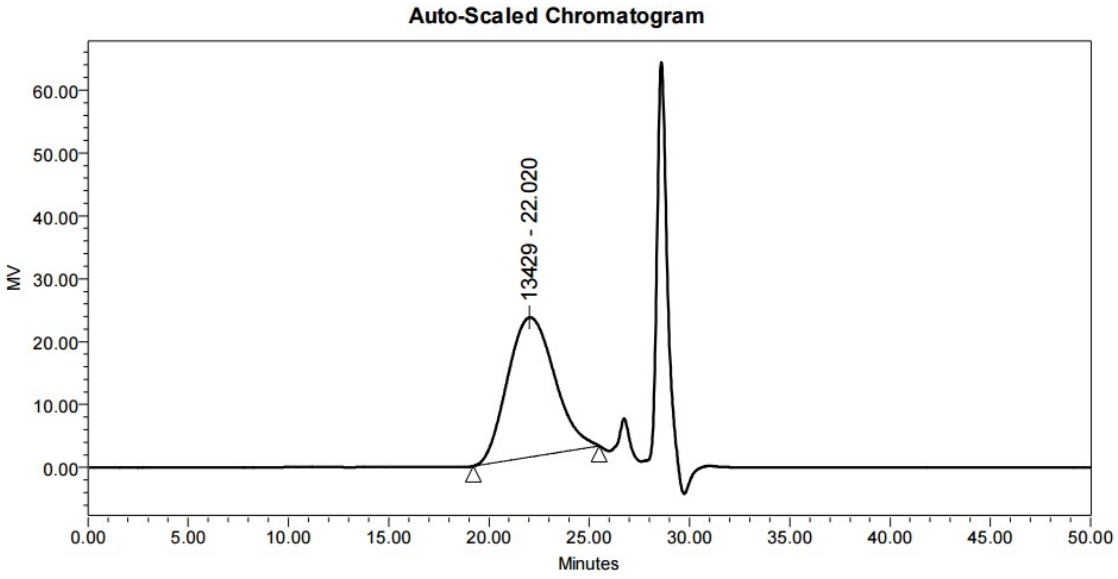

GPC Results

	Dist Name	Mn	Mw	MP	Mz	Mz+1	Mv	Polydispersity	MW Marker 1	MW Marker 2
1		10230	14698	13429	19930	25534		1.436661		

Fig. S42t. GPC trace of polyester synthesized from ^{t}BGE/PA using **2** and PPNCl in toluene (Table 4, Entry 4).

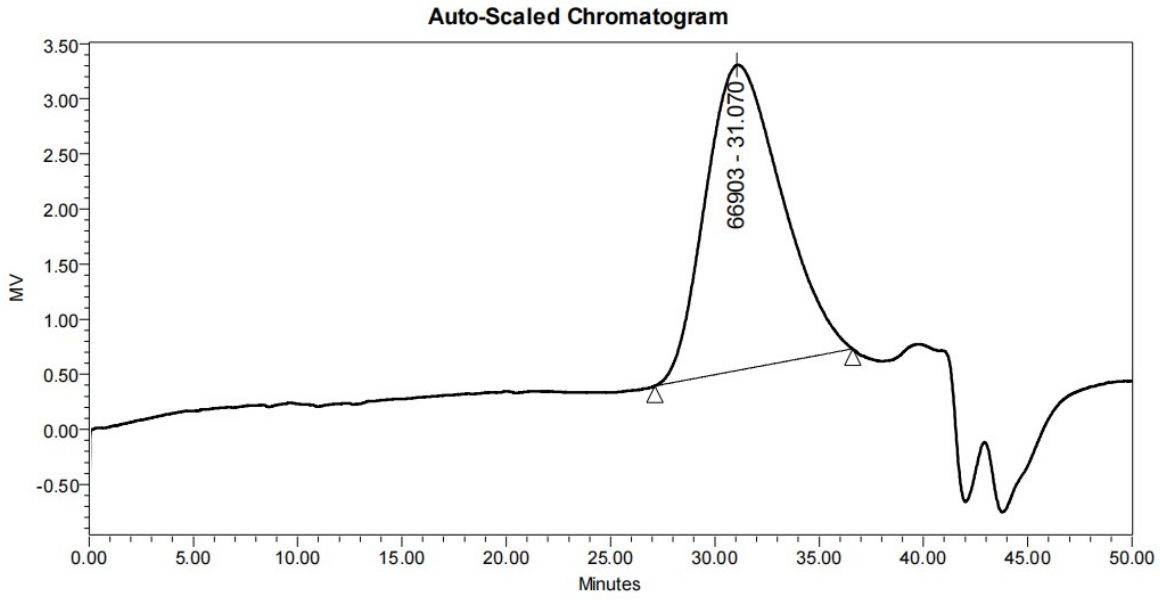

GPC Results

	Dist Name	Mn	Mw	MP	Mz	Mz+1	Mv	Polydispersity	MW Marker 1	MW Marker 2
1		40013	68436	66903	101872	135041		1.710346		

Fig. S42u. GPC trace of PLLA synthesized using **1** (Table 2, Entry 1).

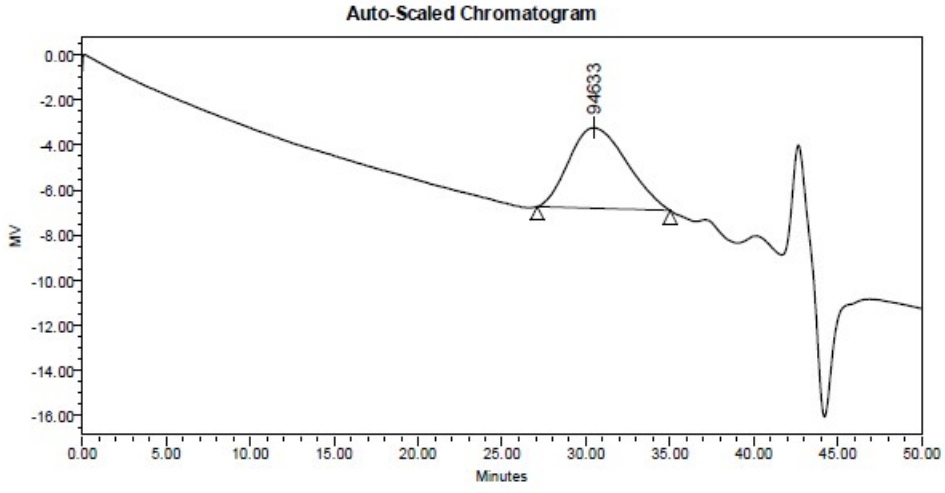

GPC Results

	Dist Name	Mn	Mw	MP	Mz	Mz+1	Mv	Polydispersity	MW Marker 1	MW Marker 2
1		63498	100536	94633	145432	189402		1.583309		

Fig. S42v. GPC trace of PLLA synthesized using **2** (Table 2, Entry 2).

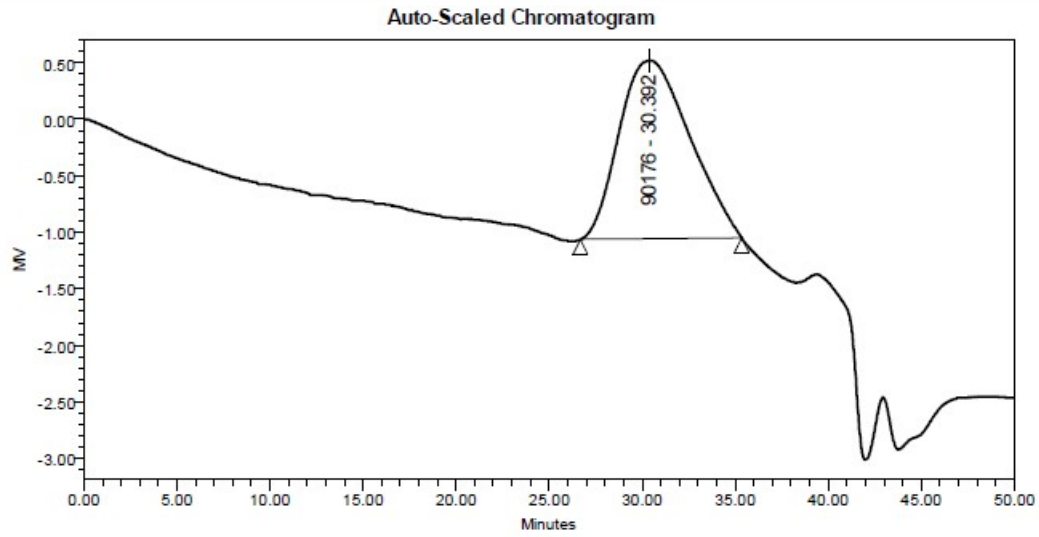

GPC Results

	Dist Name	Mn	Mw	MP	Mz	Mz+1	Mv	Polydispersity	MW Marker 1	MW Marker 2
1		55931	94211	90176	140019	183923		1.684412		

Fig. S42w. GPC trace of PLLA synthesized using **3** (Table 2, Entry 3).

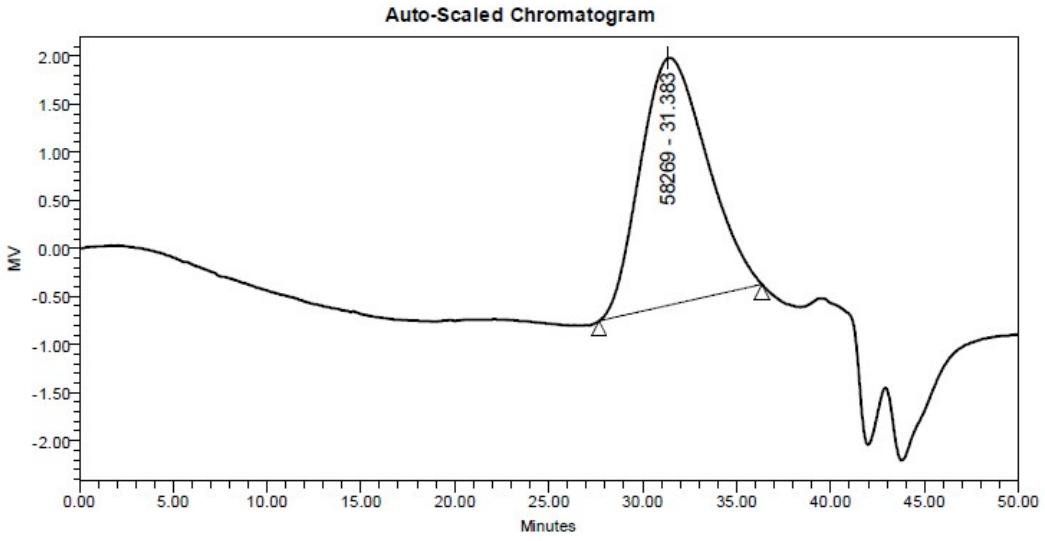

GPC Results

	Dist Name	Mn	Mw	MP	Mz	Mz+1	Mv	Polydispersity	MW Marker 1	MW Marker 2
1		37283	60728	58269	88475	115742		1.628821		

Fig. S42x. GPC trace of PLLA synthesized using **4** (Table 2, Entry 4).

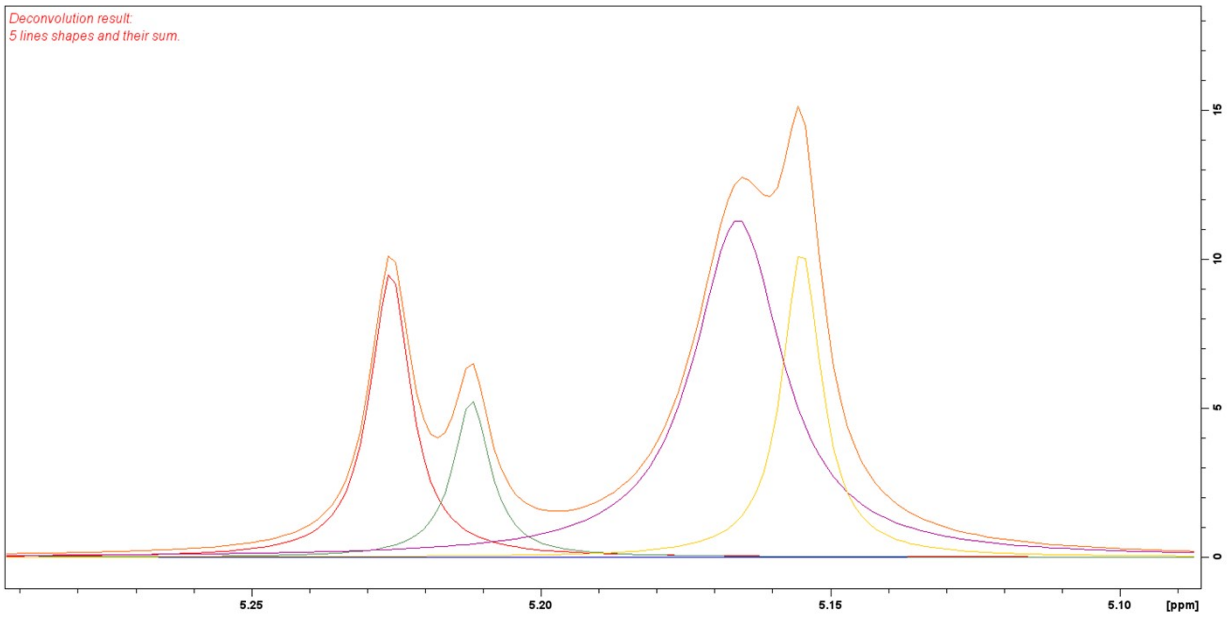

Fig. S43a. Methine region (δ= 5.10–5.25 ppm) of the homonuclear decoupled ^{1}H NMR spectrum (500 MHz, $CDCl_3$, 300 K) of a PLA prepared with **2** (P_m = 0.58) (Table 1, Entry 2).

From the spectrum it can be evaluated that,

the area of integration of (mmm), (rmm), (rmr), (mrm) is 0.602, 0.123, 0.112 and 0.163 respectively.

Therefore, for (mmm), $(P_m)^2 + \frac{(P_m)(P_r)}{2}$ **= 0.602**

Or, $2(P_m)^2 + P_m(1 - P_m) = 1.204$

$$P_m = \frac{-1 \pm \sqrt{1 - [4(1)(-1.494)]}}{2(1)}$$

P_m = 0.70

(rmm), $\frac{(P_r)(P_m)}{2}$ = 0.123

Similarly, P_m = 0.44

(rmr), $\frac{(P_r)^2}{2}$ = 0.112; $\frac{(1-P_m)^2}{2}$ = 0.112

P_m = 0.53

(mrm), $\frac{(P_r)^2 + (P_r)(P_m)}{2}$ = 0.163

P_m = 0.67

The average P_m = (0.70 + 0.44 + 0.53 + 0.67) / 4 = 0.58

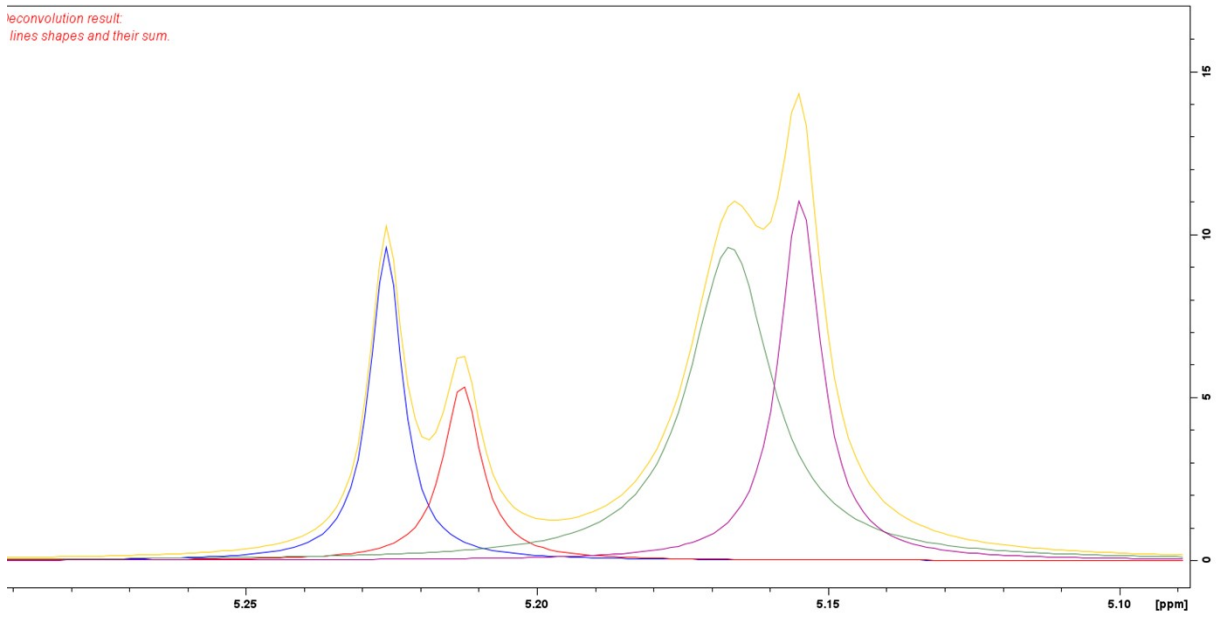

Fig. S43b. Methine region (δ = 5.10–5.25 ppm) of the homonuclear decoupled ^{1}H NMR spectrum (500 MHz, $CDCl_3$, 300 K) of a PLA prepared with **4** (P_r = 0.51) (Table 1, Entry 4).

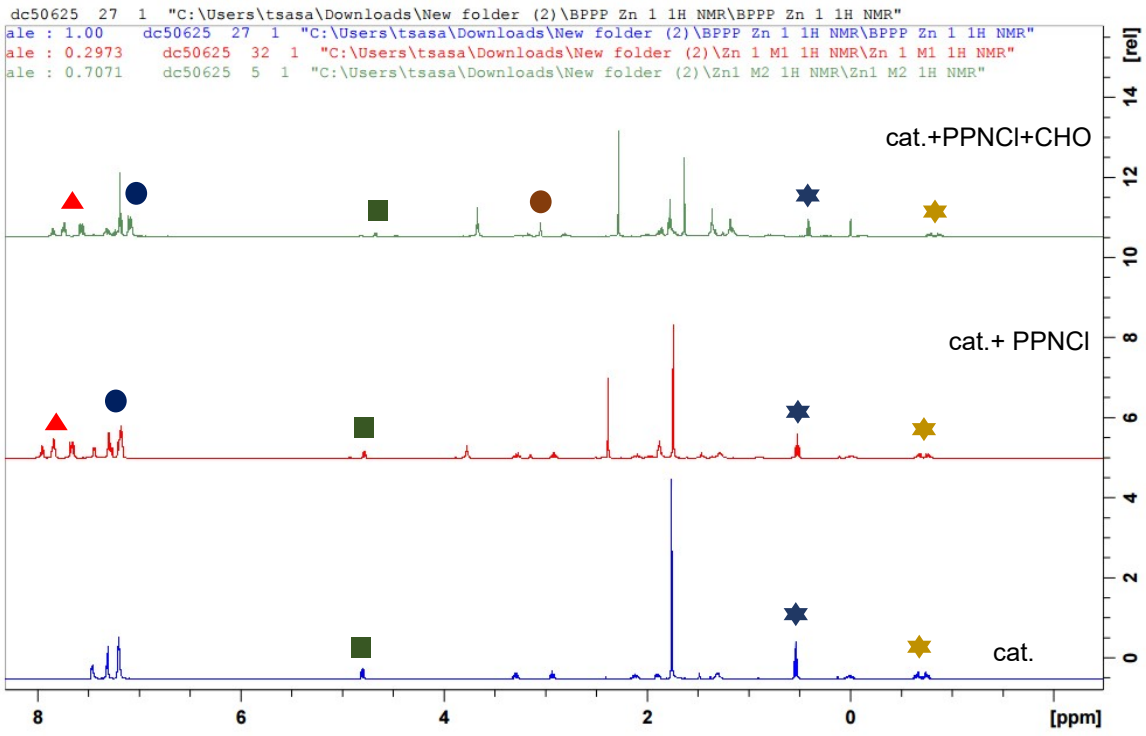

Fig. S44. Stacked ^{1}H NMR spectrum ($CDCl_3$, 500 MHz) a) Cat. **1**; b) Cat. **1** + PPNCl (1:1 mixture); c) Cat. **1** + PPNCl + CHO (1:1:2 mixture). Green rectangle: NC**H** proton signal; Blue circle: catalytic pair signal; Red triangle: phosphonium ion signal; Blue star: $ZnCH_2C\mathbf{H}_3$ protons signal; yellow star: $ZnC\mathbf{H}_2CH_3$ proton signal; Brown circle: CHO and homopolymerized product signal.

Signal	Cat.	Cat. + PPNCl	Cat. + PPNCl + CHO
N-C**H**	4.76	4.70	4.67
$H_3CC\mathbf{H}_2$–Zn	-0.80	-0.84	-0.87
$\mathbf{H}_3CCH_2$–Zn	0.50	0.46	0.43

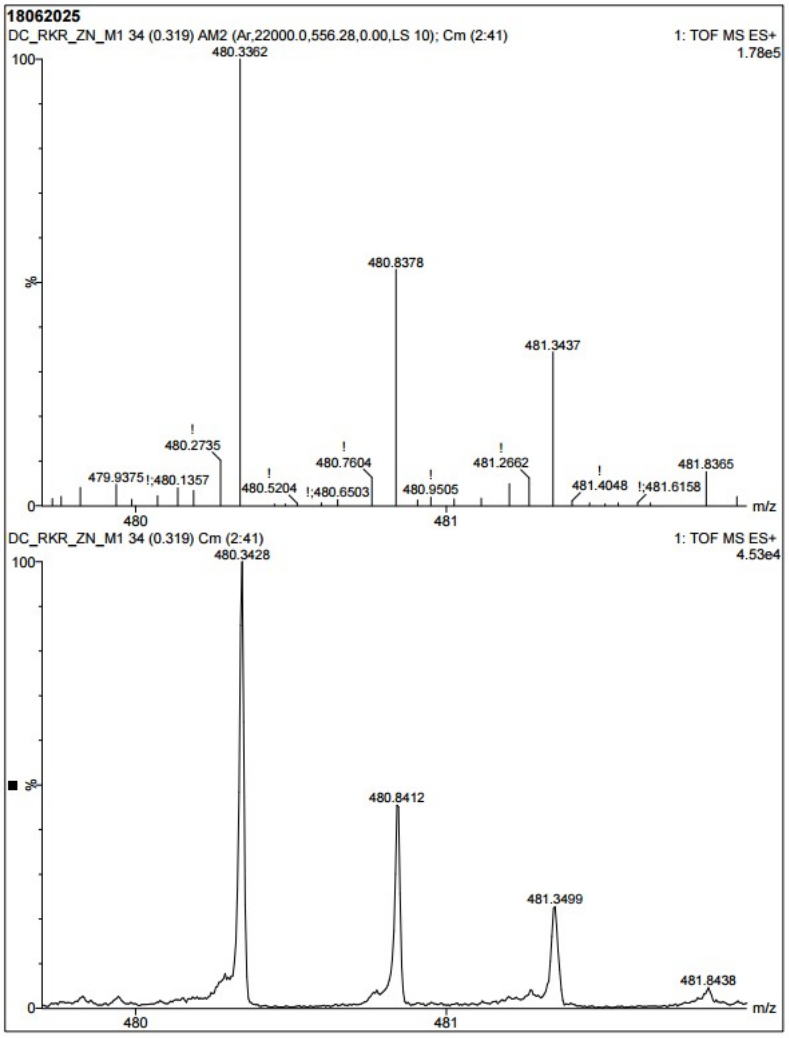

Fig. S45a. Simulated (above) and experimental (below) ESI-MS of intermediate **2b**.

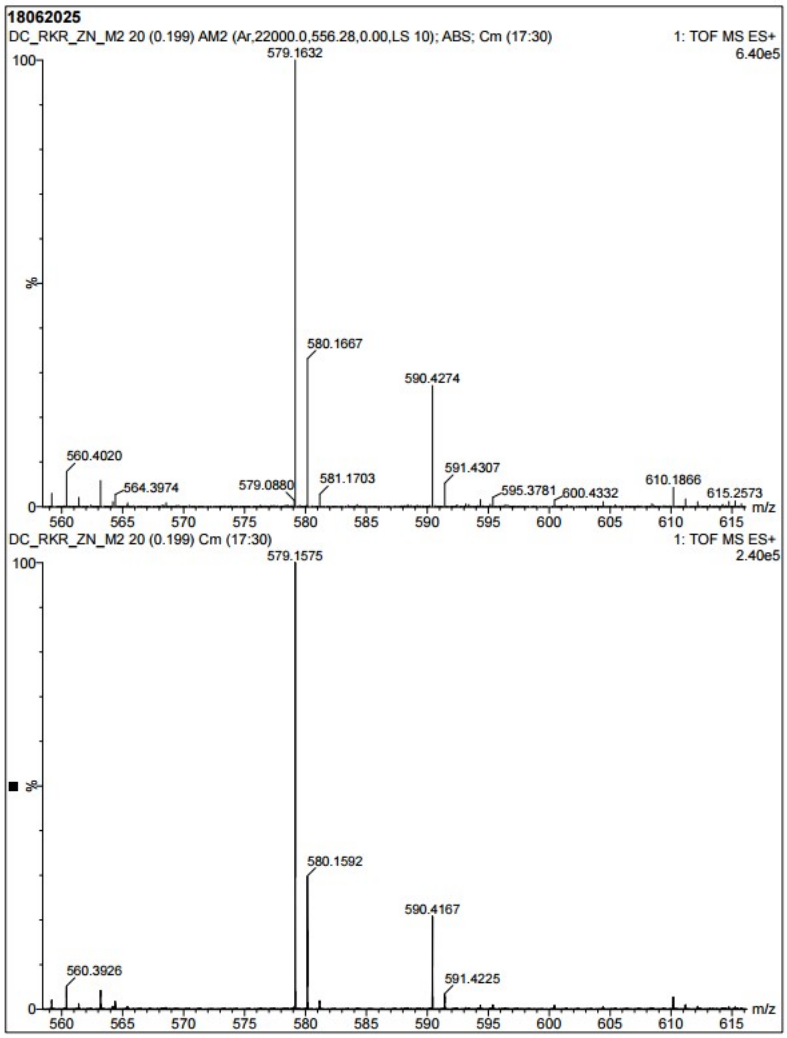

Fig. S45b. Simulated (above) and experimental (below) ESI-MS of intermediate **2c**.

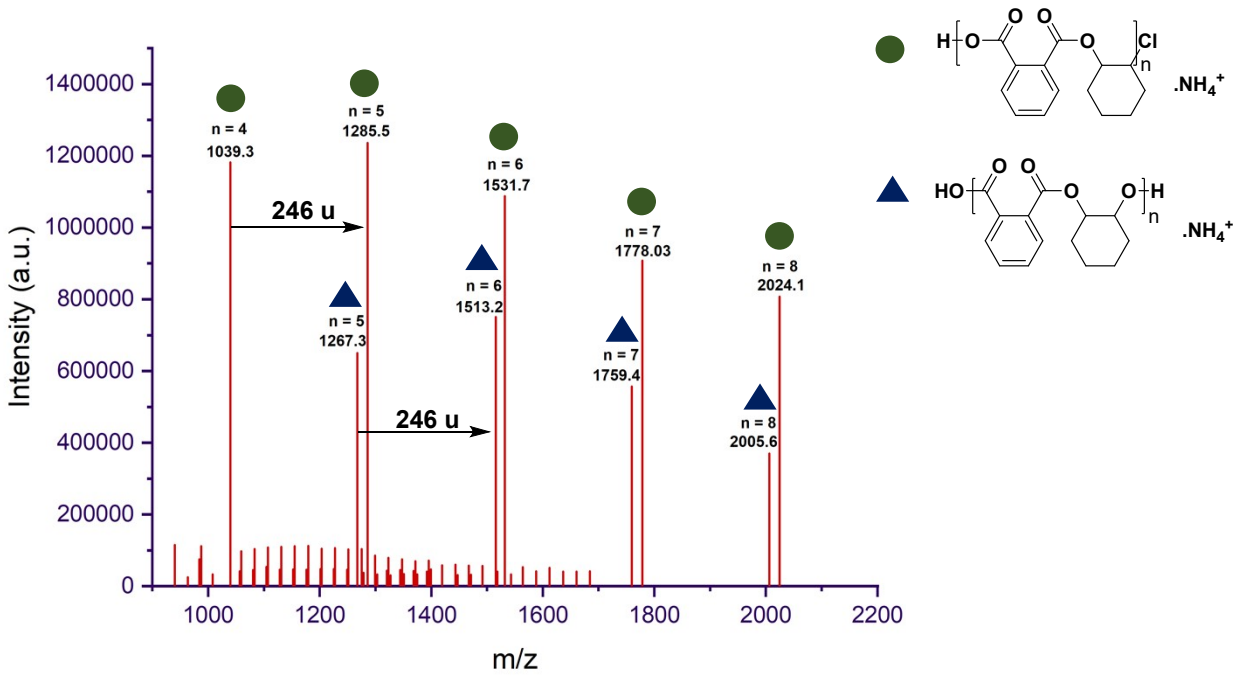

Fig. S46. MALDI-TOF spectrum of oligomer prepared from ROCOP of CHO and PA using **1**.

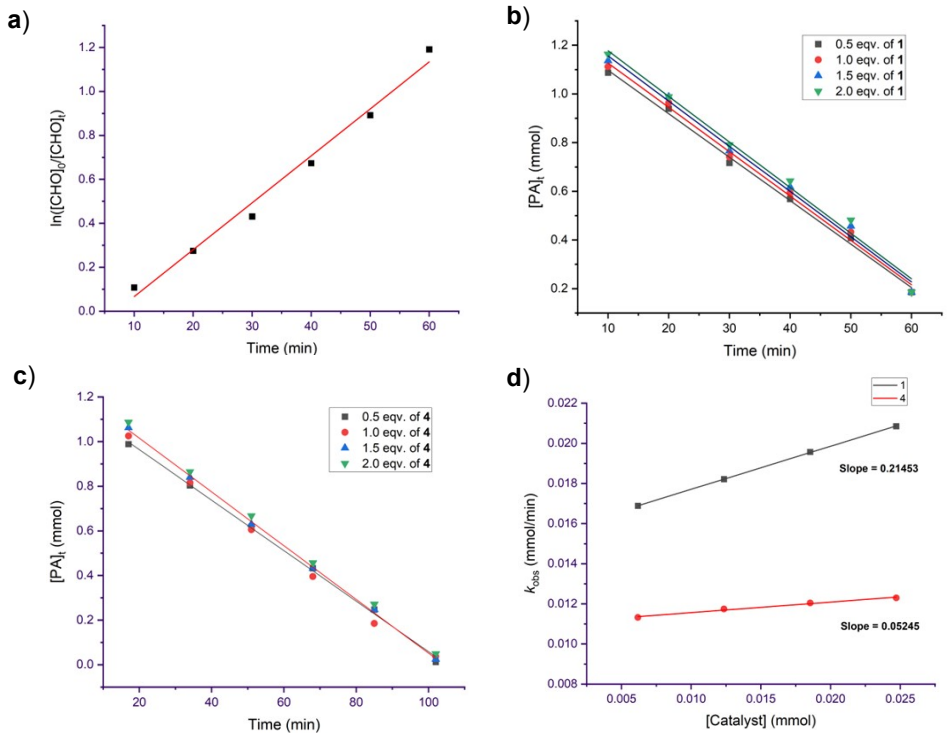

Fig. S47. a) Plot of $\ln([CHO]_0/[CHO]_t)$ vs Time; b) Plot of $[PA]_t$ vs. Time With 0.5 eqv., 1 eqv., 1.5 eqv. And 2 eqv. Of **1**; b) Plot of $[PA]_t$ vs. Time. With 0.5 eqv., 1 eqv., 1.5 eqv. And 2 eqv. Of **4**; c) Plot of k_{obs} vs [catalyst].

Table S2. Experimental data for the plots to determine the order of ROCOP of CHO and PA with respect to catalyst **1** and **4**.

Entry	[**1**] (mmol)	Initial rate [a] (mmol/min) (Compound **1**)	Initial rate [a] (mmol/min) (Compound **4**)
1	0.00618	0.03747	0.01132
2	0.01235	0.04071	0.01174
3	0.01853	0.04232	0.01204
4	0.02471	0.04404	0.0123

[a] the rate of polyester formation (CHO/PA) was determined from the slope of the linear range of conversion of PA with time. The data was obtained by taking aliquots at specific reaction times and analyzing them for individual composition by ^{1}H NMR

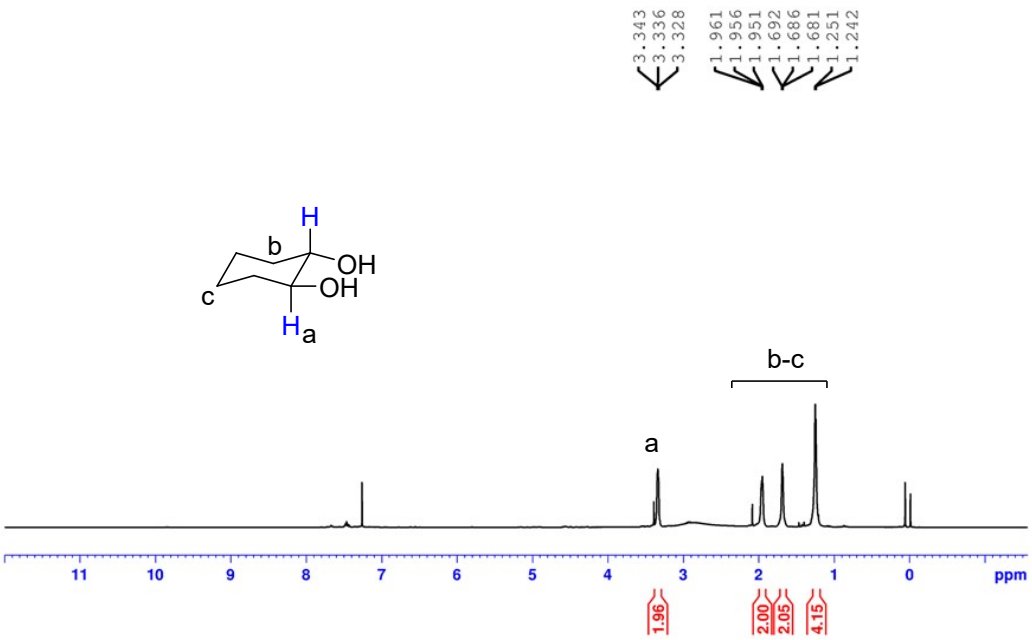

Fig. S48. ^{1}H NMR ($CDCl_3$, 500 MHz) spectrum of the hydrolyzed polyester

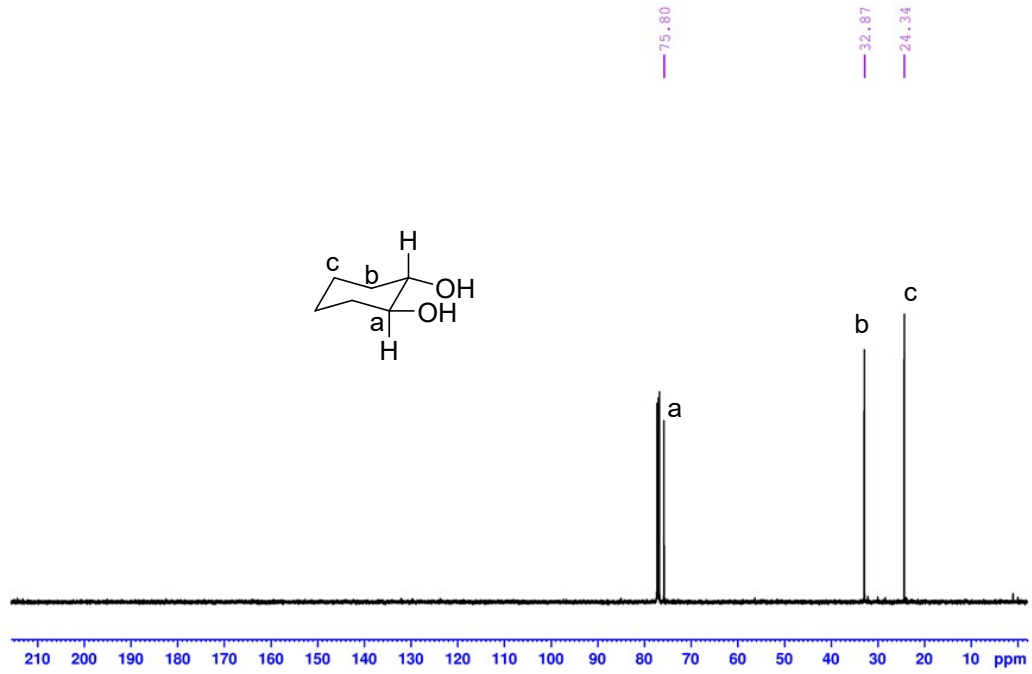

Fig. S49. ^{13}C NMR ($CDCl_3$, 500 MHz) spectrum of the hydrolyzed polyester

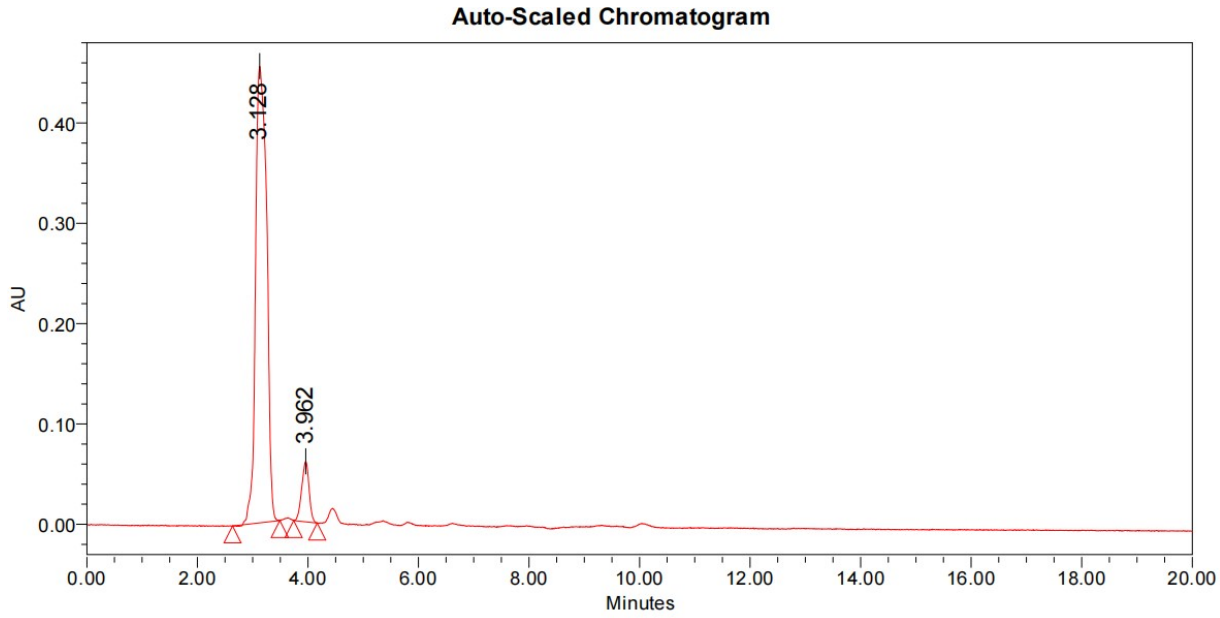

Peak Results

	Name	RT	Area	Height	% Area
1		3.128	6357697	455237	91.92
2		3.962	558482	60305	8.08

Fig. S50a. HPLC chromatogram of polyester upon hydrolysis prepared from catalyst **2 (Table S3, Entry 1)**.

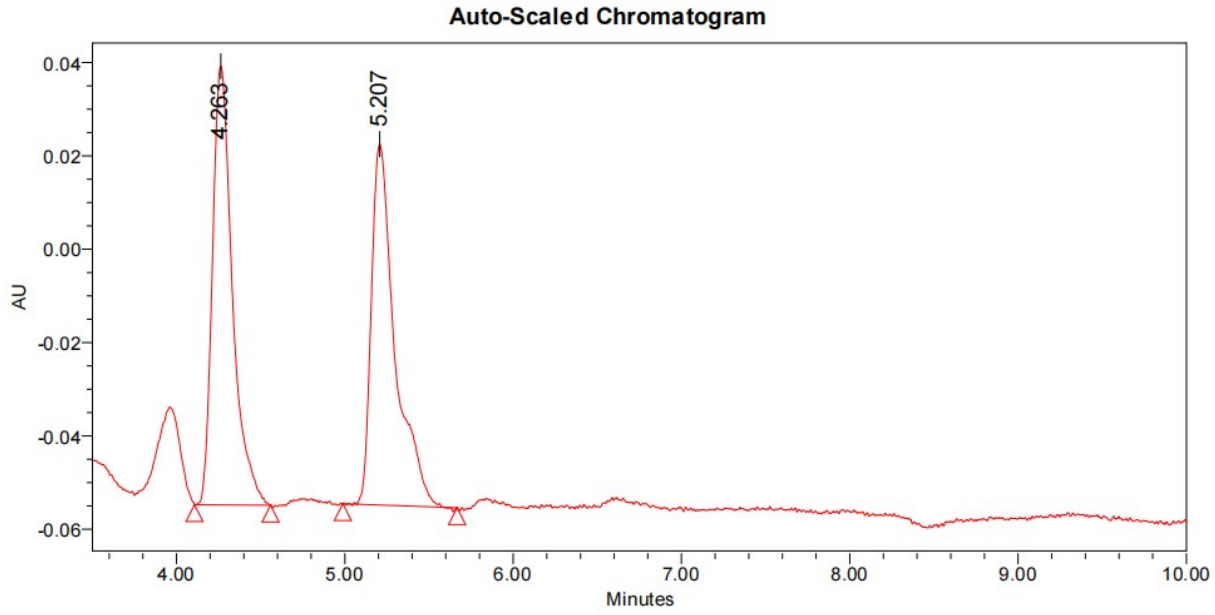

Peak Results

	Name	RT	Area	Height	% Area
1		4.263	775949	94005	50.68
2		5.207	755179	77321	49.32

Fig. S50b. HPLC chromatogram of polyester upon hydrolysis prepared from catalyst **4 (Table S3, Entry 2)**.

Table S3. Enantiomeric excess of 1,2-cyclohexanediol obtained upon hydrolysis of polyester.

Entry	Catalyst	(*S, S*) diol	(*R, R*) diol	%ee = {[(R-S)/(R+S)]x100}
1	**2**	91.92	8.08	[(91.92-8.08)/(91.92+8.08)]x100 = 83.84
2	**4**	50.68	49.32	[(50.68-49.32)/(50.68+49.32)]x100 = 1.36

Theoretical details:

The geometry Optimizations for the Zn Complexes **2**-**2g** was performed at B3LYP[S8] with dispersion correction term D3[S9] with basis set LANL2DZ[S10]in singlet electronic state, with Gaussian16[S11] package in gaseous phase. The geometry optimization is favoured by minima on the potential energy surface followed by no negative frequency, with the Phenyl group replaced by methyl group for convenience of calculation. The NBO[S12] calculations of the complexes, Mulliken charges, Molecular Electrostatic potential were performed by using NBO 6.0 program[S13] by using the optimized coordinates at B3LYP-D3(BJ)/LANL2DZ level of theory.

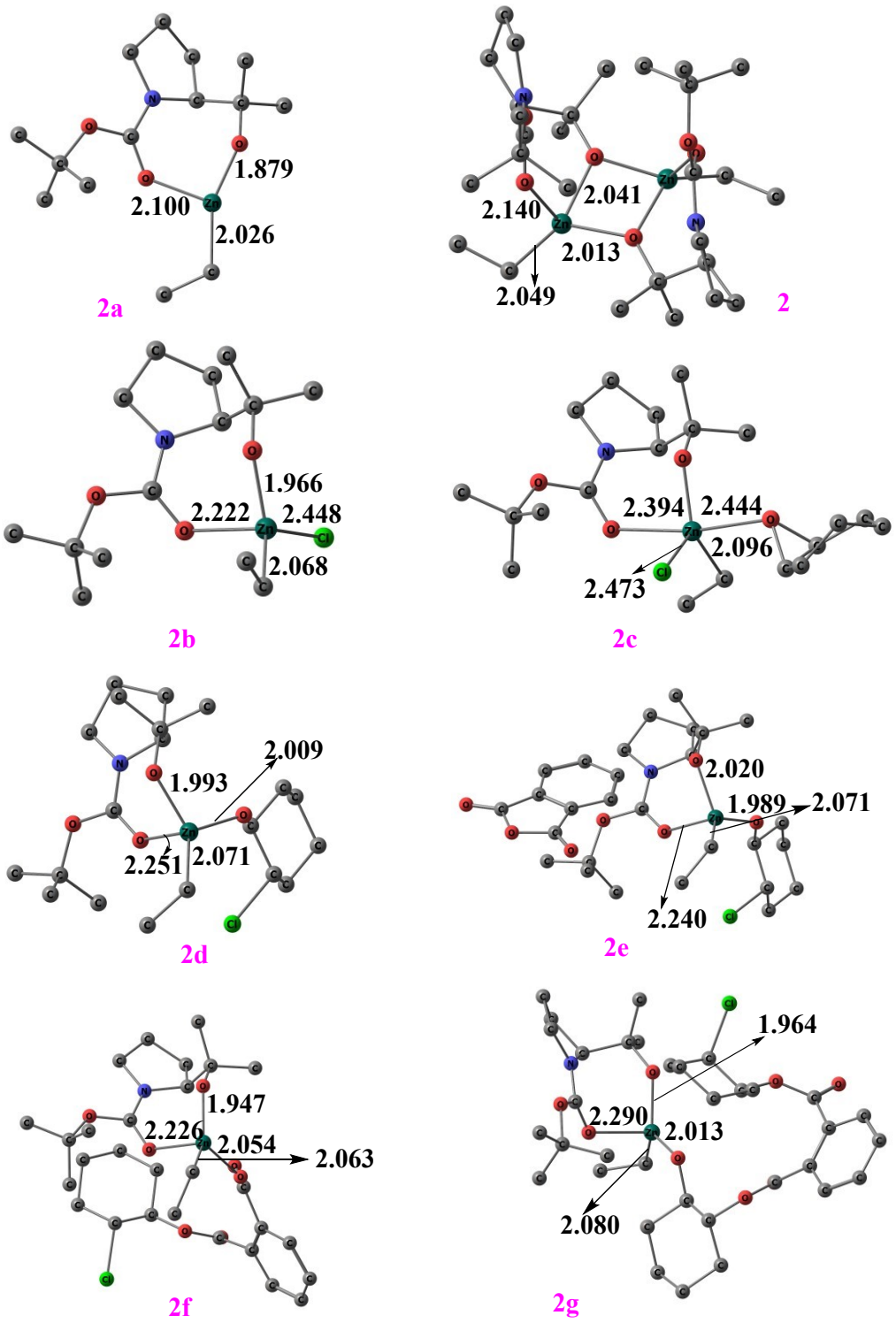

Fig. S51: The calculated bond length for **2-2g** at B3LYP-D3(BJ)/LANL2DZ level of theory. Hydrogens are omitted for clarity.

Table S4. The computed and experimentally characterized geometrical parameters of **2** [Selected bond length (Å) and angels (°)].

	2	
	Theoretical	Experimental
Zn 1-Zn 2	3.056	3.038
Zn1 - O4	2.013	1.986
Zn1 - O5	2.041	2.002
Zn1 -O6	2.140	2.146
Zn1 - C3	2.049	1.976
C3 - Zn1 - O6	108.0	109.4
Zn1 - O4 - Zn2	97.9	99.6

2a

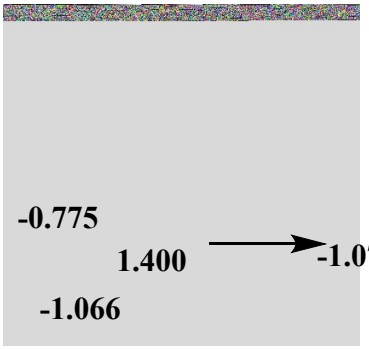

2

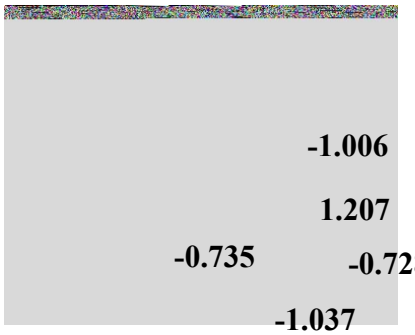

2b

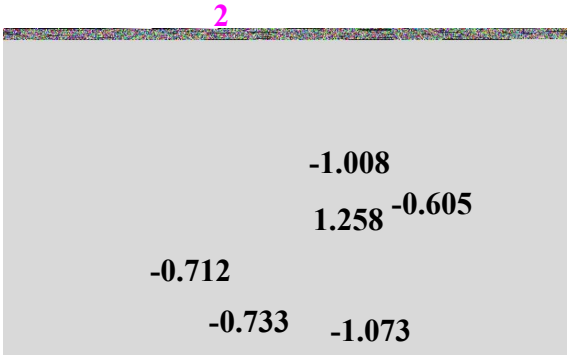

2c

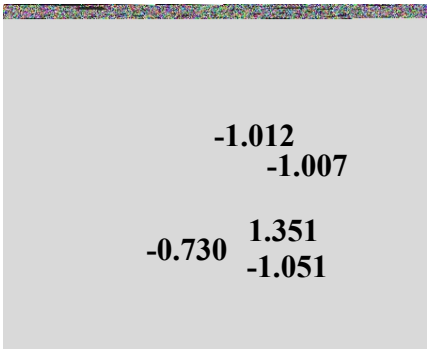

2d

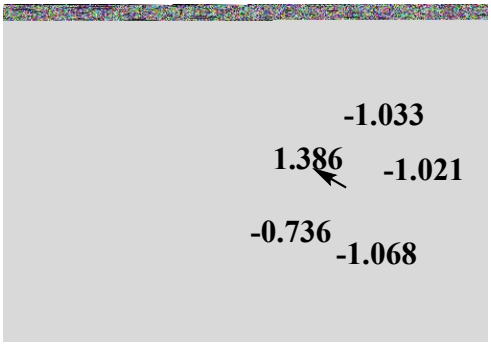

2e

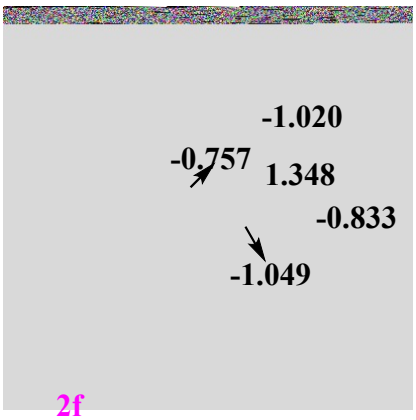

2f

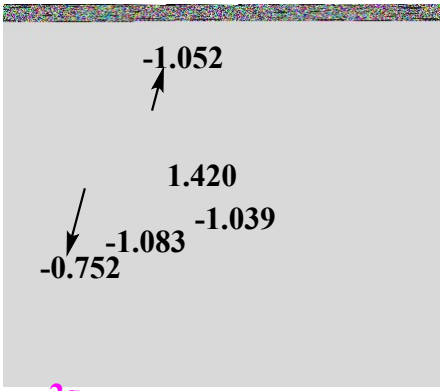

2g

Fig. S52: The Calculated NBO partial charges for **2-2g** at B3LYP-D3(BJ)/LANL2DZ level of theory. Hydrogens are omitted for clarity.

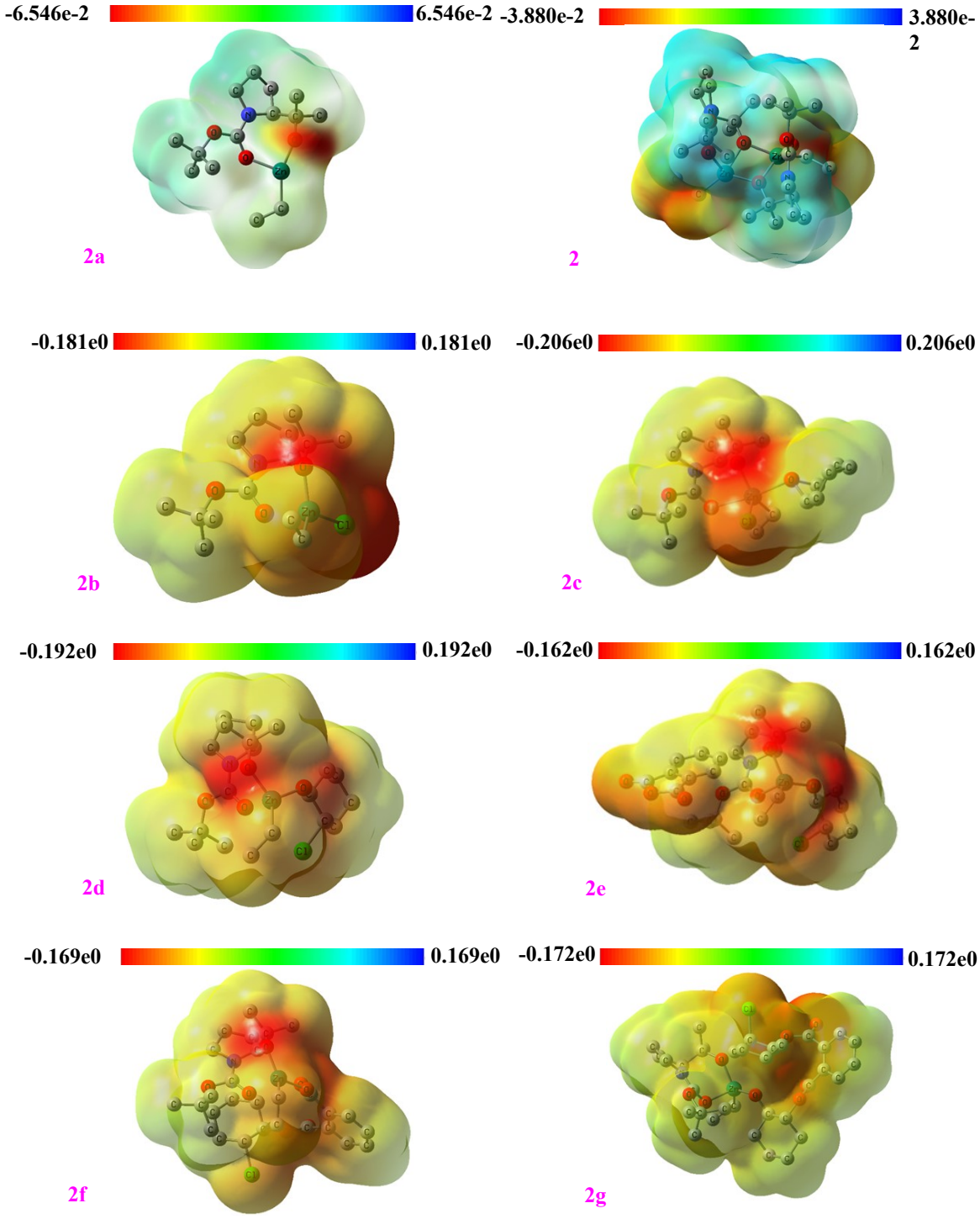

Fig. S53: The ESP Plots for **2-2g** as generated at B3LYP-D3(BJ)/LANL2DZ level of theory. Red colour indicates higher electron density which decreases from yellow to green and lowest for blue colour. Hydrogens are omitted for clarity.

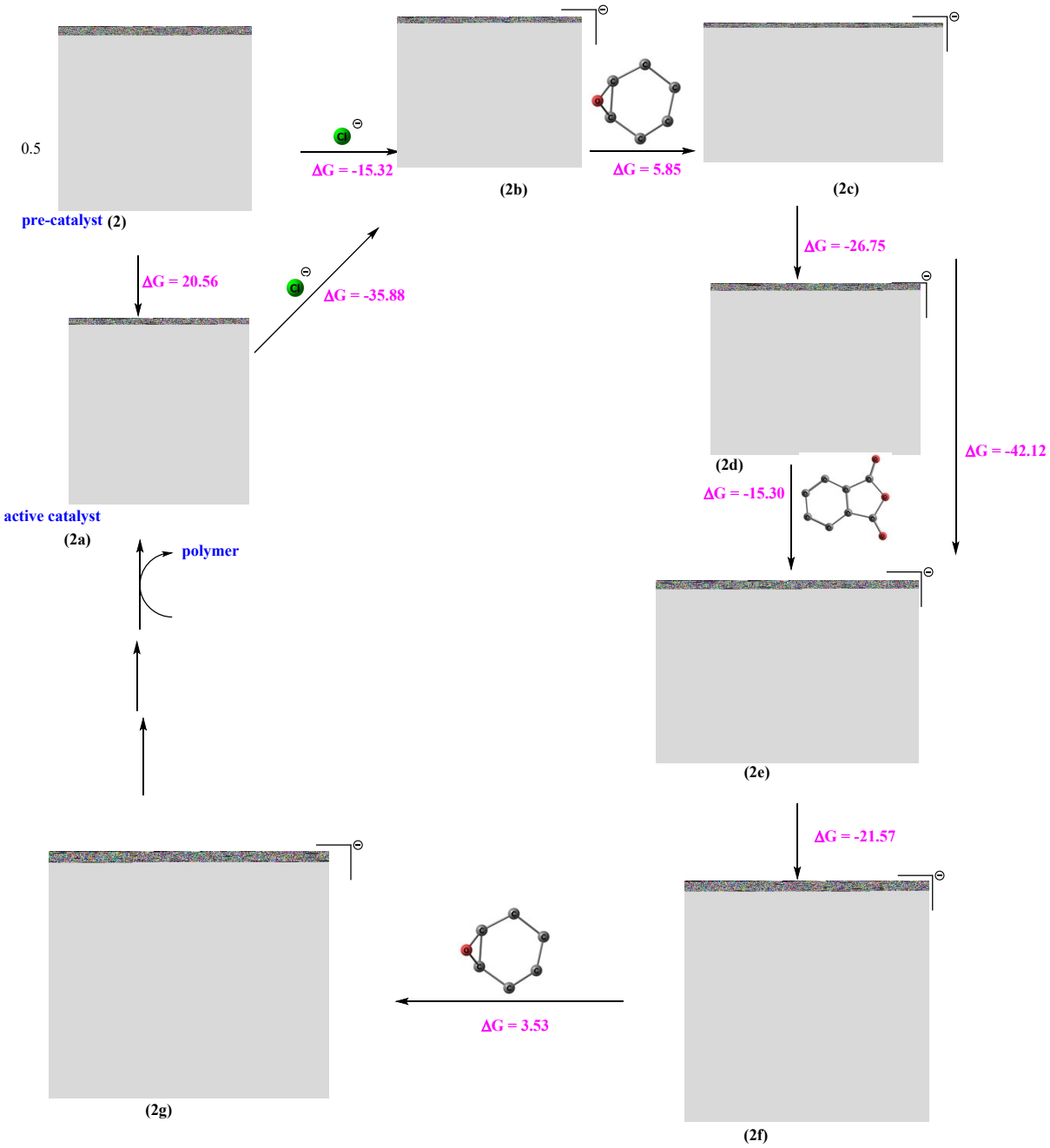

Fig. S54. The optimized structures of proposed Mechanism for Dimer Complex of Zn. The calculations are done at B3LYP-D3(BJ)/LANL2DZ level of theory and ΔG values are in Kcal/mol. Hydrogens are omitted for clarity.

Hirshfeld Surface Analysis and Fingerprint plots

A detailed Hirshfeld surface and fingerprint plot examination of the compound has been conducted and is presented below. The $\mathbf{d_i}$ represents the distance from a point on Hirshfeld surface to nearest atom internal to the surface (within same molecule), $\mathbf{d_e}$ represents the distance from a point on Hirshfeld surface to nearest atom external to the surface (nearest atom in a neighboring molecule). These parameters define the type and intensity of intermolecular interactions. On Hirshfeld surface maps, red areas indicate close atomic contacts (short distances), green indicates moderate separations, and blue defines larger distances (Scheme S3, ESI). The normalized contact distance, $\boldsymbol{d_{norm}}$, which combines $\boldsymbol{d_i}$, $\boldsymbol{d_e}$, and the van der Waals (*vdW*) radii of the atoms involved. It cab be calculated using the following formula:

$$d_{norm} = \frac{d_i - r_i^{vdW}}{r_i^{vdW}} + \frac{d_e - r_e^{vdW}}{r_e^{vdW}}$$

In $\boldsymbol{d_{norm}}$ the color scale is different from that used for $\boldsymbol{d_i}$ and $\boldsymbol{d_e}$: red areas show contacts that are shorter than the sum of van der Waals radii, which indicates strong interactions such as hydrogen bonds; white regions indicate distance approximately equal to the van der Waals separation, which indicates moderate or neutral interactions; and blue areas indicates longer contacts, suggesting weak or negligible intermolecular interactions.

Curvedness is a quantitative measure of the local geometry of a surface, particularly its flatness or curvature**.** Low values show planar/flat regions, high values show sharp edges. Low values shown in green or red indicate flatter regions, which may be due to areas of π-stacking or planar molecular packing. In compared with, high curvedness values (shown in blue) indicate sharp edges or pronounced surface features.

The Shape index provides a qualitative view of the topology of molecular surface, differenciate between concave (red) and convex (blue) regions. Shape Index show shape features like hollows (concave) and bumps (convex). It is useful in identifying π-π stacking. The fragment patch feature shows interaction zones on the Hirshfeld surface by assigning distinct colors to regions in contact with individual neighboring molecules, enabling clear visual identification of separate molecular interactions within the crystal structure.

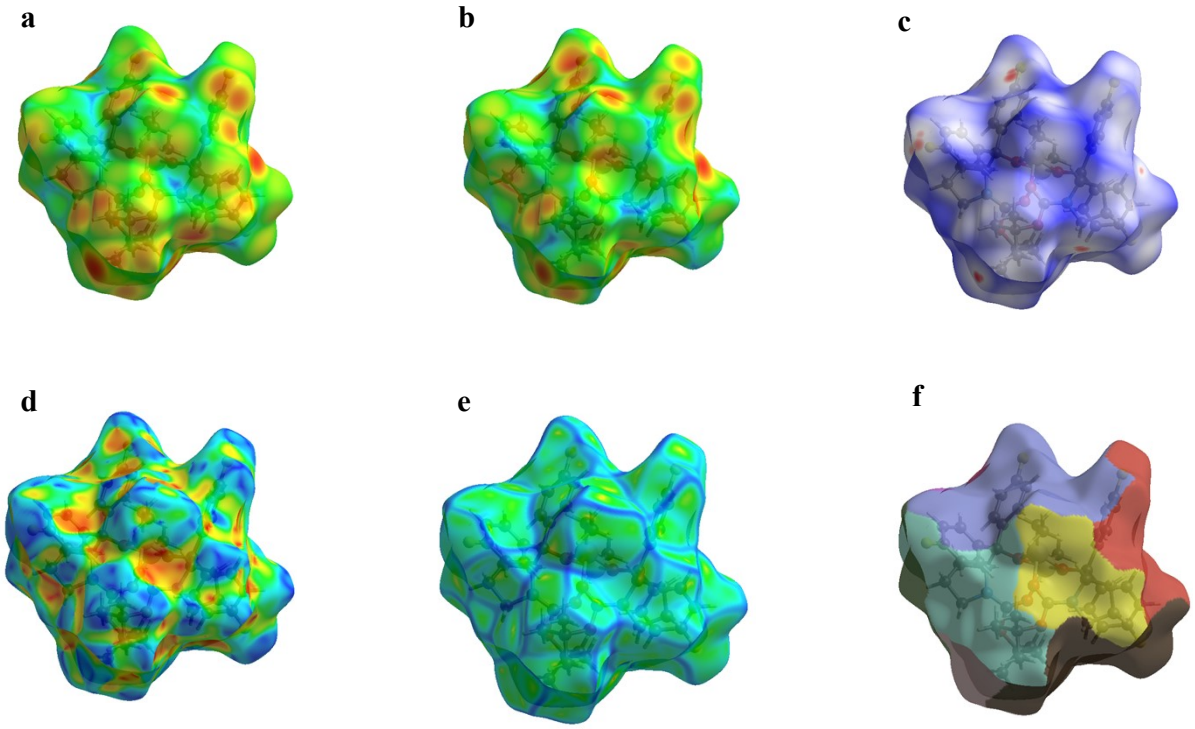

Fig. S55. A compilation of (a) d_i – internal distance, (b) d_e – external distance, (c) Shape index, (d) Curvedness, (e) Fragment patch, (f) d_{norm} mapped on the Hirshfeld surface.

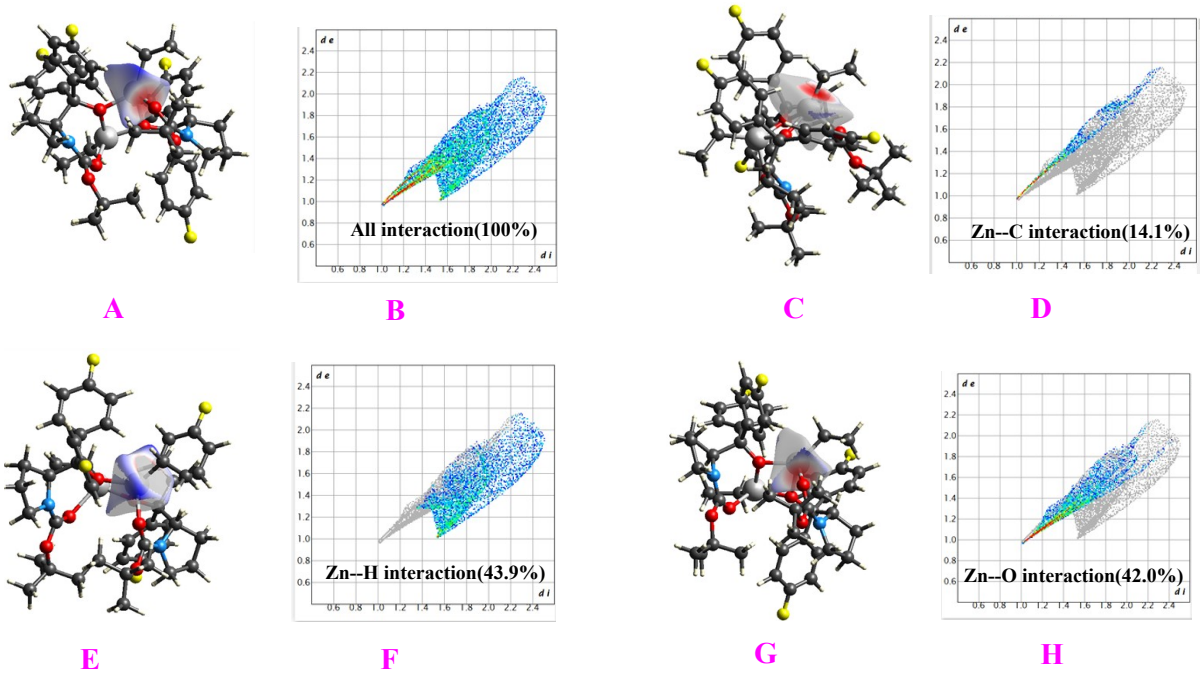

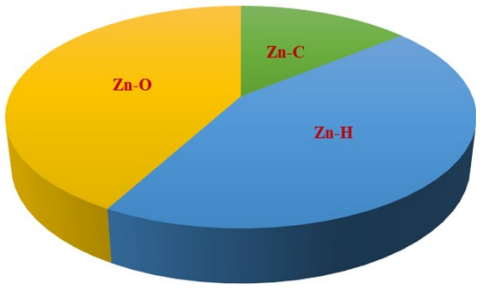

Fig. S56. Fingerprint plots from the Hirshfeld surface generated for Zn atom for **2**

2D fingerprint plots of complex, shows the contributions from different types of intermolecular interactions. The complete fingerprint plot is shown in gray color and the specific contributions (in percentage) to the Hirshfeld surface area are shown in blue within the 1.0–2.2 Å range.

Optimized coordinates of Zn Complexes at B3LYP-D3BJ/LANL2DZ level.

Compound **2a**

Energies are in Hartree

E_{hf} = -895.8075787

30	0.229599000	-2.077557000	-0.137364000
6	1.693682000	-3.465593000	0.049383000
8	-1.406764000	-1.455755000	-0.821504000
8	0.839541000	-0.202548000	0.585781000
1	2.020931000	-3.778916000	-0.954910000
6	2.903001000	-2.927242000	0.857454000
6	-2.497000000	-0.640520000	-0.392331000
6	0.372471000	0.944741000	0.273642000
1	3.701906000	-3.679801000	0.957602000
1	3.346276000	-2.042329000	0.379372000

1	2.607300000	-2.624870000	1.871912000
6	-2.017322000	0.352904000	0.727411000
7	-0.931883000	1.277445000	0.283898000
8	1.178754000	1.994489000	-0.082696000
1	-1.618320000	-0.273405000	1.536504000
6	-3.075537000	1.350868000	1.261564000
6	-1.394269000	2.671341000	0.056987000
6	2.680138000	1.831190000	-0.234882000
1	-4.089403000	0.950557000	1.195067000
1	-2.871258000	1.567535000	2.317521000
6	-2.896863000	2.638610000	0.417234000
1	-1.213029000	2.969944000	-0.980492000
1	-0.825098000	3.350509000	0.701039000
6	2.968741000	0.793173000	-1.331900000
6	3.294017000	1.450654000	1.121745000
6	3.101413000	3.239780000	-0.671235000
1	-3.502799000	2.590048000	-0.490847000
1	-3.192487000	3.536198000	0.969627000
1	4.039751000	0.807877000	-1.568315000
1	2.700129000	-0.214059000	-1.007210000
1	2.412335000	1.037089000	-2.244445000
1	4.387742000	1.451223000	1.034657000
1	3.010733000	2.183001000	1.887067000
1	2.964989000	0.458437000	1.436114000
1	4.188381000	3.275791000	-0.809924000

1	2.617019000	3.511168000	-1.615482000
1	2.820048000	3.976584000	0.088909000
6	-3.589762000	-1.559488000	0.210120000
1	-4.526437000	-1.034993000	0.438838000
1	-3.801035000	-2.349998000	-0.517701000
1	-3.220916000	-2.038367000	1.127716000
6	-3.042376000	0.095318000	-1.635200000
1	-3.256797000	-0.655306000	-2.402854000
1	-3.962745000	0.656471000	-1.428361000
1	-2.281580000	0.775133000	-2.036534000
1	1.285316000	-4.364844000	0.536172000

Compound **2**

E_{hf} = -1791.7111681

30	0.795740000	-1.667489000	-1.305701000
30	-0.791533000	-1.666786000	1.306091000
6	1.591724000	-2.922358000	-2.717058000
8	-1.107538000	-1.427189000	-0.695562000
8	1.111590000	-1.426399000	0.695740000
8	1.649914000	0.273601000	-1.588855000
6	-1.583842000	-2.922707000	2.718691000
8	-1.650835000	0.271779000	1.588442000
1	1.355463000	-3.970688000	-2.467311000
1	1.105972000	-2.720128000	-3.688275000
6	3.126937000	-2.753234000	-2.871279000
6	-2.364372000	-1.488947000	-1.386852000

6	2.368218000	-1.483247000	1.387778000
6	2.172374000	1.084820000	-0.765662000
1	-1.348915000	-3.970893000	2.467062000
1	-1.094829000	-2.721806000	3.688553000
6	-3.118462000	-2.752928000	2.877958000
6	-2.175435000	1.081079000	0.764688000
1	3.552419000	-3.379220000	-3.673806000
1	3.388414000	-1.708490000	-3.097897000
1	3.654807000	-3.026323000	-1.943339000
6	-3.394554000	-0.663517000	-0.543861000
6	3.396185000	-0.655508000	0.544348000
7	2.959461000	0.745363000	0.279766000
1	-3.541781000	-3.379333000	3.681310000
1	-3.378663000	-1.708215000	3.106119000
1	-3.649390000	-3.025003000	1.951444000
7	-2.961759000	0.738756000	-0.280375000
1	-3.481382000	-1.176237000	0.421113000
6	-4.785959000	-0.454149000	-1.188666000
1	3.484587000	-1.168717000	-0.420215000
6	4.786913000	-0.441699000	1.189167000
6	3.699932000	1.756263000	1.077599000
6	1.281823000	3.069790000	-2.045231000
6	-3.705184000	1.746983000	-1.078845000
6	-1.289576000	3.068981000	2.042838000
1	-5.053283000	-1.268280000	-1.867023000

1	-5.548860000	-0.413023000	-0.401827000
6	-4.702759000	0.912859000	-1.915321000
1	5.056482000	-1.254577000	1.868136000
1	5.549777000	-0.398973000	0.402380000
6	4.699770000	0.925598000	1.914806000
1	3.011004000	2.336411000	1.698659000
1	4.203658000	2.455077000	0.400708000
6	-0.186092000	2.617807000	-2.022206000
6	1.997768000	2.696386000	-3.353400000
6	1.412505000	4.567032000	-1.738264000
1	-3.017939000	2.328622000	-1.700390000
1	-4.210814000	2.444843000	-0.402389000
6	-2.004617000	2.694600000	3.351204000
6	-1.423813000	4.565725000	1.734900000
6	0.179321000	2.620232000	2.019941000
1	-4.328441000	0.784538000	-2.934310000
1	-5.678575000	1.404977000	-1.977317000
1	4.325721000	0.796998000	2.933859000
1	5.674190000	1.420513000	1.976520000
1	-0.725663000	3.128864000	-2.830445000
1	-0.264133000	1.539941000	-2.169732000
1	-0.660142000	2.876875000	-1.071421000
1	1.545585000	3.251752000	-4.184562000
1	3.059328000	2.965979000	-3.298215000
1	1.910527000	1.626558000	-3.554823000

1	0.899221000	5.150807000	-2.511596000
1	0.962245000	4.800059000	-0.766953000
1	2.466188000	4.865570000	-1.713199000
1	-1.553888000	3.251646000	4.182021000
1	-3.066854000	2.961487000	3.295804000
1	-1.914736000	1.625115000	3.553283000
1	-0.911581000	5.151246000	2.507609000
1	-0.974450000	4.799024000	0.763252000
1	-2.478173000	4.861870000	1.709994000
1	0.717802000	3.132956000	2.827860000
1	0.259785000	1.542640000	2.168304000
1	0.652767000	2.879595000	1.068966000
6	2.170049000	-0.923918000	2.810571000
1	1.376301000	-1.495427000	3.306364000
1	3.076540000	-1.005688000	3.422417000
1	1.857502000	0.125041000	2.767923000
6	2.841158000	-2.954568000	1.445694000
1	3.790070000	-3.080242000	1.982660000
1	2.073693000	-3.548013000	1.955642000
1	2.954909000	-3.354038000	0.430009000
6	-2.832752000	-2.961818000	-1.442719000
1	-2.063897000	-3.553509000	-1.952628000
1	-2.944450000	-3.360446000	-0.426468000
1	-3.781711000	-3.091006000	-1.978763000
6	-2.168690000	-0.930665000	-2.810385000

1	-1.373355000	-1.500232000	-3.305883000
1	-3.075194000	-1.016000000	-3.421741000
1	-1.859409000	0.119312000	-2.769113000
8	-2.033150000	2.446975000	0.877149000
8	2.026769000	2.450266000	-0.879209000

Compound **2b**

E_{hf} = - 910.8760345

30	0.858551000	-1.734067000	-0.103828000
6	-0.055163000	-3.465648000	0.562037000
8	1.331970000	-0.310793000	1.166829000
8	-0.776802000	-0.417374000	-0.830240000
1	0.592517000	-4.331162000	0.336776000
6	-0.359685000	-3.423067000	2.083517000
6	1.972949000	0.927748000	0.901895000
6	-1.035578000	0.747851000	-0.419258000
1	-0.851722000	-4.338659000	2.467434000
1	0.566048000	-3.279949000	2.660274000
1	-1.010610000	-2.571989000	2.335469000
6	1.322943000	1.575699000	-0.379365000
7	-0.151381000	1.748822000	-0.232720000
8	-2.339631000	1.164926000	-0.148824000
1	1.511885000	0.871370000	-1.198415000
6	1.764617000	3.012054000	-0.746366000
6	-0.558850000	3.136639000	0.069010000
6	-3.462078000	0.164616000	-0.154501000

1	2.796046000	3.209675000	-0.442031000
1	1.704339000	3.145900000	-1.834354000
6	0.753124000	3.955565000	-0.039774000
1	-1.009346000	3.203487000	1.066602000
1	-1.315701000	3.463509000	-0.654118000
6	-3.172292000	-0.949123000	0.867342000
6	-3.662008000	-0.385195000	-1.578209000
6	-4.655358000	1.027004000	0.282686000
1	1.112980000	4.220383000	0.958436000
1	0.596560000	4.885587000	-0.599141000
1	-4.066137000	-1.576630000	0.984511000
1	-2.340099000	-1.576587000	0.545668000
1	-2.922373000	-0.512900000	1.841894000
1	-4.553984000	-1.025764000	-1.601502000
1	-3.807038000	0.440160000	-2.286868000
1	-2.792132000	-0.968949000	-1.885111000
1	-5.567811000	0.417896000	0.309737000
1	-4.477096000	1.442922000	1.280888000
1	-4.803345000	1.856724000	-0.418521000
6	3.482376000	0.704358000	0.611205000
1	4.045731000	1.640730000	0.474064000
1	3.910665000	0.161199000	1.463080000
1	3.592531000	0.077263000	-0.281234000
6	1.805736000	1.817524000	2.159769000
1	2.200508000	1.254446000	3.013358000

1	2.342122000	2.776043000	2.091273000
1	0.740718000	2.001867000	2.348206000
1	-0.991268000	-3.620530000	-0.007509000
17	2.325320000	-1.650353000	-2.061589000

Compound **2c**

E_{hf} = - 1220.7041734

30	0.649905000	-0.378472000	-0.460257000
6	1.168560000	-0.013736000	-2.458406000
8	-0.047454000	0.849456000	0.915212000
8	-1.691030000	-0.727382000	-0.822432000
1	2.061627000	-0.618922000	-2.708640000
6	0.035847000	-0.361198000	-3.456317000
6	-0.458343000	2.176415000	0.647621000
6	-2.606771000	-0.120522000	-0.212764000
1	0.303061000	-0.187958000	-4.517666000
1	-0.253697000	-1.417013000	-3.353447000
1	-0.872367000	0.221525000	-3.242489000
6	-1.606666000	2.148388000	-0.434787000
7	-2.701963000	1.223911000	-0.056800000
8	-3.718952000	-0.761740000	0.330458000
1	-1.143476000	1.770853000	-1.354476000
6	-2.378702000	3.466128000	-0.681367000
6	-3.888637000	1.902706000	0.494087000
6	-3.718851000	-2.259520000	0.492306000
1	-1.752350000	4.345677000	-0.503486000

1	-2.722312000	3.502471000	-1.723756000
6	-3.602081000	3.413166000	0.276503000
1	-4.026032000	1.657358000	1.554401000
1	-4.787933000	1.567273000	-0.036623000
6	-2.556886000	-2.669139000	1.410820000
6	-3.644259000	-2.944063000	-0.884485000
6	-5.081754000	-2.499773000	1.159294000
1	-3.357925000	3.888865000	1.230579000
1	-4.474195000	3.928756000	-0.143006000
1	-2.643704000	-3.737652000	1.652089000
1	-1.582245000	-2.508769000	0.942636000
1	-2.594388000	-2.095464000	2.345350000
1	-3.793781000	-4.025130000	-0.758837000
1	-4.429477000	-2.556540000	-1.547158000
1	-2.669552000	-2.767500000	-1.341479000
1	-5.220284000	-3.572037000	1.347763000
1	-5.135180000	-1.963109000	2.113565000
1	-5.893894000	-2.144869000	0.512919000
6	0.718847000	3.016349000	0.071249000
1	0.474121000	4.082011000	-0.060742000
1	1.563427000	2.925981000	0.764686000
1	1.035027000	2.600527000	-0.893830000
6	-0.929004000	2.797977000	1.986365000
1	-0.097400000	2.713788000	2.695381000
1	-1.219958000	3.856424000	1.903977000

1	-1.764815000	2.213217000	2.388449000
1	1.465628000	1.046738000	-2.591907000
6	6.165113000	0.466300000	0.731761000
6	5.133444000	1.284637000	-0.083920000
6	4.017740000	0.429050000	-0.666614000
6	3.827514000	-0.991759000	-0.242207000
6	4.736219000	-1.632804000	0.783595000
6	5.479249000	-0.581681000	1.636548000
1	6.783305000	1.150181000	1.331571000
1	6.842968000	-0.058257000	0.039239000
1	5.642205000	1.820741000	-0.898293000
1	4.666053000	2.043563000	0.559225000
1	3.608281000	0.730478000	-1.626817000
1	3.293695000	-1.671554000	-0.899271000
1	4.116656000	-2.288249000	1.408049000
1	5.464387000	-2.268131000	0.253135000
1	6.223773000	-1.079729000	2.274161000
1	4.757078000	-0.081489000	2.294385000
8	2.923147000	0.074103000	0.314571000
17	0.997711000	-2.698487000	0.322206000

Compound **2d**

E_{hf} = -1220.7109898

30	-0.223291000	0.038177000	1.935730000
6	-0.580514000	1.481542000	3.377257000
8	1.417056000	-1.093359000	1.976666000

8	0.600406000	0.909861000	0.030601000
1	-0.157342000	1.159058000	4.346461000
6	-0.019166000	2.878835000	3.005355000
6	1.622966000	-2.255446000	1.189587000
6	1.523258000	0.482036000	-0.710721000
1	-0.257173000	3.670057000	3.744322000
1	1.078342000	2.847835000	2.911316000
1	-0.419993000	3.210608000	2.035201000
6	1.158960000	-1.961266000	-0.284352000
7	1.872424000	-0.807834000	-0.912378000
8	2.296128000	1.341259000	-1.497388000
1	0.101739000	-1.701685000	-0.182734000
6	1.385740000	-3.070301000	-1.338888000
6	2.874764000	-1.210007000	-1.922773000
6	2.043165000	2.822555000	-1.456991000
1	1.357427000	-4.068418000	-0.893654000
1	0.595602000	-3.020313000	-2.101339000
6	2.760079000	-2.752440000	-1.983180000
1	3.877711000	-0.875556000	-1.632047000
1	2.639586000	-0.739249000	-2.885323000
6	2.337370000	3.354688000	-0.044686000
6	0.601394000	3.124874000	-1.907181000
6	3.066231000	3.345200000	-2.476322000
1	3.564887000	-3.212108000	-1.402377000
1	2.834419000	-3.118624000	-3.014249000

1	2.272831000	4.451244000	-0.043892000
1	1.620168000	2.960071000	0.675086000
1	3.348281000	3.063180000	0.266154000
1	0.473470000	4.211190000	-2.008299000
1	0.405146000	2.661497000	-2.883035000
1	-0.122542000	2.746795000	-1.183051000
1	3.001913000	4.438687000	-2.543843000
1	4.081730000	3.067882000	-2.170797000
1	2.871781000	2.916908000	-3.466772000
6	0.739828000	-3.417731000	1.729094000
1	0.904747000	-4.380717000	1.219633000
1	0.969546000	-3.542324000	2.794687000
1	-0.314701000	-3.128981000	1.635739000
6	3.121680000	-2.636641000	1.271057000
1	3.382757000	-2.727170000	2.331995000
1	3.359593000	-3.585869000	0.766127000
1	3.731620000	-1.829530000	0.845253000
1	-1.675368000	1.550692000	3.504759000
6	-3.443787000	-1.896739000	-2.257971000
6	-2.752252000	-2.062240000	-0.889675000
6	-2.219399000	-0.726822000	-0.278398000
6	-3.403689000	0.264074000	-0.244313000
6	-4.113948000	0.455683000	-1.590584000
6	-4.614953000	-0.898355000	-2.145279000
1	-3.801677000	-2.868523000	-2.631608000

1	-2.717516000	-1.515404000	-2.994256000
1	-1.895232000	-2.745318000	-0.955562000
1	-3.449839000	-2.501123000	-0.160243000
1	-1.485573000	-0.299732000	-0.999905000
1	-4.943651000	1.165954000	-1.479766000
1	-3.400209000	0.896388000	-2.301040000
1	-5.096182000	-0.740396000	-3.122166000
1	-5.379331000	-1.313520000	-1.469386000
8	-1.663601000	-0.988195000	0.982673000
1	-4.086528000	-0.009196000	0.565791000
17	-2.788526000	2.007629000	0.294762000

Compound **2e**

E_{hf} = -1753.6464745

30	-1.017936000	-0.622905000	-1.666838000
6	0.091386000	-2.146036000	-2.525814000
8	-0.323942000	1.242428000	-2.013585000
8	-0.493788000	-0.270477000	0.482192000
1	0.832848000	-1.698099000	-3.215407000
6	0.801717000	-3.097023000	-1.527445000
6	-1.037689000	2.438786000	-1.714149000
6	-0.194153000	0.785858000	1.098509000
1	1.351934000	-3.922261000	-2.017158000
1	1.531160000	-2.555213000	-0.906723000
1	0.072784000	-3.547462000	-0.839814000
6	-1.633174000	2.315312000	-0.267292000

7	-0.606508000	2.040161000	0.788362000
8	0.598867000	0.778951000	2.239361000
1	-2.301834000	1.452823000	-0.325252000
6	-2.345494000	3.562576000	0.308232000
6	-0.358964000	3.191457000	1.686379000
6	1.011067000	-0.530468000	2.869862000
1	-2.777380000	4.185686000	-0.479277000
1	-3.162571000	3.247513000	0.971757000
6	-1.263319000	4.312535000	1.125650000
1	0.702607000	3.467005000	1.689861000
1	-0.625374000	2.921958000	2.715731000
6	1.913446000	-1.323441000	1.912211000
6	-0.249235000	-1.320684000	3.266537000
6	1.791781000	-0.049760000	4.100389000
1	-0.685845000	4.973603000	0.472956000
1	-1.690494000	4.920880000	1.931197000
1	2.269980000	-2.228587000	2.421317000
1	1.365933000	-1.617271000	1.017304000
1	2.782134000	-0.725118000	1.622334000
1	0.045474000	-2.199368000	3.855004000
1	-0.909747000	-0.697606000	3.883612000
1	-0.794922000	-1.658589000	2.382764000
1	2.171237000	-0.912513000	4.661646000
1	2.641801000	0.568532000	3.790144000
1	1.147310000	0.545628000	4.757744000

6	-2.226402000	2.587082000	-2.701562000
1	-2.797422000	3.519161000	-2.569523000
1	-1.822048000	2.567669000	-3.721110000
1	-2.894034000	1.725669000	-2.578776000
6	-0.070994000	3.639024000	-1.856762000
1	0.386489000	3.585179000	-2.851455000
1	-0.575591000	4.610854000	-1.755046000
1	0.733740000	3.574612000	-1.113507000
1	-0.593840000	-2.738682000	-3.158445000
6	-5.916758000	0.029331000	0.998828000
6	-5.005031000	0.204093000	-0.232505000
6	-3.701761000	-0.652108000	-0.181386000
6	-4.120547000	-2.117135000	0.059991000
6	-5.023068000	-2.327396000	1.281576000
6	-6.296513000	-1.455881000	1.175876000
1	-6.821480000	0.648013000	0.899909000
1	-5.387549000	0.374061000	1.902160000
1	-4.696648000	1.250854000	-0.354928000
1	-5.545083000	-0.074354000	-1.149800000
1	-3.133688000	-0.343026000	0.725698000
1	-5.280844000	-3.389669000	1.379338000
1	-4.462802000	-2.043490000	2.183662000
1	-6.916535000	-1.601020000	2.072777000
1	-6.895298000	-1.781431000	0.310742000
8	-2.977979000	-0.461923000	-1.370788000

6	4.122109000	1.483054000	0.519608000
6	2.881657000	1.676654000	-0.121830000
6	4.880689000	0.379036000	0.122513000
1	2.251955000	2.512321000	0.166706000
6	2.412741000	0.799933000	-1.127108000
6	4.420743000	-0.506007000	-0.875711000
1	1.424530000	0.991476000	-1.580381000
6	3.189728000	-0.318368000	-1.510608000
1	2.825238000	-1.009251000	-2.263210000
1	4.477218000	2.153123000	1.296692000
6	5.440011000	-1.563257000	-1.067154000
6	6.196455000	-0.085183000	0.606306000
8	6.518850000	-1.275541000	-0.135464000
8	5.499848000	-2.529215000	-1.818053000
8	6.957664000	0.365013000	1.461204000
1	-4.539160000	-2.535872000	-0.859833000
17	-2.554076000	-3.198676000	0.342201000

Compound **2f**

E_{hf} = -1753.685842

30	-0.699242000	-2.255667000	-1.198647000
6	-0.684970000	-2.522703000	-3.244385000
8	-2.066711000	-2.737051000	0.100895000
8	-1.173125000	-0.111671000	-0.835779000
1	-1.710427000	-2.546643000	-3.655508000
6	0.143706000	-1.408065000	-3.937312000

6	-2.090528000	-2.565641000	1.512952000
6	-2.164463000	0.270415000	-0.144321000
1	0.224231000	-1.529132000	-5.034342000
1	-0.294455000	-0.414469000	-3.753302000
1	1.165680000	-1.377542000	-3.532320000
6	-1.638582000	-1.101109000	1.871665000
7	-2.422839000	-0.071983000	1.130729000
8	-3.094289000	1.187589000	-0.629264000
1	-0.586443000	-1.026101000	1.581540000
6	-1.838144000	-0.647364000	3.334442000
6	-3.491170000	0.551812000	1.939137000
6	-3.187354000	1.468068000	-2.107247000
1	-1.770426000	-1.485836000	4.032786000
1	-1.051290000	0.067997000	3.600888000
6	-3.231636000	0.040012000	3.380996000
1	-4.480623000	0.262117000	1.565679000
1	-3.419415000	1.642341000	1.863668000
6	-3.452416000	0.150131000	-2.854249000
6	-1.913698000	2.174266000	-2.602034000
6	-4.400782000	2.406281000	-2.170043000
1	-4.003862000	-0.680267000	3.666122000
1	-3.258115000	0.863919000	4.103890000
1	-3.664156000	0.366401000	-3.909662000
1	-2.591890000	-0.518635000	-2.805043000
1	-4.318443000	-0.363956000	-2.420796000

1	-2.045927000	2.465864000	-3.652023000
1	-1.727093000	3.081084000	-2.015467000
1	-1.051734000	1.510162000	-2.526307000
1	-4.587919000	2.706467000	-3.208620000
1	-5.292144000	1.902141000	-1.780137000
1	-4.218447000	3.305362000	-1.569572000
6	-1.083757000	-3.535852000	2.187847000
1	-1.114845000	-3.499561000	3.287198000
1	-1.323516000	-4.555669000	1.862045000
1	-0.067373000	-3.294498000	1.858370000
6	-3.530030000	-2.878780000	1.989752000
1	-3.781193000	-3.889676000	1.648128000
1	-3.644299000	-2.837357000	3.083021000
1	-4.237766000	-2.185149000	1.518972000
1	-0.236585000	-3.506839000	-3.470590000
6	5.548051000	-0.245591000	0.302460000
6	6.201944000	-1.286457000	-0.378955000
6	4.152958000	-0.286502000	0.490504000
1	7.278919000	-1.247557000	-0.525526000
6	5.454050000	-2.368349000	-0.883245000
6	3.405088000	-1.392205000	0.025683000
1	5.951707000	-3.169678000	-1.425134000
6	4.064119000	-2.416625000	-0.678930000
1	3.461419000	-3.238292000	-1.052548000
1	6.105341000	0.607323000	0.679867000

6	1.932981000	-1.556525000	0.363014000
6	3.507198000	0.897963000	1.131362000
8	1.518413000	-1.060308000	1.462899000
8	1.231099000	-2.238466000	-0.497315000
8	3.911659000	1.473765000	2.160678000
8	2.474241000	1.375495000	0.357791000
6	1.633076000	2.448260000	0.908519000
6	0.612267000	1.841055000	1.892779000
6	-0.397102000	2.903061000	2.370793000
6	-1.115921000	3.562129000	1.174270000
6	-0.088509000	4.151556000	0.178939000
6	0.908181000	3.078544000	-0.270386000
1	2.273684000	3.181077000	1.414774000
1	1.157412000	1.396444000	2.730121000
1	0.102378000	1.020682000	1.384705000
1	-1.129409000	2.432669000	3.040146000
1	0.122933000	3.678676000	2.955996000
1	-1.785463000	4.363743000	1.517335000
1	-1.738980000	2.821181000	0.660743000
1	-0.590622000	4.572055000	-0.699887000
1	0.465694000	4.969877000	0.659642000
1	0.454297000	2.304407000	-0.890116000
17	2.174037000	3.912541000	-1.435749000

Compound **2g**

E_{hf} = -2063.5249721

30	-1.258265000	0.655946000	1.524835000
8	-1.744184000	-1.224833000	1.236762000
6	-1.679894000	1.747728000	3.244640000
8	-2.844658000	1.243116000	-0.018958000
6	-2.944945000	-1.899627000	1.573991000
1	-1.630465000	1.074924000	4.119467000
1	-0.903338000	2.517751000	3.405204000
6	-3.076084000	2.423232000	3.185029000
6	-3.352913000	0.404268000	-0.816265000
6	-4.169634000	-1.106981000	0.977306000
1	-3.318842000	3.029175000	4.078607000
1	-3.160053000	3.083451000	2.307566000
1	-3.874535000	1.670851000	3.079413000
7	-3.989024000	-0.730309000	-0.447808000
1	-4.240886000	-0.178408000	1.556151000
6	-5.523028000	-1.856020000	0.928934000
6	-4.700937000	-1.617748000	-1.388130000
6	-2.715983000	1.776783000	-2.832752000
1	-5.614783000	-2.588433000	1.736180000
1	-6.346070000	-1.136478000	1.032008000
6	-5.574330000	-2.520585000	-0.475217000
1	-3.989239000	-2.199788000	-1.986228000
1	-5.298712000	-1.015965000	-2.081457000
6	-3.303405000	3.078416000	-2.256352000
6	-3.114721000	1.596405000	-4.304808000

6	-1.193509000	1.688401000	-2.647975000
1	-5.155976000	-3.529520000	-0.433735000
1	-6.599682000	-2.595946000	-0.855088000
1	-2.962204000	3.926050000	-2.865698000
1	-4.400192000	3.048482000	-2.288007000
1	-2.983443000	3.222062000	-1.223644000
1	-2.640267000	2.374290000	-4.916330000
1	-2.784877000	0.615511000	-4.664754000
1	-4.202700000	1.664908000	-4.424175000
1	-0.730610000	2.595315000	-3.062984000
1	-0.897840000	1.599890000	-1.596473000
1	-0.796350000	0.824983000	-3.192211000
6	-3.130195000	-1.941899000	3.115283000
1	-2.266901000	-2.457805000	3.551335000
1	-0.106152000	-2.181097000	0.558107000
1	-4.048041000	-2.462940000	3.428045000
6	-2.845513000	-3.342421000	1.021072000
1	-1.936691000	-3.799482000	1.426236000
1	-3.705037000	-3.971529000	1.294168000
1	-2.737536000	-3.326533000	-0.069282000
8	3.181613000	0.985048000	1.788737000
6	3.555147000	0.933729000	0.605394000
6	4.674700000	0.060850000	0.124671000
6	4.791442000	-1.286223000	0.525480000
6	3.766882000	-2.056201000	1.325880000

8	0.244570000	1.150332000	0.279437000
8	4.125201000	-2.683404000	2.339587000
6	5.930857000	-2.021828000	0.139772000
1	6.018459000	-3.051133000	0.472998000
6	6.923471000	-1.442514000	-0.666420000
1	7.791048000	-2.027346000	-0.961684000
6	5.665097000	0.636021000	-0.695949000
1	5.540291000	1.665459000	-1.015299000
6	6.786205000	-0.108331000	-1.094625000
1	7.544493000	0.346390000	-1.727204000
6	0.345195000	-1.785330000	-2.884555000
6	-0.381095000	-1.698652000	-1.529892000
6	0.448527000	-2.259350000	-0.377772000
6	1.821040000	-1.599312000	-0.321462000
6	2.585654000	-1.771191000	-1.645392000
6	1.746329000	-1.145751000	-2.787995000
1	-0.251176000	-1.280474000	-3.658315000
1	0.440763000	-2.839102000	-3.181395000
1	-1.350932000	-2.203244000	-1.552675000
1	-0.570214000	-0.653175000	-1.263890000
1	-3.145097000	-0.920032000	3.514485000
1	1.606366000	-0.540013000	-0.104217000
1	3.557729000	-1.279982000	-1.620618000
1	2.746218000	-2.840992000	-1.829661000
1	2.289835000	-1.259161000	-3.737333000

1	1.644184000	-0.068224000	-2.593865000
8	2.483275000	-2.184953000	0.886031000
17	0.644507000	-4.174947000	-0.632674000
8	-3.374861000	0.579753000	-2.192349000
6	0.841691000	2.391681000	0.648097000
6	-0.142454000	3.594812000	0.538538000
6	0.509063000	4.915089000	1.000461000
6	1.774736000	5.225238000	0.170668000
6	2.754848000	4.030319000	0.189723000
6	2.036822000	2.747662000	-0.262315000
1	1.208596000	2.364651000	1.687809000
1	-1.022673000	3.367682000	1.147964000
1	-0.484877000	3.685213000	-0.503379000
1	-0.207595000	5.746001000	0.922530000
1	0.783348000	4.826154000	2.062859000
1	2.279133000	6.126033000	0.549633000
1	1.480298000	5.433568000	-0.870592000
1	3.614161000	4.223154000	-0.467944000
1	3.138086000	3.880825000	1.208569000
1	1.668193000	2.849028000	-1.290531000
8	3.063155000	1.673550000	-0.433995000

References:

S1. Bruker (2021)– APEX4-SAINT Bruker AXS Inc., Madison, Wisconsin, USA.

S2. SADABS-2016/2 - Bruker AXS area detector scaling and absorption Correction, Krause, L., Herbst-Irmer, R., Sheldrick G.M. & Stalke D., *J. Appl. Cryst*., 2015, **48**, 3-10.

S3. G.M. Sheldrick "SHELXT - Integrated space-group and crystal-structure determination", *Acta Cryst*., **2015**, A71, 3-8.

S4. G.M. Sheldrick , Crystal structure refinement with SHELXL", *Acta Cryst*., **2015**, C71, 3-8.

S5. L. J. Farrugia, WinGX for Windows, *J. Appl. Crystallogr.* 2012, **45**, 849-854.

S6. (a) J. A. Garden, P. K. Saini and C. K. Williams, *J. Am. Chem. Soc.* 2015, **137**, 15078–15081. (b) A. Thevenon, J. A. Garden, A. J. White and C. K. Williams, *Inorg. Chem.* 2015, **54**, 11906–11915.

S7. R. Evans, G. D. Poggetto, M. Nilsson and G. A. Morris, *Analytical chemistry*, 2018, **90**, 3987-3994.

S8. (a) A. D. Becke, *J. Chem. Phys.* 1993, **98**, 1372-1377. (b) A. D. Becke, *Phys. Rev.A*, 1988, **38**, 3098. (c) A. D. Becke, *J. Chem. Phys.* 1996, **104**, 1040. (d) P. J. Stephens, F. J. Delvin, C. F. Chabalowski, M. J. Frisch, *J. Phys. Chem.*, 1994, **98**, 11623-11627. (e) C. Lee, W. Yang, R. G. Parr, *Phys. Rev. B.*, 1988, **37**, 785-789. (f) S. Grimme, S. Ehrlich, L. Goerigk, *J. Comput. Chem.* 2011, **32**, 1456-1465.

S9. F. Weigend, R. Ahlrichs, *Phys. Chem. Chem. Phys.* 2005, **7**, 3297-3305.

S10. (a) P. J. Hay, W. R. J. Wadt, *Chem. Phys.*, 1985, **82**, 299. (b) W. R. Wadt, P. J. Hay, *J. Chem. Phys.*, 1985, **82**, 284. (c) P. J. Hay, W. R. J. Wadt, *Chem. Phys*., 1985**, 82**, 270. (d) T. H. Dunning, P. J. Hay, In Modern Theoretical Chemistry; H. F. Schaefer, III, Ed.; Plenum: New York, 1976; pp 1-28.

S11. E. D. Glendening, C. R. Landis, F. J. Weinhold, *Comput. Chem.* 2013, **34**, 1429-1437.

S12. AIMAll (Version 10.05.04), Todd A. Keith, **2010** (aim.tkgristmill.com)

S13. A. E. Reed, L. A. Curtiss, F. Weinhold, *Chem. Rev.* 1988, **88**, 899-926.